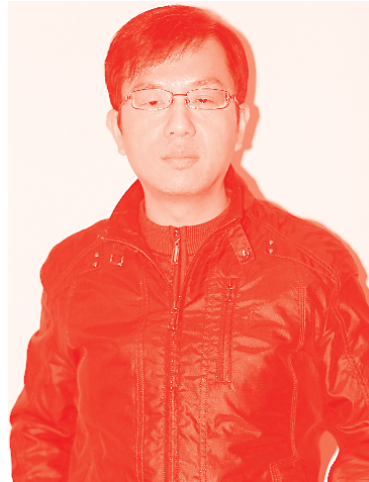# Pheochromocytoma, Paraganglioma and Neuroblastoma

*Edited by Pasquale Cianci,
Enrico Restini and Amit Agrawal*

Pheochromocytoma, Paraganglioma and Neuroblastoma

Edited by Pasquale Cianci, Enrico Restini and Amit Agrawal

IntechOpen

Supporting open minds since 2005

Pheochromocytoma, Paraganglioma and Neuroblastoma
http://dx.doi.org/10.5772/intechopen.92492
Edited by Pasquale Cianci, Enrico Restini and Amit Agrawal

Contributors
María-Dolores Chiara, Andrés San José Martinez, Enol Álvarez-González, Tamara Cubiella, Lucía Celada, Nuria Valdés, Diana Loreta Paun, Alexandra Mirica, Sorin Paun, Radu Mihail Mirica, Nagindra Prashad, Paola Defilippi, Giorgia Centonze, Jennife Chapelle, Costanza Angelini, Dora Natalini, Davide Cangelosi, Vincenzo Salemme, Alessandro Morellato, Emilia Turco, Amit Agrawal, Rakesh Mishra, Pasquale Cianci, Giandomenico Sinisi, Sabino Capuzzolo

Notice
Statements and opinions expressed in the chapters are these of the individual contributors and not necessarily those of the editors or publisher. No responsibility is accepted for the accuracy of information contained in the published chapters. The publisher assumes no responsibility for any damage or injury to persons or property arising out of the use of any materials, instructions, methods or ideas contained in the book.

We are IntechOpen,
the world's leading publisher of Open Access books
Built by scientists, for scientists

5,400+
Open access books available

132,000+
International authors and editors

160M+
Downloads

156
Countries delivered to

Our authors are among the
Top 1%
most cited scientists

12.2%
Contributors from top 500 universities

BOOK CITATION INDEX
CLARIVATE ANALYTICS
INDEXED

WEB OF SCIENCE™

Selection of our books indexed in the Book Citation Index
in Web of Science™ Core Collection (BKCI)

Interested in publishing with us?
Contact book.department@intechopen.com

Numbers displayed above are based on latest data collected.
For more information visit www.intechopen.com

Meet the editors

Pasquale Cianci, MD, Ph.D., AACS, is a general surgeon at "Lorenzo Bonomo" Hospital-Andria, Italy. He obtained a Ph.D. from the Department of Medical and Surgical Sciences, University of Foggia, Italy. He is an associate member of the American College of Surgeons (ACS) and a contract professor of Emergency Surgery, and Human Physiology, University of Foggia - Nursing Science and Physiotherapy Courses. He is also a Professor of Surgical Anatomy. Dr. Cianci is a member of The European Association for Endoscopic Surgery (EAES), Italian Society of Endoscopic and Minimally Invasive Surgery (SICE), Association of Italian Hospital Surgeons (ACOI), Polispecialistic Society of Young Surgeons (SPIGC), Società Italiana Unitaria Colonproctologia (SIUCP), and Associate of American College of Surgeons AACS. He has authored sixty national and international scientific papers. He is an editorial board member and reviewer for numerous journals. He has spoken at many surgical congresses. His special interests include laparoscopic surgery, robotic surgery, endocrine surgery, and coloproctology.

Enrico Restini, MD, is head of the Department of Surgery and Traumatology-Andria, Italy. He is a contract professor in Surgery and Health Management and an expert in advanced technologies and their impact on health organizations (HTA) (LUM University-BA). Since 2007, Dr. Restini has been honorary president of the Apulian section of Aistom. He is a member of the Society of American Gastrointestinal and Endoscopic Surgeons (SAGES), the Italian Society of Endoscopic and Minimally Invasive Surgery (SICE), SICOB, SIC, Italian Society of Private Hospital Surgery, and Association of Italian Hospital Surgeons (ACOI). He is a founding member of ARTOI, and has been a SICE National Councilor since 2012. He has spoken at numerous national and international surgical congresses and authored fifty national and international scientific papers. His special interests include laparoscopic surgery, robotic surgery, endocrine surgery, and digestive surgery.

Amit Agrawal MCh completed his neurosurgery training at the National Institute of Mental Health and Neurosciences, Bangalore, India, in 2003. Dr. Agrawal is a self-motivated, enthusiastic, and results-oriented professional with more than seventeen years of rich experience in research and development as well as teaching and mentoring in the field of neurosurgery. He is proficient in managing and leading teams for running successful process operations and has experience in developing procedures and service standards of excellence. He has attended and participated in many international and national symposiums and conferences and delivered lectures on vivid topics. He has published more than 750 articles in the medical field covering various topics in various

national and international journals. His expertise is in identifying training needs, designing training modules, and executing the same while working with limited resources. He has excellent communication, presentation, and interpersonal skills with proven abilities in teaching and training for various academic and professional courses. Presently, he is working at the All India Institute of Medical Sciences, Bhopal, Madhya Pradesh.

Contents

Preface

Well-differentiated cellular elements, tissues, and organs can originate from the cells of the neural crest. The multipotent differentiation potential of these cell lines is well known, and therefore it is not surprising that the tumors derived from them represent a group of heterogeneous neoplasms. These neoplasms can arise in localizations of the body where cells derived from the neural crest are normally present; however, they can also occur in unusual tissues and locations and in this case, the explanation could be associated with the presence of stem cells that have been shown to be present also in tissues not originating from the neural crest. The classification of tumors derived from neural crest cells has undergone various changes over time. Previously some tumors had been declared of neural crest origin, such as neuroendocrine tumors of the gastrointestinal tract, but a different embryological origin was subsequently demonstrated. Primitive neuroectodermal tumors have always been considered to originate from the cells of the neural crest, but their origin is still unknown today. Pheochromocytoma, paraganglioma and neuroblastoma are the most common neural crest-derived tumors in adults and children, respectively. These neoplasms are associated with significant morbidity and mortality. Although these tumors have different clinical manifestations, courses, and prognoses, their origin can be considered common. Various genetic studies are underway to identify their similarities and differences. Currently being investigated is the role of Stathmin 1 signaling in the pathogenetic mechanism of neuroblastoma and pheochromocytoma, such as the relevance of the PHOX2B gene. Protein is still being studied in the pathogenesis of pheochromocytoma, despite having a fundamental role in the development of precursor cells derived from the neural crest. In this book, we review the current concept of neural crest-cells derived tumors, focusing on pheochromocytoma/paraganglioma and neuroblastoma. In conclusion, I would like to thank everyone who has helped and supported us in this ambitious, long, and demanding job.

Pasquale Cianci
University of Foggia,
Department of Surgery and Traumatology,
ASL BAT,
Andria, Italy

Enrico Restini
"Lorenzo Bonomo" Hospital,
ASL BAT,
Andria, Italy

Amit Agrawal
All India Institute of Medical Sciences,
India

Section 1

Introduction

Introductory Chapter: Neural Crest Cell-Derived Tumors. An Introduction on Pheocromocytoma, Paraganglyoma and Neuroblastoma

Pasquale Cianci, Giandomenico Sinisi and Sabino Capuzzolo

1. Introduction

In the embryonic period, the nervous system originates from a layer of ectodermal cells which is called neuroectoderm. The neuroectoderm extends along the axis of the body to form the neural plate. The latter, turns inward and surrounds itself of neural folds, which then merge together giving life to the neural tube that will develop all the components of the central nervous system and the spinal cord. Finally, from the posterior portion of the neural tube, specialized cells will separate to form the neural crest. Various differentiated cell types, tissues and organs develop from neural crest cells, the mechanisms for this are not well known. However, these cells are multipotent and their subsequent specialization it could be conditioned by the activity of particular genes and by the microenvironment into which they migrate [1]. Hence, neural crest cells have a multipotent differentiation potential. From these cells originate neurons and glial cells, melanocytes, Schwann cells, parafollicular cells of the thyroid, cells of the adrenal medulla, endothelial cells of large vessels and some components of the connective and skeletal tissue of the head [2] (**Figure 1**). Based on these concepts, the tumors that develop from the cells of the neural crest represent a very varied and heterogeneous group of neoplasms, these can affect different body locations where the neural crest cells-derived are normally present. However, neural crest stem cells are also present in some adult tissues that normally do not originate from the neural crest, such as skin and bone marrow [3]. Heterogeneity of tumors originating from neural crest cells is confirmed by the fact that some of them can arise in both peripheral sites or in the central nervous system, while others are specific to the central nervous system or affect only other peripheral locations. Neural crest cell-derived tumors can be grouped into: tumors of peripheral and cranial nerves, melanocytic tumors, peripheral neuroblastic tumors, embryonal tumors of the central nervous system, paraganglioma group, and other tumors of neural crest origin. Most of these are sporadic, some can be hereditary (hereditary paraganglioma-pheochromocytoma syndrome, von Hippel–Lindau disease, neurofibromatosis, schwannomatosis, and multiple neuroendocrine neoplasia (MEN I). Pheochromocytoma/Paraganglyoma
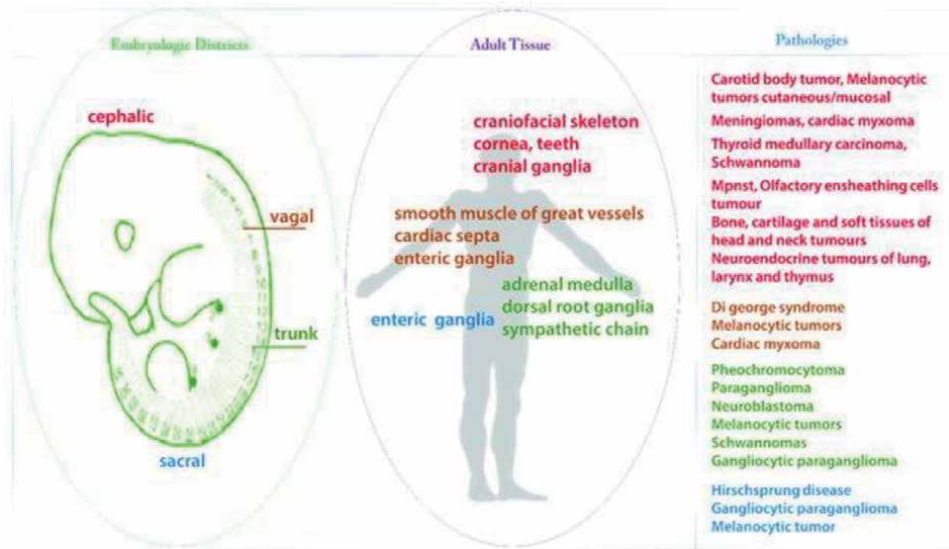
Figure 1.
Segments of neural crest with relative adult tissues and pathologies derivate [2].

and neuroblastoma are the most common neural crest-derived tumors in adults and children, respectively. These neoplasm are both associated with significant morbidity and mortality.

2. Sympatho-adrenal lineage neoplasms

Neural crest cell-derived of the truncal area after a ventral migration reach the vertebral parasympathetic ganglia of the trunk and the chromaffin cells secreting catecholamines of the adrenal medulla and paraganglia [4, 5]. Tumors arising from the cell line involving the sympathetic ganglia can have variable aggressiveness, they can develop from neuroblastomas to ganglioneuromas. Pheochromocytomas and paragangliomas are tumors that develop from neural crest cells that have migrated into the adrenal medulla and paraganglia, they can occur sporadically or within familial syndromes.

2.1 Neuroblastoma

Neuroblastoma is the most frequent extracranial malignancy in children, accounting for 8–10% of pediatric malignancy and with a mortality of 15%. About 38% of primary tumors are located in the adrenal medulla and 1–2% of newly diagnosed neuroblastomas are related to the family history of the disease [6]. At diagnosis, 50% of patients present with lymph node, liver, cortical bone and bone marrow metastases. Due to the presence of an expanding mass, compression of nearby vascular and neuronal structures may occur. The disease can also manifest itself with paraneoplastic syndromes including opsoclonus-myoclonus and intractable watery diarrhea, due to autoimmune cerebellar destruction or production of vasoactive intestinal peptide, respectively [6]. The prognosis is varied, ranging from spontaneous regressions of the disease, neuroblastoma can change into more differentiated ganglioneuromas or have a clearly aggressive course with poor survival [7]. Tumor regression is an unknown process, but may be due to expression of the nerve growth factor (NGF) receptor TrkA, which promotes differentiation in

the presence of NGF and apoptosis in its absence, as described below. Familial type of neuroblastoma is quite rare, it is associated with mutated PHOX2B. Its sporadic form is also frequently associated with the mutated PHOX2B, but the most significant lesion is MYCN amplification. The molecular and genetic characteristics of neuroblastoma are complex and are responsible for the clinical course and prognosis of the disease. The presence of MYCN amplification, chromosomal abnormalities, DNA ploidy, degree of stromal differentiation, tumor stage, and patient age all impacting outcome [8, 9]. This tumor characterized by a remarkable plasticity and by its wide spectrum of presentation remains a stimulating and fascinating subject for both doctors and researchers who deal with it in a specialized way.

2.2 Pheocromocytoma and paraganglioma

Pheochromocytoma and paraganglioma (PPGL) have a prevalence in autopsy studies of 0.05%, which indicates that during the life of many people it is not diagnosed [10, 11]. Amar in 2005 reports an average delay in diagnosis of about 3 years [12]. Their prevalence varies from 0.2% to 0.6% in hypertensive patients to less than 0.05% in the general population, with an annual incidence of about 5 cases per million per year. Two recent retrospective series reported that two thirds were discovered as incidentalomas [13, 14]. PPGL are tumors originating from tissues arising from the neural crest respectively in the paraxial autonomic ganglia or in the chromaffin cells of the adrenal medulla, these tumors are highly vascularized. PPGL arise from tissues derived from the neural crest, respectively in the paraxial autonomic ganglia or in the chromaffin cells of the adrenal medulla. Pheochromocytoma and truncal paraganglioma arising from the sympatho-adrenal lineage cells secrete catecholamines and are highly vascularized. Clinical symptoms can be characterized by tachycardia, hypertension, and a high risk for stroke [15]. In contrast, paragangliomas arising from the parasympathic ganglia are generally nonsecretory and are most commonly found in the head and neck [16, 17], these tumors present as a mass and cause symptoms from compression of adjacent vascular or neuronal structures. In 35% of cases, PPGLs are caused by autosomal dominant germ-line mutations in the succinate dehydrogenase genes or they are found in multitumor syndromes such as neurofibromatosis type 1and MEN2A/2B [18, 19]. Compared to sporadic cases, patients with hereditary forms are younger, with a higher incidence of metastases and a more aggressive disease [20]. Familial syndromes are associated with loss-of-function mutations in the SDH mitochondrial enzyme complex II genes, including the four subunits of SDH and SDHAF2, which flavinates SDHA [21].

3. Future perspectives

The neural crest is an example of a unique and transient developmental structure, endowed with plasticity, proliferative capacity, migratory capacity, and remarkable self-limitation. Its biological and behavioral similarity of the malignant metastatic cell has led to make comparisons between them and to develop the idea that mutual cancer development programs for invasion and proliferation can be exploited [22] (**Figure 2**). In neuroblastoma, clinical maturation from aggressive "precursor-like" lesions to well-differentiated ganglioneuromas speaks to the plasticity of the NC and the normal developmental limitation of pluripotency. Based on these theories and shares regarding the development of the neural crest and cancer, we can understand the importance of studying these growth mechanisms and how fundamental these implications are for the treatment of malignancy. Cancer is
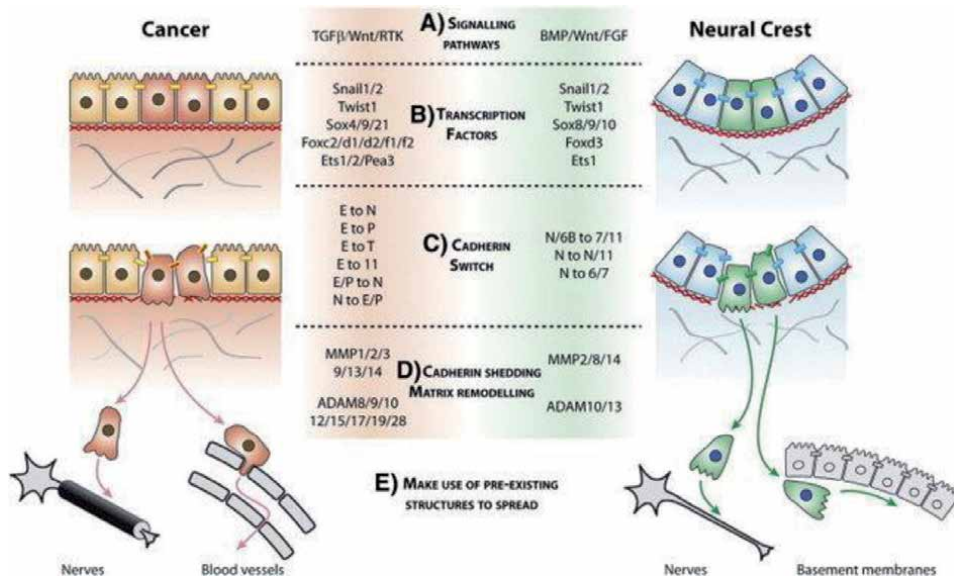
Figure 2.
Cancer metastasis and neural crest cell migration exhibit striking similarities [22].

usually treated surgically, but also in a multidisciplinary way with chemotherapy and radiotherapy. Each of these disciplines has led to many improvements in the survival of these patients but also to an increase in morbidity. Designing targeted therapies is a priority in order to achieve more effective treatment with less collateral damage. Azmi [23] in 2013 and Muller [24] in 2014 tested the therapeutic potential of Snail and c-Myc inhibitory molecules, respectively. Also Chua [25] in 2012 carried out a study aimed at identifying inhibitors of epithelial – mesenchymal transition in order to inhibit cell invasiveness and metastasis. The future direction should point to a complete identification of these factors which are very important for both neural crest development and tumor growth and metastasis, including cell survival, proliferation, motility, invasiveness, and differentiation. Only a more complete understanding of molecular similarities, we will then be poised to develop targeted therapies aimed at modulating those processes that are critical to tumor growth and metastasis. Testing potential new anti-cancer drugs is also an important future step, but is often slow, expensive, and limited to cultured cancer cells or artificial tumor models. NC development study can certainly represent a fundamental topic through which to develop new strategies and new drugs for cancer therapy.

In this book we want to offer the reader some elements of epidemiology, genetics and treatment of pheochromocytoma, paraganglioma and neuroblastoma. Our work does not reach definitive conclusions but aims to provide elements of knowledge regarding non-common neoplasms that have a unique denominator: they are Neural crest cell-derived tumors.

Author details

Pasquale Cianci[1]* , Giandomenico Sinisi[2] and Sabino Capuzzolo[2]

1 Department of Surgery and Traumatology, Lorenzo Bonomo Hospital, ASL BAT, University of Foggia, Andria, Italy

2 Department of Surgery and Traumatology, Dimiccoli Hospital, ASL BAT, Barletta, Italy

*Address all correspondence to: ciancidoc1@virgilio.it

IntechOpen

References

[1] Hall, B.K. The neural crest and neural crest cells: discovery and significance for theories of embryonic organization. J. Biosci. 2008; 33, 781-793. https://doi.org/10.1007/s12038-008-0098-4

[2] Donato G, Presta I, Arcidiacono B, Vismara MFM, Donato A, Garo NC, Malara N. Innate and Adaptive Immunity Linked to Recognition of Antigens Shared by Neural Crest-Derived Tumors. Cancers (Basel). 2020; Apr; 12(4): 840. Published online 2020 Mar 31. doi: 10.3390/cancers12040840

[3] Nagoshi N, Shibata S, Nakamura M, Matsuzaki Y, Toyama Y, Okano H. Neural crest-derived stem cells display a wide variety of characteristics. J Cell Biochem. 2009; 107:1046-1052

[4] Anderson DJ, Carnahan JF, Michelsohn A, Patterson PH. Antibody markers identify a common progenitor to sympathetic neurons and chromaffin cells in vivo and reveal the timing of commitment to neuronal differentiation in the sympathoadrenal lineage. J Neurosci. 1991; 11:3507-3519.

[5] Huber K. The sympathoadrenal cell lineage: specification, diversification, and new perspectives. Dev Biol. 2006; 298:335-343.

[6] Maris JM, Hogarty MD, Bagatell R, Cohn SL. Neuroblastoma. Lancet. 2007; 369:2106-2120.

[7] D'Angio G, Evans A, Koop CE. Special pattern of widespread neuroblastoma with a favourable prognosis. Lancet. 1971; 297: 1046-1049.

[8] Cohn SL, Pearson AD, London WB, Monclair T, Ambros PF, Brodeur GM, Faldum A, Hero B, Iehara T, Machin D, Mosseri V, Simon T, Garaventa A, Castel V, Matthay KK. The International Neuroblastoma Risk Group (INRG) classification system: an INRG Task Force report. J Clin Oncol. 2009; 27:289-297.

[9] Cheung NV, Dyer MA. Neuroblastoma: developmental biology, cancer genomics and immunotherapy. Nat Rev Cancer. 2013; 13: 397-411.

[10] McNeil AR, Blok BH, Koelmeyer TD, Burke MP, Hilton JM. Phaeochromocytomas discovered during coronial autopsies in Sydney, Melbourne and Auckland. Aust N Z J Med. 2000; Dec;30(6):648-52. doi: 10.1111/j.1445-5994.2000.tb04358.x.

[11] Lo CY, Lam KY, Wat MS, Lam KS. Adrenal pheochromocytoma remains a frequently overlooked diagnosis. American journal of surgery. 2000; 179:212-215. [PubMed: 10827323]

[12] Amar L, Servais A, Gimenez-Roqueplo AP, Zinzindohoue F, Chatellier G, Plouin PF. Year of diagnosis, features at presentation, and risk of recurrence in patients with pheochromocytoma or secreting paraganglioma. The Journal of clinical endocrinology and metabolism. 2005; 90:2110-2116.

[13] Falhammar H, Kjellman M, Calissendorff J. Initial clinical presentation and spectrum of pheochromocytoma: a study of 94 cases from a single center. Endocrine connections. 2018; 7:186-192. [PubMed: 29217652]

[14] Gruber LM, Hartman RP, Thompson GB, McKenzie TJ, Lyden ML, Dy BM et al. Pheochromocytoma Characteristics and Behavior Differ Depending on Method of Discovery. The Journal of clinical endocrinology and metabolism. 2019; 104:1386-1393. [PubMed: 30462226]

[15] Bravo EL. Pheochromocytoma. Cardiol Rev. 2002; 10:44-50.

[16] Dahan A., Taschner P.E.M., Jansen J.C., van der Mey A., Teppema L.J., Cornelisse C.J. (2004) Carotid Body Tumors in Humans Caused by a Mutation in the Gene for Succinate Dehydrogenase D (SDHD). In: Champagnat J., Denavit-Saubié M., Fortin G., Foutz A.S., Thoby-Brisson M. (eds) Post-Genomic Perspectives in Modeling and Control of Breathing. Advances in Experimental Medicine and Biology, vol 551. Springer, Boston, MA. https://doi.org/10.1007/0-387-27023-X_12

[17] Bardella C, Pollard PJ, Tomlinson I. SDH mutations in cancer. Biochim Biophys Acta. 2011; 1807:1432-1443.

[18] Raygada M, Pasini B, Stratakis CA. Hereditary paragangliomas. Adv Otorhinolaryngol. 2011; 70:99-106.

[19] Fishbein L, Merrill S, Fraker DL, Cohen DL, Nathanson KL. Inherited mutations in pheochromocytoma and paraganglioma: Why all patients should be offered genetic testing. Ann Surg Oncol. 2013; 20:1444-1450.

[20] Burnichon N, Rohmer V, Amar L, Herman P, Leboulleux S, Darrouzet V, Niccoli P, Gaillard D, Chabrier G, Chabolle F, Coupier I, Thieblot P, Lecomte P, Bertherat J, Wion-Barbot N, Murat A, Venisse A, Plouin PF, Jeunemaitre X, Gimenez-Roqueplo AP. The succinate dehydrogenase genetic testing in a large prospective series of patients with paragangliomas. J Clin Endocrinol Metab. 2009; 94:2817-2827.

[21] Hao HX, Khalimonchuk O, Schraders M, Dephoure N, Bayley JP, Kunst H, Devilee P, Cremers CWRJ, Schiffman JD, Bentz BG, Gygi SP, Winge DR, Kremer H, Rutter J. SDH5, a gene required for flavination of succinate dehydrogenase, is mutated in paraganglioma. Science. 2009; 325:1139-1142.

[22] Theveneau E, Mayor R. Neural crest delamination and migration: from epithelium-to-mesenchyme transition to collective cell migration. Dev Biol. 2012 Jun 1;366(1):34-54. doi: 10.1016/j.ydbio.2011.12.041. Epub 2012 Jan 9.

[23] Azmi AS, Bollig-Fischer A, Bao B, Park BJ, Lee SH, Yong-Song G, Dyson G, Reddy CK, Sarkar FH, Mohammad RM. Systems analysis reveals a transcriptional reversal of the mesenchymal phenotype induced by SNAIL-inhibitor GN-25. BMC Syst Biol. 2013; 7: 85.

[24] Muller I, Larsson K, Frenzel A, Oliynyk G, Zirath H, Prochownik EV, Westwood NJ, Henriksson MA. Targeting of the MYCN protein with small molecule c-MYC inhibitors. PLoS One. 2014: 9: e97285.

[25] Chua KN, Sim WJ, Racine V, Lee SY, Goh BC, Thiery JP. A cell-based small molecule screening method for identifying inhibitors of epithelial-mesenchymal transition in carcinoma. PLoS One. 2012; 7:e33183.

Section 2

Pheochromocytoma and Paraganglioma

Pheochromocytomas and Paragangliomas: Genotype-Phenotype Correlations

Diana Loreta Paun and Alexandra Mirica

Abstract

Pheochromocytomas and paragangliomas are rare neuroendocrine tumors, with genetic background in about 40% of cases, involving more than 30 susceptibility genes. The susceptibility genes can be divided into three main molecular clusters: pseudohypoxic, kinase signaling, and Wnt signaling. Biochemical characterization of these particular tumors should be integrated into the diagnostic algorithm because it can help apply personalized medicine principles and targeted therapy. These tumors can present with very different genotype-phenotype correlations, and their characterization can help the clinical practitioner make optimal clinical management decisions and prioritize genetic testing. This chapter summarizes the most important aspects of genetics and clinical characteristics, together with new genotype-phenotype correlation data.

Keywords: pheochromocytomas, paragangliomas, genotype-phenotype correlations

1. Introduction

Pheochromocytomas (Pheos) and paragangliomas (Pgls) are chromaffin cell-derived tumors that can develop from the adrenal medulla or the extra-adrenal paraganglia. There are two types of Pgls: sympathetic and parasympathetic. Both Pheos and sympathetic Pgls are catecholamine-producing tumors. Frequently parasympathetic Pgls are located in the head and neck region, they do not have chromaffin cell phenotypic features, and they are in a vast majority of non-secreting tumors [1, 2].

Pheos are rare tumors, with an annual incidence of 2 to 9.1 per 1 million for adults patients [3].

The prevalence of Pheos and Pgls in patients with hypertension is between 0.2 and 0.6% [4].

The early detection of Pheos/Pgls is mandatory because if they go undiagnosed and untreated, the cardiovascular morbidity and mortality rates are high. Furthermore, the risk of metastatic disease (the presence of metastases in nonchromaffin tissue) is increased between 10 and 20% [5, 6].

In the last two decades and especially in the last seven years of medical researches, clinical medical studies showed that 40% of these tumors are associated with underlying germline or somatic mutations in about 30 susceptibility genes. Next-Generation Sequencing (NGS) technology has made the sequencing of the whole exome routinely available, and many clinical research papers reported specific genes associated with Pheos and Pgls [2].

Catecholamines are produced within chromaffin cells, and their derivatives are metabolized within the same cells by an enzyme called catechol-O-methyltransferase. Norepinephrine and epinephrine are metabolized to normetanephrine and metanephrine. Also, dopamine is metabolized to 3-methoxytyramine [7].

Depending on biochemical secretory characteristics, Pheos and sympathetic Pgls can be divided into three different biochemical or secretory phenotypes. Pheos and sympathetic Pgls with the noradrenergic phenotype secrete especially norepinephrine. Besides, Pheos and sympathetic Pgls with the adrenergic phenotype produce epinephrine predominantly. Supplementary, Pheos, and sympathetic Pgls, which secrete dopamine, are categorized into a third category named the dopaminergic phenotype [8].

Congruent to The Endocrine Society Clinical Practice Guidelines [4], the clinical evaluation of Pheos or Pgls should start with measurements of plasmatic free metanephrines preferentially carried out using blood samples collected in the supine position or urinary fractionated metanephrines, altogether with urinary creatinine determination. Also, in suspicious dopamine secreting tumors, the plasmatic dosage of 3-methoxytyramine is indicated [7].

If the initial biochemical evaluation indicates elevated 3-fold or more above the upper cutoffs of catecholamines, the next clinical step should be imaging studies to localize the tumor. The preferred initial imaging method is computed tomography, followed by magnetic resonance imaging to detect metastatic disease, and 123I-metaiodobenzylguanidine (MIBG) scintigraphy is recommended [4].

Catecholamine hypersecretion syndrome can induce numerous lethal conditions due to the high impact on the cardiovascular system, potentially causing sudden deaths. Clinical consequences of catecholamine excess can be myocardial infarction, cardiac arrhythmias, severe acute hypertension, pulmonary edema, heart failure, hypertensive encephalopathy, and cardiogenic shock [9, 10].

In addition to catecholamines' secretion, Pheos and Pgls could also secrete a wide diversity of biomarkers, such as chromogranin A, which can monitor disease progression [11, 12]. Subsequently, chromogranin A is released by exocytosis from the storage granules and catecholamines into the bloodstream to sympathetic or adrenal stimulation. Therefore, chromogranin A level corresponds to the norepinephrine and epinephrine serum levels in the context of Pheos/Pgls [12].

Moreover, chromogranin A levels were reported to be proportional to the tumor mass, metastatic disease, especially liver disease, and the presence of the SDHB gene mutation [13].

Furthermore, Pheos and Pgls could be responsible in rare situations of ectopic secretion syndromes, with mostly cited cases of ectopic ACTH secretion syndrome, PTH/PTHrp, and interleukin 6 secretion [14]. However, the majority of ectopic secretion is encountered in non-metastatic tumors.

These particular tumors can present with very different genotype-phenotype correlations. Depending on the affected gene and its activated intracellular signaling pathways, each tumor is clinically different.

The genetic involvements, together with the good predictive value of histological PASS -Pheochromocytoma of the Adrenal Gland Scaled Score and GAPP algorithms, provide novel prognostic biomarkers and new therapeutic approaches for Pheos and Pgls [15].

2. Genetic background

More than 30 genes are currently associated with hereditary Pheos and Pgls, leading to genetic cause in about 40% of these tumors. Given this high frequency of genetic mutations, all patients with Pheos and Pgls should undergo genetic testing [16].

Genetic screening should be done mostly in patients with a positive family history, young age at diagnosis, bilateral adrenal Pheos, and metastatic or multifocal Pheos/Pgls [4].

NGS technique of targeted gene panels is now the recommended genetic screening method in all patients diagnosed with Pheos/Pgls [17].

Depending on the main signaling transduction pathways, these genes have been grouped into three clusters: pseudohypoxemia, the tyrosine kinase, and the WNT pathways [18].

Gene clusters have different molecular routes to tumorigenesis and provide a specific substrate to explore. Furthermore, each cluster is associated with particular clinical characteristics and with a specific phenotype.

2.1 Pseudohypoxic cluster

The pseudohypoxic pathway involves the Krebs cycle modulation. It is characterized by mutations in genes encoding the endothelial pas domain protein 1/hypoxia-inducible factor type 2A (EPAS1/HIF2A), von Hippel-Lindau tumor suppressor (VHL), succinate dehydrogenase subunits SDHx (SDHA, SDHB, SDHC, SDHD), succinate dehydrogenase complex assembly factor 2 (SDHAF2), egl-9 prolyl hydroxylase 1 and 2 (EGLN1/2), fumarate hydratase (FH), malate dehydrogenase 2 (MDH2), prolyl hydroxylase types 1 and 2 (PHD1 and PHD2), and isocitrate dehydrogenase (IDH) [19, 20].

Furthermore, the hypoxia/pseudohypoxia cluster is divided into two subgroups. The first is associated with germline mutations that affect Krebs cycle and especially the succinate dehydrogenase subunits (SDHA, SDHB, SDHC, SDHD, and SDHAF2), the fumarate hydratase (FH), the malate dehydrogenase 2 (MDH2), and isocitrate dehydrogenase (IDH). The second subgroup involves mutation VHL/EPAS1 genes, with a high rate of angiogenesis and over-expression of vascular endothelial-vessel growth factor (VEGF), which increases neo-angiogenesis [3].

Tumors caused by these specific genetic mutations are pseudohypoxic. Hence the upregulation of HIF-α is not caused by hypoxia but by other molecular pathways. Mutations in genes encoding enzymes lead to the misregulation of cellular metabolism, chromatin remodeling, DNA methylation changes, and reactive oxygen species production. These specific genetic mutations can induce a metabolic alteration that results in an increased dependence on glycolysis, promotion of angiogenesis, and succinate, fumarate, and L-malate accumulation. Thus, these high concentrations of Krebs cycle metabolites lead to activation of the oncogenetic pathway [16, 21].

Furthermore, the hypoxia pathway activation in these types of tumors implicates the glycolytic shift, a typical biochemical feature of these tumors [3].

Tumors in this cluster are more clinically aggressive and are often diagnosed with metastatic disease. Also, multiple and multifocal tumors are persistent, and the prognostic of patients in this gene's cluster is most deficient than other susceptibility gene mutations. Moreover, almost all tumors associated with cluster 1 (except for VHL- gene) gene mutations are extra-adrenal, and they have the noradrenergic phenotype, secreting norepinephrine [22, 23].

2.2 Kinase signaling cluster

Dysregulation of the receptor kinase signaling pathway consists of germline or somatic mutations in the RET proto-oncogene (RET), neurofibromin 1 (NF1) tumor suppressor, H-RAS and K-RAS proto-oncogenes, transmembrane protein 127

(TMEM127), Myc-associated factor X (MAX), chromatin remodeler ATRX, and cold shock domain-containing E1 (CSDE1) [24, 25].

Patients with tumors caused by gene mutations in this cluster have an excellent general prognosis, except for those with ATRX mutations, where recurrence and metastatic disease are more common [26].

Furthermore, Pheos and Pgls from this cluster have a more differentiated cellular adrenergic phenotype, they are mostly adrenal tumors, and they rarely develop secondary lesions, except for those with ATRX gene mutations [16].

2.3 Wnt signaling cluster

The Wnt pathway plays an essential role in the development, organogenesis and is vital for cell survival, migration, and chemotaxis. The Wnt signaling pathway is demodulated in different diseases such as cancer, bone diseases, cardiovascular diseases, hereditary colorectal cancer, intellectual disability syndrome, neuropsychiatric diseases [3, 27].

Tumors overexpressing genes of the Wnt and Hedgehog pathways consist of the Wnt-altered subgroup. These tumors are related to somatic mutations in CSDE1 and the mastermind, like transcriptional coactivator 3 (MAML3) [27].

These genotypes display mixed characteristics regarding catecholamine secretion phenotype, involving both noradrenergic and adrenergic phenotype. Moreover, Wnt pathway genes are associated with tumors with a high frequency of metastatic or recurrent disease [28, 29].

Furthermore, Wnt-altered tumors exhibit high expression of CHGA, a gene that encodes chromogranin A, inducing high levels of this biomarker, useful for diagnosing and monitoring disease progression [16, 21].

Moreover, somatic mutations in the TERT promoter (SDHx-deficient PPGL) and the chromatin modifier KMT2D have also been identified, but they remain validated by future researches [23]. However, the somatic mutations in genes associated with telomere preservation (inactivation of the ATRX gene or transcriptional activation of TERT) are associated with tumors with more aggressive clinical features [23].

3. Biochemical diagnosis and specific secretory phenotypes

Patients with Pheos can present with a complex spectrum of nonspecific symptoms, making it challenging for clinical physicians to diagnose correctly.

The biochemical phenotype of the tumor influences the clinical presentation. These tumors' hormonal phenotypes have systemic effects, especially on the cardiovascular system and gastrointestinal, ocular, renal systems.

Most patients present with typical clinical signs and symptoms of catecholamine excess, including sustained or paroxysmal hypertension episodes, sweating, headache, and palpitations. Symptoms may be precipitated due to external factors, including a tyramine-rich diet, specific drugs such as histamine, tricyclic antidepressants, monoamine oxidase inhibitors, and anesthesia [30, 31]. Moreover, in 10 to 20% of cases, patients may be entirely asymptomatic, with Pheos/Pgls diagnosed as incidentalomas on imaging studies [15].

These clinical characteristics can be grouped into three distinct biochemical phenotypes: noradrenergic, adrenergic, and dopaminergic, defined by elevations in epinephrine, norepinephrine, and dopamine [23].

Besides, there is a rare subset of Pgls, which are non-secreting tumors, and they are referred to as biochemically silent, although elevated levels of chromogranin A or specific neuronal enolase can be detected [12].

Studies reported that tumors with the adrenergic phenotype are more differentiated than the noradrenergic phenotype, which may be more differentiated than the dopaminergic phenotype, influencing catecholamine secretion levels [6].

Numerous reports showed a positive correlation between tumor dimensions and plasma and urinary concentrations of metanephrines. Moreover, patients with metastatic disease have high levels of metanephrines corresponding to the tumor burden. Also, chromogranin A levels were associated with tumor mass and metastatic disease, especially with secondary liver determinations [11, 13].

3.1 The noradrenergic phenotype

The noradrenergic phenotype consists of tumors producing norepinephrine as the main secretion pattern. The measurement of plasmatic free normetanephrine clinically diagnoses this phenotype. In most cases, these types of tumors are localized in extra-adrenal regions, but some medical reports describe them within the adrenal glands [23].

Tumors secreting predominantly norepinephrine are associated with a lack of signs and symptoms related to catecholamine excess syndrome, and they are more frequently clinically silent. Patients can have sustained hypertension due to norepinephrine's physiological action on the α1 receptors, inducing vasoconstriction. Also, the noradrenergic phenotype can have greater intra-operative hemodynamic instability compared with patients with adrenergic phenotype [23]. Furthermore, α receptor blockage in these patients is the first line of therapy for pre-operative patients' management [32, 33].

Additionally, norepinephrine's vasoconstrictor effect can cause vasospasms of the cerebral, ocular, gastrointestinal, and renal circulation leading to an ischemic episode or stroke, optic neuropathy, intestinal necrosis or ischemia, and renal artery stenosis, respectively. Moreover, norepinephrine cause reduced intestinal motility, leading to constipation, paralytic, ileus, and intestinal pseudo-obstruction. Furthermore, intestinal circulation vasospasms can also lead to decreased intestinal motility with bowel ischemia and gastrointestinal bleeding, increasing the risk of developing colonic perforation and abdominal sepsis [34, 35].

Noradrenergic phenotype is suggestive of mutations in cluster 1 category or the pseudohypoxic pathway, consisting of the next following genes: succinate dehydrogenase subunits SDHx (SDHA, SDHB, SDHC, SDHD), succinate dehydrogenase complex assembly factor 2 (SDHAF2), von Hippel-Lindau tumor suppressor (VHL), egl-9 prolyl hydroxylase 1 and 2 (EGLN1/2), malate dehydrogenase 2 (MDH2), endothelial pas domain protein 1/hypoxia-inducible factor type 2A (EPAS1/HIF2A), fumarate hydratase (FH), and isocitrate dehydrogenase (IDH) [6, 25].

3.2 The adrenergic phenotype

Tumors classified as the adrenergic phenotype are characterized by increased production and secretion of epinephrine. Epinephrine has numerous physiological systemic effects, and it primarily stimulates only β1 and β2 receptors [10].

Patients with Pheos and sympathetic Pgls secreting epinephrine have more frequently paroxysmal symptoms of hypertension, palpitations, headache, flushing, and sweating because of their effect on hemodynamics and metabolism [36]. Moreover, the adrenergic phenotype catecholamines can be associated with a decline in the left ventricular systolic function due to the catecholamine-induced myocarditis, also called pheochromocytoma-associated catecholamine cardiomyopathy [37, 38].

These types of tumors are also well-differentiated, and they are frequently localized within the adrenal gland. Initially, it was presumed that the increased expression of the Phenylethanolamine N-methyltransferase (PNMT) gene is involved in the pathophysiology of adrenergic phenotype, but further studies stated that the presence of glucocorticoids is not ample enough to induce the adrenergic phenotype [20].

Furthermore, adrenergic phenotype tumors are frequently associated with adrenal diabetes and dyslipidemia, caused by epinephrine's metabolic effects [39].

Mutations specific to adrenergic phenotype are grouped into cluster 2, causing activation of kinase signaling pathways. The genes included in cluster 2 are RET proto-oncogene (RET) involved in the development of MEN2 syndrome, neurofibromin 1 (NF1) tumor suppressor gene involved in neurofibromatosis type 1, H-RAS and K-RAS proto-oncogenes, transmembrane protein 127 (TMEM127), chromatin remodeler (ATRX), Myc-associated factor X (MAX), and cold shock domain-containing E1 gene (CSDE1) [31].

Patients presenting with predominantly elevated metanephrines should undergo genetic screening for RET and NF1 mutations for the first genetic approach.

All the patients should have pre-operative preparation with α-blockers or other medications to control hypertension, arrhythmia, and volume expansion [3].

3.3 The dopaminergic phenotype

The dopaminergic phenotype consists of a sporadic group of neuroendocrine tumors that produce and secrete dopamine and its metabolite, 3-methoxytyramine.

Urinary dopamine levels are unreliable markers of this phenotype. Therefore the dopaminergic phenotype can be evaluated by plasmatic determination of dopamine and 3-methoxytyramine levels [7, 40].

However, Pheos and Pgls associated with SDHx mutations can produce and/or secrete dopamine and 3-methoxytyramine.

Tumors of this subgroup are frequently found in extra-adrenal sites and may be malignant. Mainly, carotid body tumors, a specific type of head and neck Pgls, produce dopamine, which is continuously metabolized into its metabolite [41].

Regarding dopamine's physiological roles, it is well known that it acts will on D1 and D2 dopaminergic receptors.

Activation of D1 receptors, located on vascular smooth muscle cells, may lead to arterial renal vasodilatation and stimulation of the gastrointestinal tract. Therefore, studies reported case reports with patients with chronic diarrhea, nausea, vomiting, abdominal pain, weight loss [42].

In contrast, D2 receptors, located in the central nervous system, inhibit norepinephrine secretion, and have a mild negative inotropic effect on the cardiovascular system. This mechanism offers a possible explanation for the absence of hypertension and palpitations in patients with dopaminergic phenotypes [10]. Also, patients can have nausea, emesis, and hypotension.

Furthermore, 3-methoxytyramine, the O-methylated dopamine metabolite, is a biomarker useful for diagnosing extra-adrenal tumors and multifocal disease [7]. Moreover, increased levels are specific to patients with SDHB and SDHD mutations and a highly suggestive risk of malignancy [43].

The main characteristics for these tumors and genotype-phenotype correlations are summarized in **Table 1**.

The leading cause of death in patients with Pheos and Pgls is a metastatic disease that can occur in about 10–20% of cases [44, 45]. The most cited prognostic factors associated with metastasis are extra-adrenal location, a large dimension of

Biochemical phenotype	Hormones	Genetics	Risk of malignancy
Adrenergic	Epinephrine	Cluster 2 category/kinase signaling pathway	Increased risk of malignancy in ATRX gene mutations
Noradrenergic	Norepinephrine	Cluster 1 category/ pseudohypoxic pathway	Increased risk of malignancy in SDHB and SDHD gene mutations
Dopaminergic	Dopamine and 3-methoxytyramine	SDHB and SDHD mutations	Increased risk of malignancy

Table 1.
Genotype-phenotype correlations.

the primary tumor germline SDHB mutations, ATRX mutation, and catecholamine secretion (noradrenergic or dopaminergic) [6, 16, 46].

4. Peculiarities of pediatric pheochromocytoma

The subgroup of pediatric Pheos and Pgls is still poorly studied, but the latest data stated that they have peculiarities compared to the adult population.

Pediatric Pheos and Pgls have a prevalence of 8–9% in recent studies [47], with a median age between 12 and 14 years, the youngest age reported to date is four years, and a preponderance of boys between 52.7% to 65.5% [48].

In terms of diagnosing algorithms, The European practice guidelines recommend diagnosing Pheos/Pgls plasmatic metanephrines and normetanephrine, 24-hour urinary fractionated metanephrines, and optionally chromogranin A dosing [24].

In the study of [49], the authors reported a high incidence of 70% of genetic causes of Pheos/Pgls, with pathogenic mutation, detected preferably with the use of NGS.

Considering the clinical spectrum of pediatric Pheos, the prevalence of sustained hypertension is more common in children 70% than adults (50%) [50].

Furthermore, a large majority of 70–80% of pediatric catecholamine secreting tumors are functional, making the clinical diagnosis more approachable. Moreover, 10% of the tumors can be malignant, with about 20% found at multifocal sites [50–52]. Subsequently, an increased incidence of extra-adrenal tumors of about 30% was reported in recent studies [48, 49, 53].

In terms of the genetic landscape of pediatric Pheos, to date, ten genes have been described in the medical literature in association with Pheos at a pediatric age: RET, VHL, NF1, SDHD, SDHB, SDHA, FH, MAX, HIF2A, and PHD1 [24]. Thus, clinicians should always bear in mind the high frequency of the next implicated genes: VHL mutations as the most prevalent in pediatric patients ranging from 28.0% to 49.0% of cases, followed by SDHB and SDHD, RET mutations (1.0–5.4% of cases), and NF1 gene mutations (3.0% of cases) [24, 54].

Another important aspect is that about 50% of pediatric Pheos/Pgls can recur, compared with the 15–20% proportion reported in the adult population as a 10-year probability of recurrence [3]. Subsequently, in the pediatric population, a secondary tumor can be diagnosed by 30 years, underling the necessity of proper lifelong monitoring [49, 51].

5. Conclusions

New data on genetic, metabolic, and biochemical alterations of Pheos and Pgls allow us to look for genotype-phenotype correlations.

Depending on biochemical secretory characteristics, Pheos and Pgls can be divided into three different biochemical or secretory phenotypes: adrenergic, noradrenergic, and dopaminergic.

Depending on the affected gene and its activated intracellular signaling pathways, each tumor is clinically different.

Kinase signaling cluster genes are associated with tumors with an adrenergic phenotype consisting of epinephrine secretion. These tumors are mostly adrenal tumors, and they rarely develop metastatic disease, except for those associated with ATRX gene mutations.

Noradrenergic phenotype is suggestive of mutations in the pseudohypoxic pathway genes.

The dopaminergic phenotype consists of a sporadic group of neuroendocrine tumors that produce and secrete dopamine, and they are associated with SDHx mutations.

Regarding pediatric Pheos, the most affected genes are represented by VHL, followed by SDHB, SDHD, and NF1. Knowing the high incidence of germline mutations in the pediatric population, lifelong monitoring of secondary lesions is recommended.

All patients diagnosed with Pheos and Pgls should undergo genetic testing.

Genotype-biochemical phenotype correlations could help in genetic testing decision making.

Further studies are necessary for the complete identification of genotype-specific biochemical markers, which will be important in monitoring disease progression and determining treatment strategies. Furthermore, understanding of the metabolic and genetic basis of Pheos and Pgls will lead to the development of effective forms of therapy for these particular tumors.

Author details

Diana Loreta Paun[1,2] and Alexandra Mirica[1,3]*

1 Carol Davila University of Medicine and Pharmacy, Bucharest, Romania

2 C.I. Parhon National Institute of Endocrinology, Bucharest, Romania

3 Grigore Alexandrescu Clinical Emergency Hospital for Children, Bucharest, Romania

*Address all correspondence to: arix26@yahoo.com

References

[1] Alrezk R, Suarez A, Tena I, Pacak K. Update of Pheochromocytoma Syndromes: Genetics, Biochemical Evaluation, and Imaging. Front Endocrinol (Lausanne). 2018;9(November):1-13.

[2] Albattal S, Alswailem M, Moria Y, Al-Hindi H, Dasouki M, Abouelhoda M, et al. Mutational profile and genotype/phenotype correlation of nonfamilial pheochromocytoma and paraganglioma. Oncotarget. 2019;10(57):5919-5931.

[3] Farrugia FA, charalampopoulos A. Pheochromocytoma. Endocr Regul. 2019;53(3):191-212.

[4] Lenders JWM, Duh QY, Eisenhofer G, Gimenez-Roqueplo AP, Grebe SKG, Murad MH, et al. Pheochromocytoma and paraganglioma: An endocrine society clinical practice guideline. J Clin Endocrinol Metab. 2014;99(6):1915-1942.

[5] Plouin PF, Amar L, Dekkers OM, Fassnach M, Gimenez-Roqueplo AP, Lenders JWM, et al. European Society of Endocrinology Clinical Practice Guideline for long-term follow-up of patients operated on for a phaeochromocytoma or a paraganglioma. Eur J Endocrinol. 2016;174(5):G1-10.

[6] Kimura N, Takekoshi K, Naruse M. RiskStratificationonPheochromocytoma and Paraganglioma from Laboratory and Clinical Medicine. J Clin Med. 2018;7(9):242.

[7] Rao D, Peitzsch M, Prejbisz A, Hanus K, Fassnacht M, Beuschlein F, et al. Plasma methoxytyramine: Clinical utility with metanephrines for diagnosis of pheochromocytoma and paraganglioma. Eur J Endocrinol. 2017;177(2):103-113.

[8] Eisenhofer G, Pacak K, Huynh T, Qin N, Bratslavsky G, Linehan WM, et al. Catecholamine metabolomic and secretory phenotypes in phaeochromocytoma. 2013;18(1):97-111.

[9] Pacak K, Wimalawansa SJ. Pheochromocytoma and Paraganglioma. Endocr Pract. 2015;21(4):406-412.

[10] Zuber SM, Kantorovich V, Pacak K. Hypertension in pheochromocytoma: Characteristics and treatment. Endocrinol Metab Clin North Am. 2011;40(2):295-311.

[11] Mirica A, Badarau IA, Stefanescu AM, Mirica R, Paun S, Andrada D, et al. The Role of Chromogranin A in Adrenal Tumors. REVCHIM(Bucharest). 2018;69(3):34-6.

[12] Bílek R, Vlček P, Šafařík L, Michalský D, Novák K, Dušková J, et al. Chromogranin a in the laboratory diagnosis of pheochromocytoma and paraganglioma. Cancers (Basel). 2019;11(4):1-15.

[13] Mirica A BI et al. Clinical use of plasma chromogranin A in neuroendocrine tumors. Curr Heal Sci J. 2015;41(4):69-76.

[14] Angelousi A, Peppa M, Chrisoulidou A, Alexandraki K, Berthon A, Faucz FR, et al. Malignant pheochromocytomas/paragangliomas and ectopic hormonal secretion: A case series and review of the literature. Cancers (Basel). 2019;11(5).

[15] Stenman A, Zedenius J, Juhlin CC. The value of histological algorithms to predict the malignancy potential of pheochromocytomas and abdominal paragangliomas—A meta-analysis and systematic review of the literature. Cancers (Basel). 2019;11(2).

[16] Main AM, Rossing M, Borgwardt L, Toft BG,

Rasmussen ÅK, Feldt-Rasmussen U. Genotype–phenotype associations in PPGLS in 59 patients with variants in SDHX genes. Endocr Connect. 2020;9(8):793-803.

[17] Toledo RA, Burnichon N, Cascon A, Benn DE, Bayley JP, Welander J, et al. Consensus Statement on next-generation-sequencing-based diagnostic testing of hereditary phaeochromocytomas and paragangliomas. Nat Rev Endocrinol. 2017;13(4):233-247.

[18] Paun DL, Mirica A. Pheochromocytoma a focus on genetic [Internet]. Intech. 2016. 13 p. Available from: https://www.intechopen.com/books/advanced-biometric-technologies/liveness-detection-in-biometrics

[19] Else T. Pheochromocytoma, paraganglioma and genetic syndromes: A historical perspective. Endocr Relat Cancer. 2015;22(4):T147–T159.

[20] Nölting S, Grossman AB. Signaling pathways in pheochromocytomas and paragangliomas: Prospects for future therapies. Endocr Pathol. 2012;23(1):21-33.

[21] Martinelli S, Maggi M, Rapizzi E. Pheochromocytoma/paraganglioma preclinical models: which to use and why? Endocr Connect. 2020;1-26.

[22] Azizi F. Precision medicine for endocrinology. Int J Endocrinol Metab. 2016;14(3):6-8.

[23] Björklund P, Pacak K, Crona J. Precision medicine in pheochromo-cytoma and paraganglioma: current and future concepts. J Intern Med. 2016;280(6):559-573.

[24] Pereira BD, Da Silva TN, Bernardo AT, César R, Luiz HV, Pacak K, et al. A clinical roadmap to investigate the genetic basis of pediatric pheochromocytoma: Which genes should physicians think about? Int J Endocrinol. 2018;2018.

[25] Jochmanova I, Pacak K. Genomic Landscape of Pheochromocytoma and Paraganglioma. Trends in Cancer. 2018;4(1):6-9.

[26] Andrews KA, Ascher DB, Pires DEV, Barnes DR, Vialard L, Casey RT, et al. Tumour risks and genotype-phenotype correlations associated with germline variants in succinate dehydrogenase subunit genes SDHB, SDHC and SDHD. J Med Genet. 2018;55(6):384-394.

[27] Pacak K, Taïeb D. Pheochromocytoma (PHEO) and paraganglioma (PGL). Cancers (Basel). 2019;11(9):2-5.

[28] Ferolla P, Faggiano A, Mansueto G, Avenia N, Cantelmi MG, Giovenali P, et al. The biological characterization of neuroendocrine tumors: The role of neuroendocrine markers. J Endocrinol Invest. 2008;31(3):277-286.

[29] Liu IH, Kunz PL. Biologics in gastrointestinal and pancreatic neuroendocrine tumors. J Gastrointest Oncol. 2017;8(3):457-465.

[30] Canu L, Parenti G, De Filpo G, Mannelli M. Pheochromocytomas and paragangliomas as causes of endocrine hypertension. Front Endocrinol (Lausanne). 2019;10(JUN):1-5.

[31] Pang Y, Liu Y, Pacak K, Yang C. Pheochromocytomas and paragangliomas: From genetic diversity to targeted therapies. Cancers (Basel). 2019;11(4):1-16.

[32] Favier J, Amar L, Gimenez-Roqueplo AP. Paraganglioma and phaeochromocytoma: From genetics to personalized medicine. Nat Rev Endocrinol [Internet]. 2015;11(2):101-111. Available

from: http://dx.doi.org/10.1038/nrendo.2014.188

[33] van der Zee PA, de Boer A. Pheochromocytoma: A review on preoperative treatment with phenoxybenzamine or doxazosin. Neth J Med. 2014;72(4):190-201.

[34] Thosani S, Ayala-Ramirez M, Román-González A, Zhou S, Thosani N, Bisanz A, et al. Constipation: An overlooked, unmanaged symptom of patients with pheochromocytoma and sympathetic paraganglioma. Eur J Endocrinol. 2015;173(3):377-387.

[35] Osinga TE, Kerstens MN, van der Klauw MM, Koornstra JJ, Wolffenbuttel BHR, Links TP, et al. Intestinal pseudo-obstruction as a complication of paragangliomas: Case report and literature review. Neth J Med. 2014;71(10):512-517.

[36] Galetta F, Franzoni F, Bernini G, Poupak F, Carpi A, Cini G, et al. Cardiovascular complications in patients with pheochromocytoma: A mini-review. Biomed Pharmacother [Internet]. 2010;64(7):505-509. Available from: http://dx.doi.org/10.1016/j.biopha.2009.09.014

[37] Choi SY, Cho KI, Han YJ, You GI, Kim JH, Heo JH, et al. Impact of pheochromocytoma on left ventricular hypertrophy and QTc prolongation: Comparison with Takotsubo cardiomyopathy. Korean Circ J. 2014;44(2):89-96.

[38] Kvasnička J, Zelinka T, Petrák O, Rosa J, Štrauch B, Krátká Z, et al. Catecholamines induce left ventricular subclinical systolic dysfunction: A speckle-tracking echocardiography study. Cancers (Basel). 2019;11(3).

[39] Petrák O, Haluzíková D, Kaválková P, Štrauch B, Rosa J, Holaj R, et al. Changes in energy metabolism in pheochromocytoma. J Clin Endocrinol Metab. 2013;98(4):1651-1658.

[40] Grouzmann E, Tschopp O, Triponez F, Matter M, Bilz S, Brändle M, et al. Catecholamine metabolism in paraganglioma and pheochromocytoma: Similar tumors in different sites? PLoS One [Internet]. 2015;10(5):1-18. Available from: http://dx.doi.org/10.1371/journal.pone.0125426

[41] Sriphrapradang C, Choopun K, Tunteeratum A, Sura T. Genotype-phenotype correlation in patients with germline mutations of VHL, RET, SDHB, and SDHD genes: Thai experience. Clin Med Insights Endocrinol Diabetes. 2017;10:1-7.

[42] Mesmar B, Poola- Kella S, Malek R. the Physiology Behind Diabetes Mellitus in Patients With Pheochromocytoma: a Review of the Literature. Endocr Pract [Internet]. 2017;23(8):999-1005. Available from: http://journals.aace.com/doi/10.4158/EP171914.RA

[43] Corssmit EP, Romijn JA. Management of endocrine disease: Clinical management of paragangliomas. Eur J Endocrinol. 2014;171(6):R231–R243.

[44] Gkolfinopoulos S, Tsapakidis K, Papadimitriou K, Papamichael D, Kountourakis P. Chromogranin A as a valid marker in oncology: Clinical application or false hopes? World J Methodol. 2017;7(1):9.

[45] Szalat A, Fraenkel M, Doviner V, Salmon A, Gross DJ. Malignant pheochromocytoma: Predictive factors of malignancy and clinical course in 16 patients at a single tertiary medical center. Endocrine. 2011;39(2):160-166.

[46] Assadipour Y, Sadowski SM, Alimchandani M, Quezado M, Steinberg SM, Nilubol N, et al. SDHB mutation status and tumor size but not

tumor grade are important predictors of clinical outcome in pheochromocytoma and abdominal paraganglioma. Surg (United States). 2017;161(1):230-239.

[47] Cascón A, Inglada-Pérez L, Comino-Méndez I, De Cubas AA, Letón R, Mora J, et al. Genetics of pheochromocytoma and paraganglioma in Spanish pediatric patients. Endocr Relat Cancer. 2013;20(3).

[48] Mishra A, Mehrotra PK, Agarwal G, Agarwal A, Mishra SK. Pediatric and adolescent pheochromocytoma: Clinical presentation and outcome of surgery. Indian Pediatr. 2014;51(4):299-302.

[49] Makri A, Akshintala S, Derse-Anthony C, Del Rivero J, Widemann B, Stratakis CA, et al. Pheochromocytoma in Children and Adolescents with Multiple Endocrine Neoplasia Type 2B. J Clin Endocrinol Metab. 2020;104(1):7-12.

[50] Sarathi V. Characteristics of Pediatric Pheochromocytoma/ paraganglioma. 2020;21(3):470-4.

[51] Tibbetts MD, Wise R, Forbes B, Hedrick HL, Levin A V. Hypertensive retinopathy in a child caused by pheochromocytoma: Identification after a failed school vision screening. J AAPOS [Internet]. 2012;16(1):97-9. Available from: http://dx.doi.org/10.1016/j.jaapos.2011.09.010

[52] de Tersant M, Généré L, Freyçon C, Villebasse S, Abbas R, Barlier A, et al. Pheochromocytoma and Paraganglioma in Children and Adolescents: Experience of the French Society of Pediatric Oncology (SFCE). J Endocr Soc. 2020;4(5):1-12.

[53] Ross JH. Pheochromocytoma: Special considerations in children. Urol Clin North Am. 2000;27(3):393-402.

[54] Bausch B, Wellner U, Bausch D, Schiavi F, Barontini M, Sanso G, et al. Long-term prognosis of patients with pediatric pheochromocytoma. Endocr Relat Cancer. 2014;21(1):17-25.

Chapter 3

Metastatic Paragangliomas and Pheochromocytomas: An Epigenetic View

María-Dolores Chiara, Lucía Celada,

Andrés San José Martinez, Tamara Cubiella,

Enol Álvarez-González and Nuria Valdés

Abstract

Paragangliomas and pheochromocytoma (PPGLs) are hereditary tumors in about 40% of cases. Mutations in the genes encoding for components of the mitochondrial succinate dehydrogenase protein complex (*SDHB*, *SDHD*, *SDHC*) are among the most prevalent. Most PPGLs have a benign behavior, but patients with germline *SDHB* mutations may develop metastatic PPGLs in up to 30% of cases. This suggest that the SDH substrate, succinate, is key for the activation of the metastatic cascade. The last decade has witnessed significant advances in our understanding of how succinate may have oncogenic properties. It is now widely accepted that succinate is an oncometabolite that modifies the epigenetic landscape of SDH-deficient tumors via modulating the activities of DNA and histone modification enzymes. In this chapter, we summarize recent discoveries linking SDH-deficiency and metastasis in SDH-deficient PPGLs via inhibition of DNA methylcytosine dioxygenases, histone demethylases and modified expression of non-coding RNAs. We also highlight promising therapeutic avenues that may be used to counteract epigenetic deregulations.

Keywords: paraganglioma, pheochromocytoma, metastasis, epigenetic, DNA methylation, histone methylation, succinate

1. Introduction

Paragangliomas and pheochromocytomas (PPGLs) are rare neuroendocrine tumors that originate in the diffuse paraganglionic tissue and the adrenal gland, respectively. Approximately 40% of these tumors are hereditary and related to germline mutations in *SDHB, SDHC, SDHA, SDHD* and *SDHAF2* (collectively called *SDHx*), as well as *RET, VHL, NF1, TMEM127, MAX, FH, KIF1B* and *EGLN1* among others [1]. Mutations in genes encoding different subunits of the succinate dehydrogenase (SDH) complex are the most prevalent in hereditary PPGLs being present in about 50% of cases. Among these genes, *SDHB*, *SDHD* and *SDHC* are the most frequently affected. Somatic mutations affecting *SDHx* genes can be also detected in non-hereditary PPGLs [2]. The strong association of *SDHx* mutations and PPGLs reveals that the activity of this mitochondrial complex plays an

essential, and likely unique, role in the neuroendocrine tissues conforming human paraganglia such that its deregulation cause development of neoplasia in these tissues that can, eventually, become metastatic.

One of the peculiarities of PPGLs is that they are generally slow growing, indolent tumors that are not life-threatening. However, 10–30% (according to different studies) of the PPGLs metastasize and once metastasis occurs, treatment options are rather limited and patients have poor prognosis, often with less than 50% surviving at 5 years [3]. Surgery can improve the prognosis but standard chemotherapeutic regimen with cyclophosphamide, vincristine, and dacarbazine, or radionuclide therapy with 131 Iodine-radiolabelled metaiodobenzylguanidine result in only partial responses. Thus, there is still a long road to reach therapeutic improvements. Further challenges for clinicians come from the fact that, in half of the cases, metastases are not present during the initial treatment of the patient but emerge over a period of undetermined time, which may even exceed 10 years after diagnosis of the primary tumor. For this reason, these patients receive long-term, post-treatment surveillance. However, the duration as well as the interval of the follow-up screening is poorly defined. Following these reasonings, the WHO 2017 Classification of Tumors of Endocrine Organs stated that PPGLs should be considered as tumors of undetermined biologic potential and should not be termed benign but should be classified as metastatic or not metastatic [4]. Given that all PPGLs are recognized as exhibiting malignant potential to some extent, the risk for malignant behavior must be determined to be able to pinpoint cases at risk of future metastases directly in the early post-operative period, a knowledge that would have a significant clinical impact.

Despite overwhelming advances in understanding the molecular mechanisms of PPGL development made in the last decade, the factors governing the emergence of metastasis are still very poorly understood. Considerable efforts have been made in identifying histopathological features suggestive of metastatic behavior using pre-defined algorithms. The Pheochromocytoma of the Adrenal Gland Scaled Score (PASS) and the Grading System for Adrenal Pheochromocytoma and Paraganglioma (GAPP), rely on different histopathologic features or on a combination of histopathologic, immunohistochemical (Ki-67 index) and biochemical (catecholamine production) parameters, respectively, as tools to distinguish PPGLs with potential for aggressive behavior [5]. However, these algorithms lack accuracy and have a high degree of inter-observer variability thus complicating their clinical roll-out. Hence, the guiding of therapeutic decision-making by using predictive biomarkers in PPGL patients require in-depth knowledge of the biology of this neoplasia.

2. Epigenetic and SDH-deficiency: a connection with metastatic potential

The metastatic cascade involves a succession of cell phenotypic alterations that spans from the acquisition of local invasive activity, the intravasation of cancer cells into blood and lymphatic vessels, their subsequent extravasation in the parenchyma of distant tissues and finally their growth forming macroscopic tumors. How a primary PPGL-tumor cell becomes metastatic and what are the molecular events involved in this process remain to be known. With the emergence of genomic profiling technologies, single gene/protein or multi-gene "signature"-based assays have been introduced to measure specific molecular pathway deregulations in cancer which could be used as clinically useful biomarkers. In PPGLs' patients, it is well established that the presence of inactivating germline mutations in the

SDHB gene is the most important molecular predictor of malignancy. More than 40% of patients with metastatic PPGLs (especially extra-adrenal tumors) carry germline *SDHB* mutations [6, 7]. Although mutations in other PPGL-predisposing genes, such as *FH*, *SDHC*, *SDHD*, *SDHA,* and *TMEM127* have been found in some patients with metastatic PPGLs, these mutations account for only <5% of cases. The mitochondrial 2-oxoglutarate/malate carrier *SLC25A11* gene has been proposed as a novel gene that can confer a predisposition to metastatic PPGLs but the number of patients harboring *SLC25A11*-germline mutations was rather limited to definitely assigned it a role in metastasis development [8]. Thus, *SDHB* gene germline mutation remains as the most reliable risk factor for metastasis. Nonetheless, metastases are developed in only 30% of the *SDHB*-mutation carriers and it is not known what are the mechanisms that either tip the balance towards the metastatic process or prevent it in these patients. Recent studies have pointed to several cancer-related genetic deregulations in metastatic PPGLs, especially prevalent in *SDHB*-related tumors. These include activation of telomerase and over-expression of genes involved in epithelial to mesenchymal transition [9–11]. However, these molecular alterations have been found in limited number of metastatic PPGLs and it is not known what their role is as triggers of the metastatic process. Aside *SDHB*-related metastatic PPGLs, the specific genetic traits involved in the development of the remaining 60% of metastatic PPGLs are not known. Somatic mutations in *ATRX* and *SETD2* genes, and fusions of *MAML3* gene have been identified in metastatic PPGLs [12, 13].

One of the most relevant hints on the molecular mechanisms involved in metastasis came from the The Cancer Genome Atlas (TCGA) Program. These studies revealed that metastatic *SDHx*-mutated PPGLs do not accumulate more gene mutations at the somatic level than no-metastatic PPGLs [13]. It is now becoming increasingly evident that epigenetic changes play a key role in providing properties to the primary cancer cell that have a major contribution to the metastatic process. Relevant studies revealed that PPGLs, developed in patients with mutations in *SDHx* genes, harbor a DNA hypermethylation phenotype which is not present in PPGLs developed in patients with other genetic backgrounds [14]. Although these variations are commonly found in benign and metastatic *SDHB*-mutated PPGLs, qualitative and/or quantitative deviations could cooperate to set the trigger for metastasis development.

Epigenetics is defined as heritable changes in gene expression that do not involve a change in DNA sequence. Epigenetic changes occur in many types of cancer cells and include DNA methylation, histone modification, and small RNAs. Aberrant hypermethylation can lead to silencing of tumor-suppressor genes, histone modifications control the accessibility of the chromatin and transcriptional activities inside a cell, and microRNAs (miRNAs) can negatively control their target gene expression post-transcriptionally. Herein, we provide a perspective on the recent advances and challenges in our understanding of how epigenetic deregulations may underlie the progression of SDH-deficient PPGLs towards a metastatic disease and highlight promising therapeutic avenues that may be used to counteract those epigenetic deregulations.

3. Succinate: an oncometabolite driving epigenetic deregulation in SDH-deficient PPGLs

The SDH complex links the tricarboxylic acid cycle (TCA) and the mitochondria respiratory chain by the coupling of succinate oxidation to fumarate to the reduction of ubiquinone to ubiquinol at the mitochondrial complex II (**Figure 1**). The
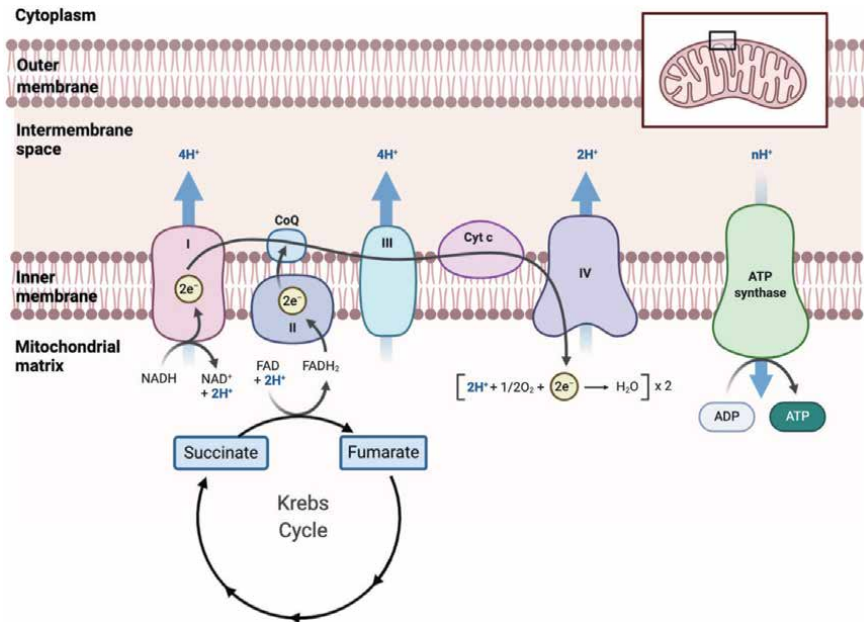
Figure 1.
Schematic representation of the SDH-mediated connection between the Krebs cycle and the mitochondrial respiratory chain. The succinate dehydrogenase complex is part of both, the Krebs cycle at the mitochondria matrix and the mitochondria respiratory chain in the inner mitochondrial membrane. It is composed of four subunits (SDHA, SDHB, SDHC and SDHD) that couples the succinate oxidation to fumarate to the reduction of ubiquinone (coenzyme Q: CoQ) to ubiquinol via FAD at the mitochondrial complex II. The mitochondria respiratory chain consists of four membrane-bound, multimeric protein complexes (complexes I, II, III, and IV) that catalyzes the oxidation of reducing equivalents, mainly nicotinamide adenine dinucleotide (NADH), using the terminal electron acceptor oxygen. This electron transfer is linked to the ATP synthase, which generates ATP.

fumarate/succinate ratio and the redox state of the ubiquinone pool act as signal transducers known to modulate the regulatory programs that control cell fate. Loss of SDH activity leads to dramatic elevation of its natural substrate, succinate. The succinate generated in the mitochondrial matrix is exported to the cytosol where it can inhibit 2-oxoglutarate (2OG)-dependent dioxygenases such as ten-eleven translocation (TET) DNA cytosine-oxidizing enzymes and prolyl hydroxylases (PHD) [15].

PHD enzymes catalyze the prolyl-hydroxylation of the hypoxia-inducible factors HIF1α and HIF2α which transcriptionally regulates HIFα-responsive genes and conform the major hub involved in oxygen-sensing (**Figure 2**). These genes serve to adapt cells to oxygen deficiencies and their over-activation under pathologic conditions may also have pro-tumorigenic activity. HIFα proteins are degraded under physiological conditions by a mechanism requiring active PHD enzymes. PHD-catalyzed prolyl-hydroxylation of HIFα proteins is required by their recognition by VHL, subsequent ubiquitination and proteasomal degradation. Low oxygen levels and succinate repress PHD activities thus leading to the stabilization and functional activation of HIFα proteins. This oxygen-sensing pathway has long been considered a driver mechanism of metastasis in tumors with SDH-deficiencies [16]. However, although HIF1α protein and HIF1α-responsive genes are over-expressed in PPGLs carrying *SDHx* mutations, this signature is much weaker than that of PPGLs carrying *VHL*-loss-of-function mutations which rarely metastasize [17, 18]. Moreover, nuclear HIF2α does accumulate in all paragangliomas of the head and neck which very scarcely develop metastasis. These observations argue against nuclear HIFα
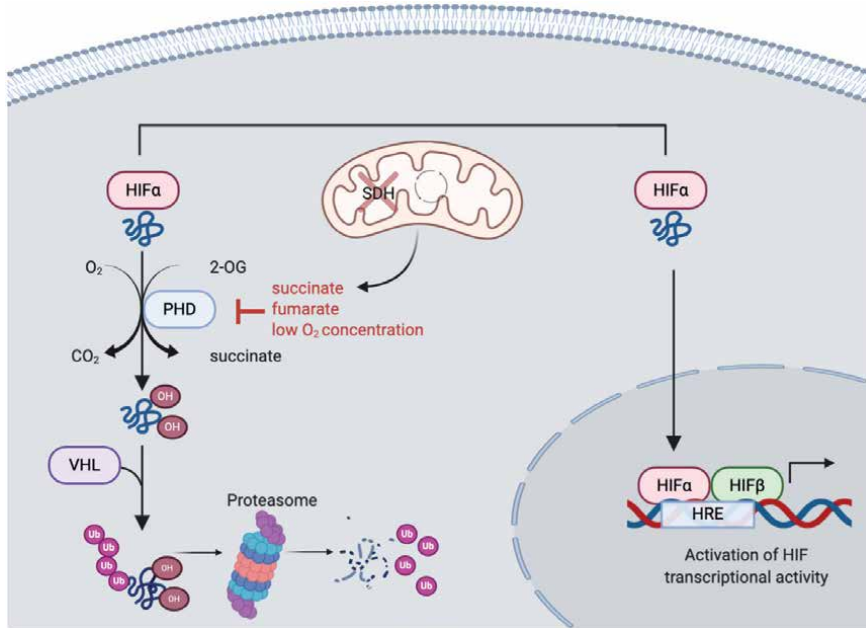
Figure 2.
Oxygen and oncometabolite dependent regulation of HIFα. Under physiological conditions, prolyl hidroxylases (PHD) hydroxylate two proline residues in HIFα subunits thus allowing their recognition by the von Hipple-Lindau protein (VHL). VHL is a component of a ubiquitination protein complex that ubiquitinate (Ub) prolyl-hydroxylated HIFα for degradation by the proteasome. PHDs activity rely on oxygen (O$_2$) and oxoglutarate (2-OG). When oxygen concentration diminishes below physiological levels the activity of PHDs is inhibited leading to the dissociation of VHL from HIFα which results in HIFα stabilization that is transported to the nucleus, binds to HIFβ and activates transcription of target genes by binding to hypoxia-responsive elements (HRE) in their promoter regions. Succinate, as well as fumarate, structurally mimics 2-OG and inhibits PHDs (product inhibition) when present at elevated concentrations, as observed in tumor cells carrying inactivating mutations-driven disfunction of SDH or fumarate hydratase.

proteins as the triggers of malignant transformation of *SDHx*-mutant PPGLs. Further research is required to demonstrate whether any, both or none of the HIFα proteins are required for malignant transformation of PPGLs.

In addition to PHDs, succinate, which can accumulate to millimolar levels in *SDHx*-mutant PPGLs, is a potent inhibitor of TET enzymes and the Jumonji domain-containing histone demethylases [19]. TET enzymes hydroxylate DNA-methylcytosines into 5-hydroxymethylcytosine leading to DNA demethylation. Increased DNA methylation in or near promoter regions, and subsequent decreased gene expression, has been associated with oncogenesis in a number of tumor types including PPGLs carrying *SDHx*-mutations [14]. A role for TET enzymes in this phenotype has been recently demonstrated [20].

In addition to DNA epigenetic alterations, metastasis in PPGLs patients has also been shown to be associated with other epigenetic traits such as aberrant expression of long non-coding RNA (lncRNA) [21] and microRNAs (miRNAs) [22, 23] although these deregulations are not specific of SDH-deficient metastatic PPGLs.

3.1 Succinate-induced DNA hypermethylation

Site-specific DNA hypermethylation in regions of DNA with a high density of cytosine-guanine (CpG) dinucleotides in promoters represent a common feature of the cancer-associated epigenetic landscape. These CpG hypermethylations are linked with repressive chromatin modifications and silencing of tumor suppressor

genes. We discuss here the current understanding of the epigenetic basis of metastasis in *SDHB*-related PPGLs uncovered by our recent studies.

To identify epigenetic alterations relevant for metastasis, we recently performed a comprehensive analysis of DNA methylation in metastatic PPGLs with and without *SDHB* mutations. This analysis revealed that over 1000 genes harbored promoter hypermethylation in the metastatic tumors but not in the not metastatic ones thus suggesting that those gene alterations have a role in the pathogenesis of the metastatic disease linked to *SDHB* mutations [24]. About 15% of these alterations had been also identified in *sdhb–/–* mouse chromaffin cells and in 41% of *SDHx*-mutated PPGLs analyzed by Letouzé et al. [14]. Although these authors did not make distinctions whether the PPGLs were or not metastatic, they did find that hypermethylation was stronger in *SDHB*-PPGLs. Therefore, it is likely that gene
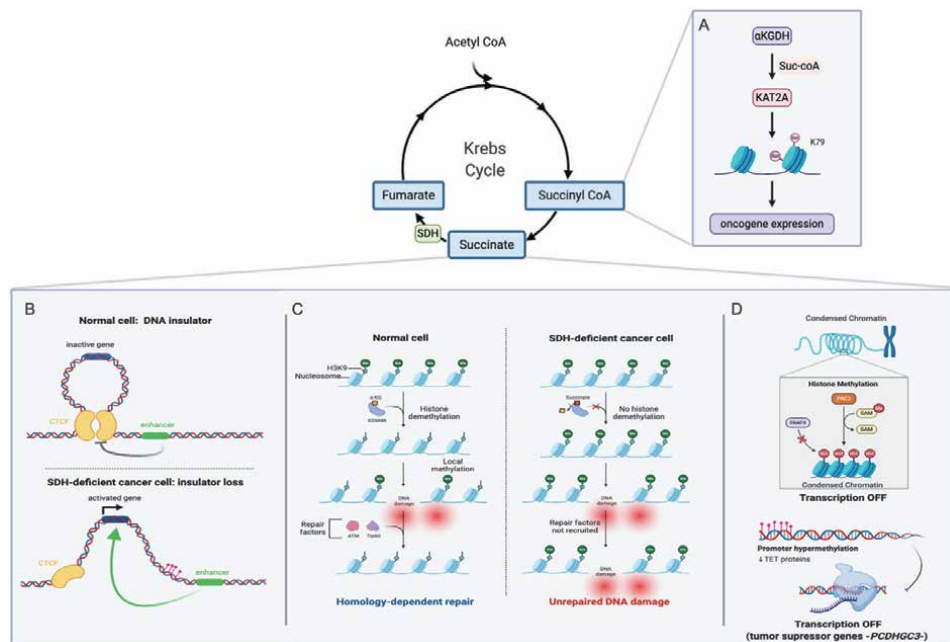

Figure 3.
Outline of the epigenetic changes induced by abnormal succinate accumulation due to SDHx-mutations. Mutations of the SDHx genes in PPGLs cause blockage of SDH activity and subsequent abnormal succinate and succinyl-CoA accumulation. Increased levels of succinate induce inhibition of 2-oxoglutarate-dependent dioxygenases such as TET enzymes and the Jumonji domain-containing histone demethylases leading to activation or repression of gene transcription. TET enzymes hydroxylate DNA-methylcytosines into 5-hydroxymethylcytosine leading to DNA demethylation. Increased DNA methylation due to impaired TET enzyme functions in or near promoter regions induces decreased gene transcription (D) that, when affects tumor suppressor genes, such as PCDHGC3, may trigger different aspects of the metastatic programs. Gene expression can also be inhibited by succinate-induced inhibition of Jumonji domain-containing histone demethylases that remove the methyl group on lysine in histone tails. Histone methylation occurs by the transfer of methyl groups from the methyl donor S-adenosylmethionine (SAM) to amino acids of histone proteins. This protein modification can either increase or decrease transcription of genes, depending on which amino acids are methylated, and how many methyl groups are attached. Succinate inhibition of demethylation of trimethylated-H3K27 by the Polycomb complex (PRC2) induce gene silencing and chromatin condensation (D). (C) Succinate also represses homology-dependent DNA repair by inhibiting the H3K9 demethylase, leading to global elevation of trimethylated H3K9 chromatin marks at loci surrounding DNA breaks. This masks a local H3K9 trimethylation signal that is essential for the proper execution of homology-dependent DNA repair. (A, B) Apart from repression of gene expression, abnormal succinate accumulation may induce gene transcription. This occurs when DNA methylation affects CTCF insulators which prevents CTCF binding to CTCF binding sites, CTCF dimerization and the assembly of long-range chromatin looping. This provokes promiscuous enhancer-promoter interactions and the subsequent induction of the affected genes (B). (A) Increased succinyl-CoA levels induce succinylation of histones associated with enhanced in vitro transcription. The figure shows the enzymatic succinylation of histone via the KAT2A histone succinyltransferase which associates with α-ketoglutarate dehydrogenase (α-KGDH).

mutations in *SDHB* induce epigenetic programs that may be involved in tumors initiation and others involved in metastasis development.

Gene set enrichment analysis revealed that the hypermethylated promoters in metastatic *SDHB*-mutated PPGLs were associated with developmental genes that are preferential targets of the polycomb repressive complex 2, PRC2. PRC2 catalyzes the mono-methylation, di-methylation and tri-methylation of histone H3 at lysine 27 required for PRC2-mediated gene silencing and for maintaining cellular identity during differentiation and development [25]. Specifically, PRC2 occupies a special set of developmental genes in embryonic stem cells that must be repressed to maintain pluripotency and that are poised for activation during cell differentiation. In cancer, aberrant promoter hypermethylation, or PRC-mediated repression, can inhibit differentiation programs, such that cancer cells are arrested at a proliferative state [26] (see **Figure 3**). In agreement with these observations, increasingly, metabolites, such as succinate, are recognized as important modulators of the regulatory programs that control cell fate [27]. Thus, it is tempting to speculate that the succinate 'oncometabolite' plays an essential role in the epigenetic reprogramming of chromaffin cells such that, when reaching high enough levels, induces the transit of mature differentiated cells towards a less differentiated state that allow them to proliferate and generate a tumor mass. This could provide an explanation for tumorigenesis in SDH-deficient tumors. However, it cannot explain why some SDH-deficient PPGLs acquire metastatic fitness, but others do not. The identification of an epigenetic signature specific for metastatic SDH-deficient PPGLs, but not present in SDH-PPGLs that do not develop metastasis, provides some clues. Our recent study revealed that, in addition to the epigenetic changes in developmentally regulated genes, high level hypermethylation of genes involved in homophilic cell-to-cell adhesion was present in metastatic but not in non-metastatic PPGLs *SDHB*-mutated PPGLs. Loss of cell–cell adhesion is a hallmark of metastatic cells required for the transformation of immobile cells into motile cells providing them the ability to invade local tissues leading to metastasis at distant organs. Among these hypermethylated genes, we identified *CNTN2*, *SDK1*, *TENM1*, *TENM4* encoding neuronal cell adhesion molecules involved in the establishment of connections in the nervous system. More strikingly, the cell–cell adhesion set of hypermethylated genes included a 1 Mb-long chromosomal region that hold clustered protocadherin genes [designated as *PCDHA*, *PCDHB* and *PCDHG* (collectively, *PCDHs*)] encompassing 50 different genes at the chromosomal locus 5q31.3 [24] (**Figure 4**). One of the *PCDH* genes, *PCDHGC3*, has been further analyzed and found to be of clinical relevance in metastatic *SDHB*-mutated PPGLs.

3.2 Long-range hypermethylation of clustered protocadherin genes in metastatic *SDHB*-mutated PPGLs

PCDH genes, organized into three closely linked gene clusters (*PCDHA*, *PCDHB* and *PCDHG*), span nearly 1 million base pairs [28] (**Figure 4**). The *PCDHA* and *PCDHG* clusters are organized into variable and constant exons. The generation of full-length *PCDHA* and *PCDHG* messenger RNA requires RNA splicing of each variable exon to three constant exons. Each of the variable exon promoters are randomly activated in individual neurons to generate individual cell-specific patterns of *PCDH* gene expression. In contrast, *PCDHB* mRNA consists of only the variable exon. These genes are involved in the regulation of neural development and engage in homophilic/heterophilic trans-interactions as multimers acting as cell-surface molecular barcodes [29–33]. Their unique genomic organization makes them sensitive to long range epigenetic silencing (LRES). Several recent studies have revealed that epigenetic silencing of clustered *PCDHs* is
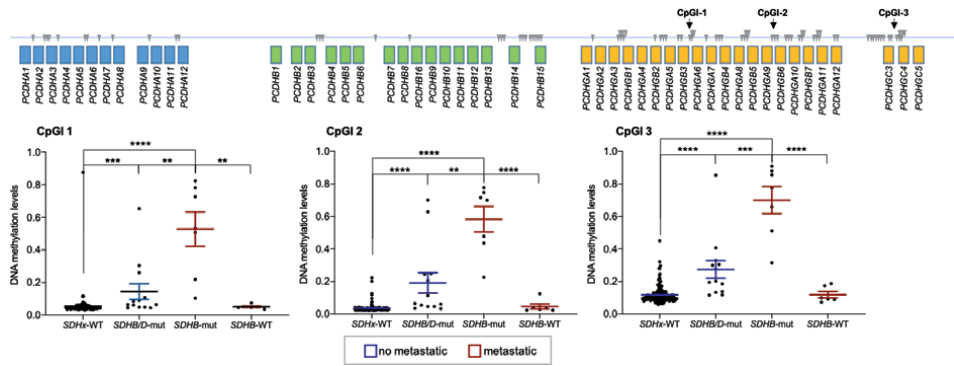
Figure 4.
High level long-range hypermethylation of the clustered PCDH genes in metastatic SDHx-mutated PPGLs. Schematic representation of the genomic organization of the clustered PCDHA, PCDHB and PCDHG genes. For PCDHA and PCDHG genes, only the first exons (blue and orange rectangles, respectively) are represented. For PCDHB genes, rectangles represent the whole gene. Inverted gray triangles point to CpG hypermethylation sites detected in the SDHx-mutated PPGLs included in the TCGA database. Graphics represent DNA methylation levels of the indicated CpG islands (CpGI) according to their genotype. Data from patients without or with metastasis are represented in blue and red, respectively. SDHx-WT: PPGLs lacking mutations in any of the SDHx genes (include PPGLs with and without mutations in other PPGL-susceptibility genes); SDHB/D-Mut: Metastatic PPGLs from patients with germline mutations in SDHB or SDHD genes; SDHB-Mut: PPGLs from patients with germline mutations in SDHB genes; SDHB-WT: Metastatic PPGLs lacking mutations in SDHB genes. ** P < 0.01; *** P < 0.001; **** P < 0.0001.

present in various human malignant tumors, such as Wilms tumor, neuroblastoma, breast, prostate, colon cancer, gastric and biliary tract cancers, and astrocytoma suggesting that this process plays roles in regulating cancer development and/or progression [34–37]. By using one of the largest cohorts of epigenetically studied *SDHB*-mutated PPGLs, we have recently found that the epigenetic silencing of one of the clustered *PCDH* genes, *PCDHGC3*, is putatively involved in the metastatic behavior of these tumors [24]. Methylation of *PCDHGC3* promoter were found to be null in normal paraganglia, null or low in most *SDHB*-mutated PPGLs that do not metastasize, high in *SDHB*-mutated metastatic PPGLs, and much higher in the metastatic tissues derived from these tumors. Similar findings have been reported in colorectal cancer, showing that *PCDHGC3* is methylated and silenced during the adenoma-to-carcinoma transition [37]. These data suggest that this epigenetic trait is progressively amplified during the transformation of the tumor cells from benign state to the invasive and metastatic states, as suggested for other oncogenes and tumor suppressor genes [38].

We also found that, not only *PCDHGC3*, but the other clustered *PCDH* genes are highly methylated in metastatic SDHx-mutated PPGLs. Indeed, the *in-silico* analysis of DNA methylation data reported by TCGA confirmed the hypermethylation of the clustered *PCDH* genes (**Figure 4**) in *SDHx*-mutated PPGLs and allowed further analysis of this phenomena. As in our report, methylation of different CpG islands were detected in the three clustered *PCDHs*, being more highly enriched in the *PCDHG* cluster. **Figure 4** shows analysis of three different CpG regions in that cluster revealing that, similarly to our findings in *PCDHGC3* promoter region, methylation levels were higher in *SDHx*-mutated PPGLs than in PPGLs that did not harbor *SDHx* mutations. More importantly, among the *SDHB*-mutated PPGLs, those having a metastatic behavior had a significantly higher levels of methylation than tumors that had not developed metastasis at the last follow-up date. Analysis of the RNAseq data confirmed the epigenetic silencing of, not only *PCDHGC3* [24], but also *PCDHGC4* gene (**Figure 5**). The *PCDHGC4* mRNA levels were found significantly decreased in *SDHx*-mutated PPGLs as compared with tumors with other
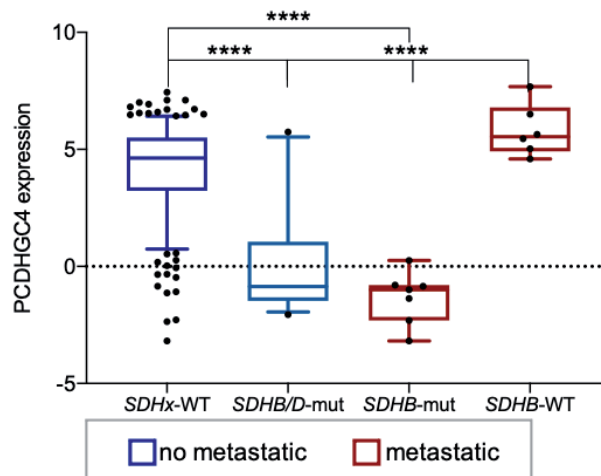
Figure 5.
*PCDHGC4 gene silencing in SDHB-mutated PPGLs that developed metastasis. PCDHGC4 mRNA levels in metastatic (red) and not-metastatic (blue) PPGLs included in the TCGA database are represented according to their genotype. SDHx-WT: PPGLs lacking mutations in any of the SDHx genes (include PPGLs with and without mutations in other PPGL-susceptibility genes); SDHB/D-Mut: PPGLs from patients with germline mutations in SDHB or SDHD genes; SDHB-Mut: Metastatic PPGLs from patients with germline mutations in SDHB genes; SDHB-WT: Metastatic PPGLs lacking mutations in SDHB genes. **** P < 0.0001.*

genotypes. More importantly, downregulation was significantly more dramatic in metastatic than in benign *SDHx*-mutated tumors. Thus, the corrupted epigenetic changes in this chromosomal region seems to amplify the positive selection of the most metastatic cells and the evolutionary capacity of cancer to spread out of the tissue of origin. Interestingly, only the PCDHGC4 isoform, among the clustered PCDH proteins, have been shown to be strictly required for postnatal viability and survival of many neuronal subsets [39].

Consistent with previous findings in colon cancer cell lines [37], we found in that decreased *PCDHGC3* gene expression in two different cancer cell lines resulted in significant increases in cell proliferation, cell migration, and collective cell invasion. Silencing of *PCDHGC3* gene also resulted in increased tumor growth in studies of xenograft tumor models *in vivo*. Consistent with this, the current published data showed that PCDHs regulate pathways for cell proliferation and death. In tumor tissues derived from PPGLs, loss of *PCDH* expression is an indicator of poor prognosis, as revealed by our data and the *in silico* analysis of published data. Importantly, in *SDHB*-mutated metastatic PPGLs with high levels of *PCDHGC3* methylation, diagnosis of primary tumor and metastatic disease was synchronous in most cases, but some patients had a metastasis-free time ranging from 1 to 19 years. Thus, it is possible that epigenetic alterations of *PCDHGC3* during tumor initiation do not automatically lead to the manifestation of full metastatic potential. Rather, metastatic potential likely evolves through quantitative amplification, ultimately providing the cell with metastatic fitness. Thus, *PCDHGC3* acts as a tumor suppressor gene in PPGLs, could be an efficient biomarker of malignancy, and could represent a novel target for personalized medicine.

Targeting any of the protocadherin genes is challenging given that they are highly expressed in nervous system where exert relevant functions for the establishment and maintenance of specific neuronal connections. It is imperative, thus, to unravel the signaling pathways downstream *PCDHGC3* to identify potential therapeutic targets activated in the absence of *PCDHGC3* expression. Current published data have shown that PCDHs are tightly linked to several major signaling pathways, including the Wnt/β-catenin and receptor tyrosine kinase signaling

pathways [40–44]. In renal cancer cell lines, we have found that *PCDHGC3* loss of expression associates with increased mTOR activity. Several reports have shown activation of the mTOR pathway in PPGLs [45]. In addition, inhibition of this pathway exerts potent antitumor activity in a rat model of pheochromocytoma [46]. The epigenetic silencing of *PCDHGC3* could, thus, serve as a biomarker for the selection of patients appropriate for therapeutic options targeting the mTOR pathway.

3.3 Succinate-induced histone methylation

Gene expression can also be altered by changes in chromatin structure via chemical modification of amino acids on histone tails. Accumulation of high levels of succinate in SDH-deficient PPGLs inhibits JmjC domain-containing histone demethylases (KDMs) [19, 47, 48]. These KDMs remove the methyl group on lysine in histone tails, which can either activate or repress transcription depending on the specifically modified lysine residues. Generally, H3K4, H3K36 and H3K79 methylations are considered to mark active transcription, whereas H3K9, H3K27 and H4K20 methylations are thought to be associated with silenced chromatin states [49].

Succinate increases methylation of H3K27 and H3K79 [19]. Trimethylation of H3K27 is a hallmark of repressed transcription. It is tightly associated with inactive gene promoters and also the gene promoters that were found hypermethylated in *SDHB*-mutated metastatic PPGLs. Instead, H3K79 methylation is linked to active transcription and may influence transcription elongation and genomic stability [50] (**Figure 4**).

Succinate induces inhibition of the activities of KDM4A which remove methylation on histone 3 lysine 9 (H3K9) [51, 52]. H3K9 methylation is the mark of heterochromatin, which is the condensed, transcriptionally inactive state of chromatin. Importantly, Sulkowski et al. have recently shown that increased succinate levels, induced by SDH silencing, can also repress homology-dependent DNA repair (HDR) by directly inhibiting the H3K9 demethylase KDM4B, leading to global elevation of trimethylated H3K9 chromatin marks at loci surrounding DNA breaks. This masks a local H3K9 trimethylation signal that is essential for the proper execution of HDR [51] (**Figure 4**). This finding underscores the notion that decreased DNA repair acts as a key oncogenic mechanism in SDH-deficient PPGLs, similarly to the underlying mechanisms of the familial breast and ovarian cancer predisposition syndromes linked to the *BRCA1* and *BRCA2* genes.

3.4 Succinate-induced loss of insulators

DNA hypermethylation outside of gene promoters may also have significant impacts on PPGL pathophysiology, especially when hypermethylation occurs at the CCCTC-binding factor (CTCF) insulators. Insulators are DNA regulatory elements that block the interaction between gene enhancers and gene promoters. They block the spreading of enhancers action and thus insulate, or shield, gene promoters from unwanted regulation [53, 54]. CTCF dimerization, when it is bound to different DNA sequences, mediates long-range chromatin looping allowing the insulation of promoters from enhancer sequences (**Figure 4**). Many proto-oncogenes are isolated in such domains and thus protected from promiscuous enhancer interactions. The CTCF insulator is methylation-sensitive and may be displaced by DNA methylation. DNA hypermethylation at CTCF insulators is traduced in promiscuous enhancer-promoter interactions with the subsequent induction of the affected genes [53, 55].

Recent studies of SDH-deficient gastrointestinal stromal tumors (GISTs) have uncovered the frequent hypermethylation of CTCF insulators where DNA methylation replaces CTCF binding [55, 56]. This ubiquitous insulator losses leads SDH-deficient cells to acquire promiscuous enhancer-promoter interactions and an altered genome topology promoting expression of genes such as *FGF4* or *KIT* involved in the oncogenic programs activated in GIST. This discovery raises the interesting possibility that SDH-deficiency in PPGLs may drive oncogenic programs, in the absence of DNA mutations, by epigenetic modifications that alter genome topology and the enhancer/promoter functions.

3.5 Succinate-induced protein succinylation

SDH inactivation induces accumulation of the immediate upstream metabolite, succinyl-CoA. Succinyl-CoA is the substrate used for the succinylation of proteins, in which succinyl group is transferred to a lysine residue of a protein. It is a recently identified common and widespread posttranslational modification that directly couples TCA cycle metabolism, via succinyl-CoA, to alterations in the structures and activities of proteins involved in diverse cellular processes [57].

Lysine succinylation can occur by a non-enzymatic chemical reaction. This suggests that the abundance of succinyl-CoA would be one of the main governing factors of protein succinylation. A recent study have demonstrated that knockdown of *SDHB* leads to global lysine hyper-succinylation in multiple cellular compartments, especially mitochondria, coupled with increased succinyl-CoA levels [58]. Succinate-induced hypersuccinylation results in apoptosis resistance suggesting a relevant role in tumorigenesis and metastasis development. Succinylation can also occur at the nuclei. In this regard, Wang et al. have demonstrated that the lysine acetyltransferase 2A (KAT2A) may also act as a histone succinyltransferase by forming a complex with α-ketoglutarate dehydrogenase (α-KGDH) that catalyzes the conversion of α-ketoglutarate (α-KG) to succinyl-CoA in the promoter regions of genes [59] (**Figure 4**). Indeed, more than one-third of nucleosomes, including histone and non-histone chromatin components, have been shown to be lysine succinylated in the absence of functional SDH activity suggesting that SDH loss has significant effects on chromatin structure and function and subsequent gene expression [60]. These succinyl marks in chromatin coincide with H3K4me3-chromatin marks, but not with H3K27me3-chromatin marks, suggesting that succinylation of chromatin at active gene promoters is functionally meaningful. Histone succinylation induces widespread gene expression changes that promote tumor growth [61, 62]. However, how histone and nonhistone protein succinylation affects tumorigenesis remains largely unexplored and deserve in-depth characterization to unravel their putative involvement in metastasis development in patients with *SDHB*-mutations and to develop drug therapies and targeted agents.

4. microRNA and lncRNA

RNA-based mechanisms of epigenetic regulation are less well understood than mechanisms involved on DNA methylation and histones but have also profound roles in gene regulation, development and tumorigenesis. Several recent studies have analyzed the pattern of expression of non-coding RNAs, including microRNAs (miRNAs) and long-non-coding RNAs (lncRNAs), in metastatic PPGLs.

Mature miRNAs (~22 nucleotides long) base-pair with target mRNAs to inhibit translation or direct mRNA degradation. Several studies have shown over-expression of miR-183 in metastatic compared with non-metastatic PPGLs, irrespective of

the genotype of the tumor [23, 63]. Higher levels of miR-483-5p have been also in metastatic tumors compared with benign tumors [23, 64]. Given the rarity of PPGLs, in general, and of metastatic PPGLs with *SDHB* mutations, in particular, the putative involvement of SDH-deficiency mediated miRNA deregulation in metastasis development is yet unknown.

miR-210 is one of the best characterized miRNAs downstream HIF1α activation and a candidate tumor-driver of metabolic reprogramming in cancer [65]. Some studies have proposed that up-regulation of miR-210 is a hallmark of the *VHL/SDHx*-mutated PPGLs [66] whereas others have ascribed it a role exclusively in *VHL*-mutated tumors [18]. One of the targets of miR-210 is the gene that codifies the iron–sulfur cluster assembly enzyme (*ISCU*) required for the assembly of maturation of Fe-S clusters, critical bioinorganic prosthetic groups essential for electron transport and multiple metabolic processes [67]. The miR-210-*ISCU* signaling pathway, a hallmark of the HIF activation in cancer, is activated in *SDHx* and *VHL*-mutated PPGLs [18]. However, the role of miR-210 in metastasis predisposition of *SDHB*-mutated PPGLs is not known. A recent report showed that the serum levels of miR-210 are decreased in metastatic PPGLs [68] although these data were grounded in a very limited number of samples and has not been confirmed in publicly available databases. For example, *in silico* analysis of the TCGA database confirms previous reports showing that miR-210 is highly over-expressed in *VHL*-mutated PPGLs and moderately up-regulated in *SDHB*-PPGLs although this was independent on whether the tumor had or not metastatic behavior (**Figure 6**). Similarly, *ISCU* mRNA levels more dramatically decreased in *VHL*-mutated than in *SDHx*-mutated PPGLs. Among *SDHB*-mutated PPGLs, the differences of *ISCU* levels were not significant enough to assign it a role as biomarker of metastasis development. miR-210 was not found over-expressed, neither was *ISCU* under-expressed, in tumors carrying somatic mutations of the gene encoding the HIF2α subunit (*EPAS1*) of the HIF transcription factor thus confirming previous reports showing that this miRNA is a substrate of HIF1α but not HIF2α [69], at least, in the context of paraganglionar tissues. Thus, the available data suggest that miR-210 should not be used as a biomarker of metastatic *SDHB*-mutated PPGLs.
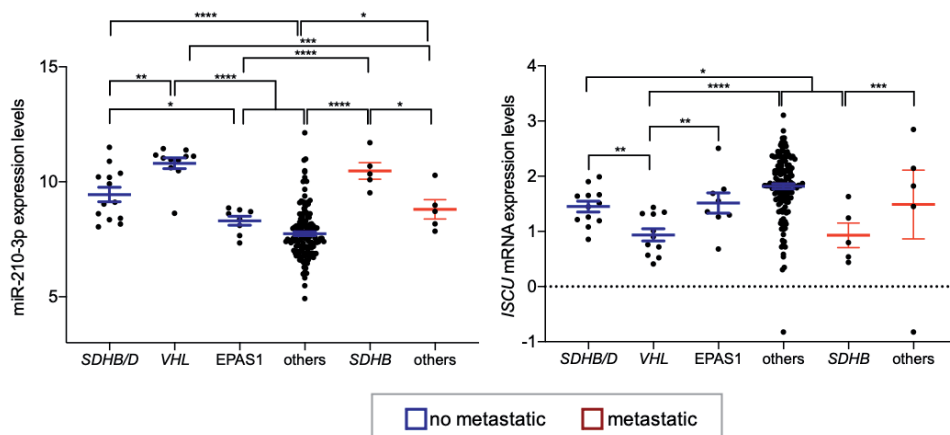
Figure 6.
miR-210-ISCU signaling is moderately activated in SDHx-mutated PPGLs irrespective of their benign or metastatic behavior. miR-210-3p and ISCU levels in PPGLs included in the TCGA database are represented according to their genotype. Data from patients without or with metastasis are represented in blue and red, respectively. SDHB/D: PPGLs from patients with germline mutations in SDHB or SDHD genes; VHL: PPGLs with mutations in VHL; EPAS1: PPGLs with mutations in EPAS1; others: PPGLs with or without mutations in other PPGL-susceptibility genes; SDHB: metastatic PPGLs from patients with germline mutations in SDHB gene; **** P < 0.0001.

lncRNAs are usually defined as non-coding RNAs greater than 200 nucleotides [70]. Although their functions are not well understood they seem to have key roles in gene regulation which depend on their localization and their specific interactions with DNA, RNA and proteins. Their tissue-specific and condition-specific expression patterns suggest that lncRNAs could be potential biomarkers. Recent reports described DGCR9, FENDRR, HIF1A-AS2, MIR210HG [71] and BC063866 [21] with significantly elevated expression in metastatic compared to benign PPGLs. Expression of BC063866 was found significantly elevated in *SDHx*-mutated metastatic PPGLs and, if validated in larger series, could be a novel biomarker to identify potentially metastatic tumors in patients carrying *SDHB* mutation.

5. Epigenetic drugs as therapeutic strategies for patients with metastatic PPGLs

Among epigenetic drugs, despite their limitations, DNA methyltransferase (DNMT) inhibitors are the most effective epigenetic therapy developed to date. Azacitidine and decitabine are cytidine analogues that incorporate themselves into replicating DNA and inhibit DNMTs. This implies that these inhibitors have broad cellular effects leading to global loss of DNA methylation. Hence their use as epigenetic drugs have to deal with strategies to minimize the off-target effects. The use of effective methods for drug delivery reduces side effects and attains a higher therapeutic index. There are various delivery systems like nanocarriers (nanogels, liposomes, dendrimers, and polymeric nanoparticles) that enhance drug stability, permeability and retention. Low doses have received regulatory approval for the treatment of myelodysplastic syndrome and acute myeloid leukemia who are not candidates for conventional induction chemotherapy. The use of the DNMT inhibitor, guadecitabine, is currently been evaluated in patients with PPGLs associated with SDH-deficiency under phase II clinical trial.

Other epigenetic drugs include the inhibitors of histone-lysine methyltransferases [72]. Multiple PRC2 inhibitors are currently being evaluated in ongoing phase I/II clinical trials in a range of cancers [73]. Most hypermethylated genes in metastatic *SDHB*-mutated PPGLs are PRC2 targets thus suggesting that patients could be benefited by the use of these epigenetic drugs [24].

The findings that overproduction of succinate suppresses HDR provide a mechanistic basis for the use novel effective strategies to exploit these defects for therapeutic gain. HDR repression in SDH-deficient tumors enhances cellular dependence on alternative, poly [ADP-ribose] polymerase (PARP) dependent DNA repair mechanisms, which appears to offer a compelling opportunity for targeted therapeutic intervention in oncometabolite-driven cancers. A large body of scientific evidence and clinical trials led to FDA approval of PARP inhibitor monotherapy for the treatment of various cancers harboring mutations in HDR machinery, including those with BRCA1/2 loss [74]. It should be explored whether the HDR defect conferred by succinate accumulation is strong enough to put into practice this therapeutic strategy in SDH-deficient driven cancers. One interesting possibility will be to add DNA-damaging therapies to PARP antagonists to maximize therapeutic efficacy. Notably, the PARP inhibitor olaparib in combination with temozolamide is currently undergoing testing in phase II clinical study in metastatic PPGLs.

Hypersuccinylation can also be a target of therapy in metastatic PPGLs. Succinyl-CoA accumulated in SDH-deficient tumors can be condensed with glycine by D-aminolevulinate synthase 1 to form 5-aminolevulinate and enter the heme biosynthesis pathway. Therefore, glycine supplementation may facilitate removal of succinyl-CoA and inhibit succinylation. Relief of hypersuccinylation by glycine

supplementation, has been shown to result in inhibited growth of hypersuccinylated tumors [59], thus shedding lights on alternative approaches for *SDHx*-mutated-PPGLs.

6. Conclusions

Metastasis is the most letal attribute of PPGLs, especially in patients with compromised SDH activity. Since the initial discovery of succinate as an oncometabolite that induces DNA hypermethylation, the knowledges that illustrate its role on epigenetic reprogramming and metastasis development continues to expand. The best characterized changes, DNA and histone methylation, could be efficiently and globally neutralized by DNA or histone hypomethylating agents, well-known epi-drugs that could be tested as single- or multi-drug therapy in metastatic SDH-deficient PPGLs. The activity of these epigenetic therapies, however, is not limited to cancer cells but have broad cellular effects leading to global loss of DNA methylation and off-target effects. Emerging scientific knowledges on the impacts that succinate-induced modification of the epigenetic code has on cancer development and progression is certainly empowering the research community to develop more effective, less toxic, and better tolerated therapies.

Acknowledgements

Conflict of interest

There are not conflict of interest.

Notes/thanks/other declarations

L.C. thanks the Spanish Ministerio de Ciencia, Innovación y Universidades for the FPU predoctoral contract. T.C. thanks to the Red Temática de Investigación Cooperativa en Cáncer, CIBERONC, Instituto de Salud Carlos III (ISCIII) for her contract. A.S.J.M. thanks to Principado de Asturias and Fondo Europeo de Desarrollo Regional (GRUPIN) for his contract. **Figures 1**–**3** were created with BioRender.com.

Acronyms and abbreviations

DNMT	DNA methyltransferase
HDR	homology-dependent DNA repair
LRES	Long-range epigenetic silencing
PARP	poly [ADP-ribose] polymerase
PPGL	paraganglioma and pheochromocytoma
PRC2	polycomb repressive complex 2
SDH	succinate dehydrogenase
TCA	tricarboxylic acid cycle
TCGA	The cancer genome atlas

Author details

María-Dolores Chiara[1,2,3*], Lucía Celada[1,3], Andrés San José Martinez[1],
Tamara Cubiella[1,3], Enol Álvarez-González[1,2,4] and Nuria Valdés[1,5]

1 Institute of Sanitary Research of Principality of Asturias, Oviedo, Spain

2 Institute of Oncology of the Principality of Asturias, University of Oviedo,
Oviedo, Spain

3 CIBERONC, Madrid, Spain

4 Department of Functional Biology, University of Oviedo, Oviedo, Spain

5 Section of Endocrinology and Nutrition, Hospital Universitario de Cabueñes,
Gijón, Spain

*Address all correspondence to: mdchiara.uo@uniovi.es

IntechOpen

References

[1] Buffet A, Burnichon N, Favier J, Gimenez-Roqueplo AP. An overview of 20 years of genetic studies in pheochromocytoma and paraganglioma. Best Practice and Research: Clinical Endocrinology and Metabolism. 2020;34(2):101416. DOI: 10.1016/j.beem.2020.101416

[2] Weber A, Hoffmann MM, Neumann HPH, Erlic Z. Somatic Mutation Analysis of the SDHB, SDHC, SDHD, and RET Genes in the Clinical Assessment of Sporadic and Hereditary Pheochromocytoma. Horm Cancer. 2012;3(4):187-192. DOI: 10.1007/s12672-012-0113-y

[3] Hamidi O. Metastatic pheochromocytoma and paraganglioma: recent advances in prognosis and management . Current Opinion in Endocrinology, Diabetes and Obesity. 2019;26(3):146-154. DOI: 10.1097/MED.0000000000000476

[4] Lam AK yin. Update on Adrenal Tumours in 2017 World Health Organization (WHO) of Endocrine Tumours . Endocrine Pathology. 2017; 28(3):213-227. DOI: 10.1007/s12022-017-9484-5

[5] Wachtel H, Hutchens T, Baraban E, Schwartz LE, Montone K, Baloch Z, et al. Predicting metastatic potential in pheochromocytoma and paraganglioma: A comparison of PASS and GAPP scoring systems. J Clin Endocrinol Metab . 2020;105(12). DOI: 10.1210/clinem/dgaa608

[6] Lee H, Jeong S, Yu Y, Kang J, Sun H, Rhee JK, et al. Risk of metastatic pheochromocytoma and paraganglioma in SDHx mutation carriers: A systematic review and updated meta-analysis. Journal of Medical Genetics. 2020;57(4):217-225. DOI: 10.1136/jmedgenet-2019-106324

[7] Crona J, Lamarca A, Ghosal S, Welin S, Skogseid B, Pacak K. Genotype-phenotype correlations in pheochromocytoma and paraganglioma: A systematic review and individual patient meta-analysis. Endocr Relat Cancer. 2019;26(5):539-550. DOI: 10.1530/ERC-19-0024

[8] Buffet A, Morin A, Castro-Vega L-J, Habarou F, Lussey-Lepoutre C, Letouzé E, et al. Germline Mutations in the Mitochondrial 2-Oxoglutarate/Malate Carrier SLC25A11 Gene Confer a Predisposition to Metastatic Paragangliomas. Cancer Res. 2018;78(8):1914-1922. DOI: 10.1158/0008-5472.can-17-2463

[9] Job S, Draskovic I, Burnichon N, Buffet A, Cros J ôme, Lepine C, et al. Telomerase activation and ATRX mutations are independent risk factors for metastatic pheochromocytoma and paraganglioma. Clin Cancer Res . 2019;25(2):760-770. DOI: 10.1158/1078-0432.CCR-18-0139

[10] Luo Z, Li J, Qin Y, Ma Y, Liang X, Xian J, et al. Differential expression of human telomerase catalytic subunit mRNA by in situ hybridization in pheochromocytomas. Endocr Pathol. 2006;17(4):387-398. DOI: 10.1007/s12022-006-0010-4

[11] Vezzosi D, Bouisson M, Escourrou G, Laurell H, Selves J, Seguin P, et al. Clinical utility of telomerase for the diagnosis of malignant well-differentiated endocrine tumours. Clin Endocrinol (Oxf). 2006;64(1):63-67. DOI: 10.1111/j.1365-2265.2005.02417.x

[12] Suh YJ, Choe JY, Park HJ. Malignancy in Pheochromocytoma or Paraganglioma: Integrative Analysis of 176 Cases in TCGA. Endocr Pathol. 2017;28(2):159-164. DOI: 10.1007/s12022-017-9479-2

[13] Fishbein L, Leshchiner I, Walter V, Danilova L, Robertson AG, Johnson AR, et al. Comprehensive Molecular Characterization of Pheochromocytoma and Paraganglioma. Cancer Cell. 2017;31(2):181-193. DOI: 10.1016/j.ccell.2017.01.001

[14] Letouzé E, Martinelli C, Loriot C, Burnichon N, Abermil N, Ottolenghi C, et al. SDH Mutations Establish a Hypermethylator Phenotype in Paraganglioma. Cancer Cell. 2013;23(6):739-752. DOI: 10.1016/j.ccr.2013.04.018

[15] Losman JA, Koivunen P, Kaelin WG. 2-Oxoglutarate-dependent dioxygenases in cancer. Nature Reviews Cancer. 2020;20(12):710-726. DOI: 10.1038/s41568-020-00303-3

[16] Pollard PJ, El-Bahrawy M, Poulsom R, Elia G, Killick P, Kelly G, et al. Expression of HIF-1α, HIF-2α (EPAS1), and their target genes in paraganglioma and pheochromocytoma with VHL and SDH mutations. J Clin Endocrinol Metab. 2006;91(11):4593-4598. DOI: 10.1210/jc.2006-0920

[17] Bernardo-Castiñeira C, Sáenz-de-Santa-María I, Valdés N, Astudillo A, Balbín M, Pitiot AS, et al. Clinical significance and peculiarities of succinate dehydrogenase B and hypoxia inducible factor 1α expression in parasympathetic versus sympathetic paragangliomas. Head Neck. 2019;41(1):79-91. DOI: 10.1002/hed.25386

[18] Merlo A, de Quiros SB, Secades P, Zambrano I, Balbín M, Astudillo A, et al. Identification of a signaling axis HIF-1α/microRNA-210/ISCU independent of SDH mutation that defines a subgroup of head and neck paragangliomas. J Clin Endocrinol Metab. 2012;97(11):E2194-200. DOI: 97(11):E2194-200

[19] Xiao M, Yang H, Xu W, Ma S, Lin H, Zhu H, et al. Inhibition of α-KG-dependent histone and DNA demethylases by fumarate and succinate that are accumulated in mutations of FH and SDH tumor suppressors. Genes Dev. 2012;26(12):1326-1338. DOI: 10.1101/gad.191056.112

[20] Morin A, Goncalves J, Moog S, Castro-Vega LJ, Job S, Buffet A, et al. TET-Mediated Hypermethylation Primes SDH-Deficient Cells for HIF2α-Driven Mesenchymal Transition. Cell Rep. 2020;30(13):4551-4566.e7. DOI: 10.1016/j.celrep.2020.03.022

[21] Job S, Georges A, Burnichon N, Buffet A, Amar L, Bertherat J, et al. Transcriptome Analysis of lncRNAs in Pheochromocytomas and Paragangliomas. J Clin Endocrinol Metab. 2020;105(3):dgz168. DOI: 10.1210/clinem/dgz168

[22] Calsina B, Castro-Vega LJ, Torres-Pérez R, Inglada-Pérez L, Currás-Freixes M, Roldán-Romero JM, et al. Integrative multi-omics analysis identifies a prognostic miRNA signature and a targetable miR-21-3p/TSC2/mTOR axis in metastatic pheochromocytoma/paraganglioma. Theranostics. 2019;9(17):4946-4958. DOI: 10.7150/thno.35458

[23] Patterson E, Webb R, Weisbrod A, Bian B, He M, Zhang L, et al. The microRNA expression changes associated with malignancy and SDHB mutation in pheochromocytoma. Endocr Relat Cancer. 2012;19(2):157-166. DOI: 10.1530/ERC-11-0308

[24] Bernardo-Castiñeira C, Valdés N, Celada L, Martinez ASJ, Sáenz-de-Santa-María I, Bayón GF, et al. Epigenetic Deregulation of Protocadherin PCDHGC3 in Pheochromocytomas/Paragangliomas Associated With SDHB Mutations. J Clin Endocrinol Metab. 2019;104(11):5673-5692.

[25] Khan AA, Lee AJ, Roh TY. Polycomb group protein-mediated

histone modifications during cell differentiation. Epigenomics. Future Medicine. 2015; 7(1):75-84. DOI: 10.2217/epi.14.61

[26] Conway E, Healy E, Bracken AP. PRC2 mediated H3K27 methylations in cellular identity and cancer. Current Opinion in Cell Biology. 2015:37:42-48. DOI: 10.1016/j.ceb.2015.10.003

[27] Baksh SC, Finley LWS. Metabolic Coordination of Cell Fate by α-Ketoglutarate-Dependent Dioxygenases. Trends in Cell Biology. 2020;31(1):24-36DOI: 10.1016/j.tcb.2020.09.010

[28] Wu Q, Zhang T, Cheng JF, Kim Y, Grimwood J, Schmutz J, et al. Comparative DNA sequence analysis of mouse and human protocadherin gene clusters. Genome Research. 2001;11(3):389-404. DOI: 10.1101/gr.167301

[29] Mountoufaris G, Chen W V., Hirabayashi Y, O'Keeffe S, Chevee M, Nwakeze CL, et al. Multicluster Pcdh diversity is required for mouse olfactory neural circuit assembly. Science. 2017;356(6336):411-414. DOI: 10.1126/science.aai8801

[30] Thu CA, Chen W V., Rubinstein R, Chevee M, Wolcott HN, Felsovalyi KO, et al. Single-cell identity generated by combinatorial homophilic interactions between α, β, and γ protocadherins. Cell. 2014;158(5):1045-1059. DOI: 10.1016/j.cell.2014.07.012

[31] Chen W V., Maniatis T. Clustered protocadherins. De . 2013;140(16):3297-3302. DOI: 10.1242/dev.090621

[32] Chen W V., Alvarez FJ, Lefebvre JL, Friedman B, Nwakeze C, Geiman E, et al. Functional significance of isoform diversification in the protocadherin gamma gene cluster. Neuron. 2012;75(3):402-409. DOI: 10.1016/j.neuron.2012.06.039

[33] Lefebvre JL, Kostadinov D, Chen W V., Maniatis T, Sanes JR. Protocadherins mediate dendritic self-avoidance in the mammalian nervous system. Nature. 2012;488(7412):517-521. DOI: 10.1038/nature11305

[34] Wang KH, Lin CJ, Liu CJ, Liu DW, Huang RL, Ding DC, et al. Global methylation silencing of clustered proto-cadherin genes in cervical cancer: Serving as diagnostic markers comparable to HPV. Cancer Med. 2015;4(1):43-55. DOI: 10.1002/cam4.335

[35] Vega-Benedetti AF, Loi E, Moi L, Blois S, Fadda A, Antonelli M, et al. Clustered protocadherins methylation alterations in cancer. Clin Epigenetics. 2019;11(1):100. DOI: 10.1186/s13148-019-0695-0

[36] Banelli B, Brigati C, Di Vinci A, Casciano I, Forlani A, Borz L, et al. A pyrosequencing assay for the quantitative methylation analysis of the PCDHB gene cluster, the major factor in neuroblastoma methylator phenotype. Lab Investig. 2012;92(3):458-465. DOI: 10.1038/labinvest.2011.169

[37] Dallosso AR, Øster B, Greenhough A, Thorsen K, Curry TJ, Owen C, et al. Long-range epigenetic silencing of chromosome 5q31 protocadherins is involved in early and late stages of colorectal tumorigenesis through modulation of oncogenic pathways. Oncogene. 2012;31(40):4409-4419. DOI: 10.1038/onc.2011.609

[38] Vanharanta S, Massagué J. Origins of Metastatic Traits. Cancer Cell. 2013;24(4):410-421. DOI: 10.1016/j.ccr.2013.09.007

[39] Garrett AM, Bosch PJ, Steffen DM, Fuller LC, Marcucci CG, Koch AA, et al. CRISPR/Cas9 interrogation of the mouse Pcdhg gene cluster reveals a crucial isoform-specific role for

Pcdhgc4. PLoS Genet. 2019;15(12). DOI: 10.1371/journal.pgen.1008554

[40] Garrett AM, Schreiner D, Lobas MA, Weiner JA. γ-Protocadherins Control Cortical Dendrite Arborization by Regulating the Activity of a FAK/PKC/MARCKS Signaling Pathway. Neuron. 2012;74(2):269-276. DOI: 10.1016/j.neuron.2012.01.028

[41] Chen J, Lu Y, Meng S, Han MH, Lin C, Wang X. α- and γ-protocadherins negatively regulate PYK2. J Biol Chem. 2009;284(5):2880-2890. DOI: 10.1074/jbc.M807417200

[42] Suo L, Lu H, Ying G, Capecchi MR, Wu Q. Protocadherin clusters and cell adhesion kinase regulate dendrite complexity through Rho GTPase. J Mol Cell Biol. 2012;4(6):362-376. DOI: 10.1093/jmcb/mjs034

[43] Keeler AB, Schreiner D, Weiner JA. Protein kinase C phosphorylation of a γ-protocadherin C-terminal lipid binding domain regulates focal adhesion kinase inhibition and dendrite arborization. J Biol Chem. 2015;290(34):20674-20686. DOI: 10.1074/jbc.M115.642306

[44] Keeler AB, Molumby MJ, Weiner JA. Protocadherins branch out: Multiple roles in dendrite development . Cell Adhesion and Migration. 2015;9(3):214-226. DOI: 10.1080/19336918.2014.1000069

[45] Oudijk L, Papathomas T, De Krijger R, Korpershoek E, Gimenez-Roqueplo AP, Favier J, et al. The mTORC1 Complex Is Significantly Overactivated in SDHX -Mutated Paragangliomas. Neuroendocrinology. 2017;105(4):384-393. DOI: 10.1159/000455864

[46] Zhang X, Wang X, Qin L, Xu T, Zhu Z, Zhong S, et al. The dual mTORC1 and mTORC2 inhibitor PP242 shows strong antitumor activity in a pheochromocytoma PC12 cell tumor model. Urology. 2015;85(1):273.e1-273.

e7. DOI: 10.1016/j.urology.2014.09.020

[47] Cervera AM, Bayley JP, Devilee P, McCreath KJ. Inhibition of succinate dehydrogenase dysregulates histone modification in mammalian cells. Mol Cancer. 2009;8:89. DOI: 10.1186/1476-4598-8-89

[48] Smith EH, Janknecht R, Maher JL. Succinate inhibition of α-ketoglutarate-dependent enzymes in a yeast model of paraganglioma. Hum Mol Genet. 2007;16(24):3136-3148. DOI: 10.1093/hmg/ddm275

[49] Hyun K, Jeon J, Park K, Kim J. Writing, erasing and reading histone lysine methylations. Experimental and Molecular Medicine. 2017;49(4):e324. DOI: 10.1038/emm.2017.11

[50] Ljungman M, Parks L, Hulbatte R, Bedi K. The role of H3K79 methylation in transcription and the DNA damage response. Mutation Research. 2019;780:48-54. DOI: 10.1016/j.mrrev.2017.11.001

[51] Sulkowski PL, Oeck S, Dow J, Economos NG, Mirfakhraie L, Liu Y, et al. Oncometabolites suppress DNA repair by disrupting local chromatin signalling. Nature. 2020;582(7813):586-591. DOI: 10.1038/s41586-020-2363-0

[52] Savani MR, Abdullah KG, McBrayer SK. Amplifying the Noise: Oncometabolites Mask an Epigenetic Signal of DNA Damage. Mol Cell . 2020;79(3):368-370. DOI: 10.1016/j.molcel.2020.07.014

[53] Flavahan WA, Drier Y, Liau BB, Gillespie SM, Venteicher AS, Stemmer-Rachamimov AO, et al. Insulator dysfunction and oncogene activation in IDH mutant gliomas. Nature. 2016;529(7584):110-114. DOI: 10.1038/nature16490

[54] Özdemir I, Gambetta MC. The role of insulation in patterning gene

expression. Genes. 2019;10(10):767. DOI: 10.3390/genes10100767

[55] Flavahan WA, Drier Y, Johnstone SE, Hemming ML, Tarjan DR, Hegazi E, et al. Altered chromosomal topology drives oncogenic programs in SDH-deficient GISTs. Nature. 2019;575(7781):229-233. DOI: 10.1038/s41586-019-1668-3

[56] Zhao Y, Feng F, Guo QH, Wang YP, Zhao R. Role of succinate dehydrogenase deficiency and oncometabolites in gastrointestinal stromal tumors. World Journal of Gastroenterology. 2020;26(34):5074-5089. DOI: 10.3748/WJG.V26.I34.5074

[57] Zhang Z, Tan M, Xie Z, Dai L, Chen Y, Zhao Y. Identification of lysine succinylation as a new post-translational modification. Nat Chem Biol . 2011;7(1):58-63. DOI: 10.1038/nchembio.495

[58] Li F, He X, Ye D, Lin Y, Yu H, Yao C, et al. NADP+-IDH Mutations Promote Hypersuccinylation that Impairs Mitochondria Respiration and Induces Apoptosis Resistance. Mol Cell. 2015;60(4):661-675. DOI: 10.1016/j.molcel.2015.10.017

[59] Wang Y, Guo YR, Liu K, Yin Z, Liu R, Xia Y, et al. KAT2A coupled with the α-KGDH complex acts as a histone H3 succinyltransferase. Nature. 2017;552(7684):273-277. DOI: 10.1038/nature25003

[60] Smestad J, Erber L, Chen Y, Maher LJ. Chromatin Succinylation Correlates with Active Gene Expression and Is Perturbed by Defective TCA Cycle Metabolism. iScience. 2018;2:63-75. DOI: 10.1016/j.isci.2018.03.012

[61] Guo Z, Pan F, Peng L, Tian S, Jiao J, Liao L, et al. Systematic Proteome and Lysine Succinylome Analysis Reveals the Enhanced Cell Migration by Hyposuccinylation in Esophageal Squamous Cell Cancer. Mol Cell Proteomics . 2020;mcp.RA120.002150. DOI: 10.1074/mcp.ra120.002150

[62] Yang G, Yuan Y, Yuan H, Wang J, Yun H, Geng Y, et al. Histone acetyltransferase 1 is a succinyltransferase for histones and non-histones and promotes tumorigenesis. EMBO Rep. 2020;e50967. DOI: 10.15252/embr.202050967

[63] Castro-Vega LJ, Letouzé E, Burnichon N, Buffet A, Disderot PH, Khalifa E, et al. Multi-omics analysis defines core genomic alterations in pheochromocytomas and paragangliomas. Nat Commun. 2015;6:6044. DOI: 10.1038/ncomms7044

[64] Meyer-Rochow GY, Jackson NE, Conaglen J V., Whittle DE, Kunnimalaiyaan M, Chen H, et al. MicroRNA profiling of benign and malignant pheochromocytomas identifies novel diagnostic and therapeutic targets. Endocr Relat Cancer. 2010;17(3):835-846. DOI: 10.1677/ERC-10-0142

[65] Bavelloni A, Ramazzotti G, Poli A, Piazzi M, Focaccia E, Blalock W, et al. Mirna-210: A current overview. Anticancer Research. 2017;37(12):6511-6521. DOI: 10.21873/anticanres.12107

[66] Tsang VHM, Dwight T, Benn DE, Meyer-Rochow GY, Gill AJ, Sywak M, et al. Overexpression of miR-210 is associated with SDH-related pheochromocytomas, paragangliomas, and gastrointestinal stromal tumours. Endocr Relat Cancer. 2014;21(3):415-426. DOI: 10.1530/ERC-13-0519

[67] Chan SY, Zhang YY, Hemann C, Mahoney CE, Zweier JL, Loscalzo J. MicroRNA-210 Controls Mitochondrial Metabolism during Hypoxia by Repressing the Iron-Sulfur Cluster Assembly Proteins ISCU1/2. Cell Metab. 2009;10(4):273-284. DOI: 10.1016/j.cmet.2009.08.015

[68] Ruff SM, Ayabe RI, Malekzadeh P, Good ML, Wach MM, Gonzales MK, et al. MicroRNA-210 May Be a Preoperative Biomarker of Malignant Pheochromocytomas and Paragangliomas. J Surg Res. 2019;243:1-7. DOI: 10.1016/j.jss.2019.04.086

[69] Merlo A, Bernardo-Castiñeira C, Sáenz-de-Santa-María I, Pitiot AS, Balbín M, Astudillo A, et al. Role of VHL, HIF1A and SDH on the expression of miR-210: Implications for tumoral pseudo-hypoxic fate. Oncotarget. 2016;8(4):6700-6717. DOI: 10.18632/oncotarget.14265

[70] Ponting CP, Oliver PL, Reik W. Evolution and Functions of Long Noncoding RNAs. Cell. 2009;136(4):629-641. DOI: 10.1016/j.cell.2009.02.006

[71] Ghosal S, Das S, Pang Y, Gonzales MK, Huynh TT, Yang Y, et al. Long intergenic noncoding RNA profiles of pheochromocytoma and paraganglioma: A novel prognostic biomarker. Int J Cancer. 2020;146(8):2326-2335. DOI: 10.1002/ijc.32654

[72] Rugo HS, Jacobs I, Sharma S, Scappaticci F, Paul TA, Jensen-Pergakes K, et al. The Promise for Histone Methyltransferase Inhibitors for Epigenetic Therapy in Clinical Oncology: A Narrative Review. Advances in Therapy. 2020; 37(7):3059-3082 p. 3059-82. DOI: 10.1007/s12325-020-01379-x

[73] Duan R, Du W, Guo W. EZH2: A novel target for cancer treatment. Journal of Hematology and Oncology. 2020;13(1):104. DOI: 10.1186/s13045-020-00937-8

[74] Slade D. PARP and PARG inhibitors in cancer treatment . Genes and Development. 2020;34 (5-6):360-394 p. 360-94. DOI: 10.1101/gad.334516.119

Chapter 4

Surgical Approach in Pheochromocytoma

Radu Mihail Mirica and Sorin Paun

Abstract

Pheochromocytomas are tumors composed of chromaffin cells that can produce, secrete and metabolise catecholamines. The surgical excision procedure of these tumors may present the risk of significant variations in blood pressure, as well as the chance of cardiovascular complications in the perioperative period. During surgery, patients may be at risk for cardiovascular events such as major variations in blood pressure, pulmonary edema, stroke, myocardial infraction and a long period of intubation. The surgical approach to pheochromocytomas must always be preceded by accurate imaging evaluation, endocrine screening and identification of associated genetic mutations. In addition, the surgical technique of choice consists in using minimally invasive surgical methods, with a transabdominal or retroperitoneal approach.

Keywords: pheochromocytomas, adrenalectomy, laparoscopic surgery, epinephrine, transabdominal approach

1. Introduction

Pheochromocytomas are rare tumors composed of chromaffin tissue that can secrete catecholamines in excess (epinephrine, norepinephrine, and dopamine) and their metabolites (metanephrine, normetanephrine, and 3-methoxytyramine). Pheochromocytomas can develop from the chromaffin cells inside the adrenal gland. Moreover, about 80–85% of these neuroendocrine tumors are localized inside the adrenal gland as pheochromocytomas and 15–20% can be extra-adrenal tumors that are named paragangliomas [1–4].

The USA has a pheochromocytoma's annual incidence of 500–1,600 cases per year with equality between genders and a peak incidence in the forth decade of life. The association with hypertension is well known; in the case of patients with hypertension, it is encountered with an incidence of 0.1–0.6% [5]. The classical mode of presentation of a pheochromocytomas case consists of headaches, diaphoresis, flushing and paroxistic hypertension [6].

The latest studies indicate a genetic cause for pheochromocytomas in about 40% of cases, from specific genetic syndromes or de novo mutation [7]. After the biochemical phenotype established, the genetic screening completed, and the imaging investigations performed, the patient has two surgery approaches: through minimally invasive surgical methods or through classical open surgery technique. The surgical method and grade of adrenalectomy can be decided depending on different factors: germline genetic test results, tumor size, body mass index, surgeon experience, and risk of malignancy [1].

The classic surgical methods approaching the adrenal pathology can be transabdominal, transthoracic and retroperitoneal. These include large incisions and extensive plans dissections to offer a reasonable control of vascular pedicles' maneuvers treatment. Usually, this is the critical point for surgical resection due to the difficulty of reaching the vascular branches and the rule of vein first, artery second (preventing releasing the catecholamine into the bloodstream). Postoperative morbidity can be influenced by the type of surgical approach to the adrenal gland. The development of minimally invasive surgery (MIS) techniques has ensured great changes for most surgical procedures. Adrenalectomy is an excellent example of this. This type of pathology fully benefits from the advantages of laparoscopy.

The first laparoscopic adrenalectomy was performed in 1991 by Dr. Lamar Snow, and in 1992 Dr. Joseph Petelin published the first description of the operation. The first laparoscopic adrenalectomy was performed on January 17th, 1992, by a Japanese surgical team led by Go H at Niigata University School of Medicine, Japan [16]. A significant moment in the evolution of laparoscopic adrenal surgery is the publication of the lateral transperitoneal procedure by Michel Gagner in 1992. This later became the most widely used laparoscopic adrenalectomy procedure. Similar to open procedures, the video-assisted approach recognizes three variants, depending on the patient's position and the access: first: anterior approach (transperitoneal), second: lateral approach (transperitoneal or retroperitoneal), and the third one is the posterior approach (retroperitoneal). Soon after it, the laparoscopic adrenalectomy became the second gold standard therapy (after cholecystectomy) in the field of surgery.

The accuracy of new imaging techniques for locating preoperative tumors is necessary because surgical exploration in the blind manner is unlikely to identify any unlocated tumor.

2. Preoperative management

The surgical approach of pheochromocytomas can include significant variations in blood pressure values and cardiovascular events such as arrhythmias and tachycardia can appear in the perioperative patient period.

Intraoperatively, patients undergoing surgical resection can have arrhythmias, sustained hypertension or hypotension and also postoperative myocardial infarction, stroke, pulmonary edema, and prolonged intubation.

Heart failure risk can be influenced by high levels of metanephrines and normetanephrines associated with large tumor size and a longer duration of surgery due to technically difficult surgical excision [8].

Preoperative alpha-blockers ensure a significant decrease in the risk of major hypertensive crises intraoperatively. Patients with pheochromocytoma are systematically examined preoperatively by the cardiologist and anesthesiologist, and the latter will be provided at the time of surgery with all necessary material and drug support (invasive monitoring of BP, central venous catheter, sufficient doses of sodium nitroprusside, etc.) [9].

However, experienced medical specialists (surgeons and endocrinologists) agree that preoperative optimisation must include a seated blood preasure of 120–130/80 mmHg, a standing systolic blood pressure over 90 mmHg, a seated heart rate between 60–70 bpm and a heart rate 70–80 bpm in standing position. In addition, is important to encourage patients to supplement their water intake along with a high sodium diet before surgery [8, 10].

Regarding specific drugs utilized in the preoperative period, Phenoxybenzamine is a non-selective alpha receptor blocker that has been associated with better perioperative hemodynamics parameters, compared with other medication [9].

However, due to the slower onset than selective alpha-blockers such as doxazosin or prazosin it is preferably to be used for 10–14 days instead of 4–7 days. In addition, alpha adrenergic blockers side effects can consists of orthostatic hypotension with secondary tachycardia, palpitation, nasal congestion and headache. In terms of pharmacological actions, alpha adrenergic blockers control volume expansion, minimize the frequency of hypertensive peaks during surgery and control blood pressure values [11, 12].

Furthermore, calcium channel blockers represents a proper variant as a primary drug choice or as an alternative medication. In addition, they can counterbalance coronary vasospasm caused by catecholamines and may induce orthostatic hypotension less frequently than alpha blockers.

Methyrosine is a pharmacological blocking agent of the enzyme tyrosine hydroxylase that inhibits the conversion of tyrosine to dihydroxyphenylalanine, thus blocking the catecholamine synthesis pathway.

This drug can be used in patients who do not tolerate treatment with alpha blockers or is reserved for cases of hypertension refractory to the use of alpha-blockers, beta-blockers and calcium channel blockers [11].

Possible unpleasant side effects of this medication include drowsiness, neurological disorders, and intestinal transit disorders.

In addition, the main medical management approaches are: the expansion of intravascular volume with a saline solution together with the control of hypertension or other cardiovascular events, the correction of metabolic and electrolyte imbalance and the treatment of possible anemia.

Beta-adrenergic receptor blockade with propranolol is used in the treatment of catecholamine induced tachycardia after at least three to four days of alpha blockade administration; beta blockers usage is contraindicated until the alpha-adrenergic receptor blockade is done, in order to prevent severe hypertensive crisis caused by unopposed alpha vasoconstriction [12].

Appropriate and smooth venous access and arterial catheters for continuous blood pressure monitoring must be placed before surgery. Communication between the anesthesiologist and surgeon is essential to ensure safe results. Ideally, the anesthesia team should be prepared to use intravenous vasoactive drugs to manage hemodynamic variations and has to remain vigilant throughout the entire medical-surgical procedure [13].

More than that, the timing of surgical dissection should be coordinated with the anesthesiologist's maneuvers even from the time of pneumoperitoneum inflation – new recordings of blood pressure (BP) of the patient should be registered every minute, according to the gas amount already introduced (until the value of 12 mmHg); if the BP is too high, a lower intraperitoneal pressure should be taken into consideration during the all-time of the procedure. Another example of surgeon-anesthesiologist cooperation can be the proper time of dissection around the gland – touching the gland (with catecholamine release and rapid increase of BP). The surgeon requires rapid measures from the anesthesiologist to control the cardiac output and possible arrhythmias [14–16].

3. Surgical intervention approach

Surgery is the curative therapy for either benign or malignant pheochromocytoma. Morbidity in adrenalectomy operations is about 40% and can be associated

with cardiac events such as arrhythmia, myocardial dysfunction, pulmonary embolism and sepsis. Mortality for adrenalectomy has improved in the last decade, with an under 2% rate of death.

Firstly, the main critical point in adrenalectomy in pheochromocytoma is the minimal manipulation of the tumor to avoid seeding the tumor in adjacent tissues and in order to prevent a hypertensive crisis during the operation (it is said that adrenalectomy should be performed by dissecting away the body from the gland, not the gland from the body). Secondly, another crucial step during the surgical procedure is the control of vascular supply together with the complete tumor resection. All of these can be provided by adequate surgical exposure in order to prevent other organs injuries.

Minimally invasive techniques can be done laparoscopically or robotically. The aim of minimally invasive procedures and open surgical approach is the minimal manipulation of the tumor, in order to prevent catecholamine release as mentioned above; if this is not respected, it can result in hemodynamic instability and tumor rupture.

Also, to diminish the risk of releasing large amounts of hormones, it is indicated to early ligature the adrenal vein. This step can be performed through the transabdominal or posterior surgical approaches.

Furthermore, the surgical approach is dependent on surgeon choise, experience and familiarity with the specific techniques. However, some factors may influence the decision of surgical approach: body mass index, tumor size and location, and patient's personal pathological history of abdominal or retroperitoneal surgical procedures [14].

Our paper will focus mainly on the minimally invasive laparoscopic approach, being the surgical procedure of choice for adrenal tumors, due to its advantages of surgical technique.

The laparoscopic approach includes normal anatomy and easy conversion to open surgery if necessary for exceptional cases [15].

Although the retroperitoneal approach can directly access the adrenal gland and would require less effort to dissect and mobilize nearby visceral organs, this technique is not easy for general surgeons due to lack of familiarity with it. In addition, the contraindications for the retroperitoneal surgical approach include tumors bigger than seven to eight cm due to the narrow working space and an increased body mass index with increased retroperitoneal fat. Simultaneously, a tumor lying around the inferior vena cava (on the right side) or close to the aorta (on the left side) can lead to a complex surgical resection by retroperitoneal access [13].

Retrospective studies from literature have shown that robotic and laparoscopic resection of pheochromocytomas are equivalent in terms of operative time, blood loss volumes, intraoperative hemodynamic events, rates of morbidity and mortality, and rates of conversion from minimally invasive approach to open surgery technique [9].

Furthermore, the main advantages of robotic adrenalectomy include: the three dimensional acces, improved wrist mobilization for the surgeon, and a stable camera port. Disadvantages of robotic adrenal surgery include increased cost, insufficient learning curve and lack of tactile feedback.

When invasive malignant pheochromocytoma is suspected or concerned clinically, open approach is the first choice. Open treatment may benefit from a greater risk of tumor rupture, which may lead to pheochromocytoma disease. For patients with confirmed SDHB mutations, that are associated with a higher metastatic disease rate, the open approach is prefered [16].

For patients with pheochromocytoma associated with different syndromes, minimally invasive or open surgical methods can also be used for cortical sparing

(partial) adrenalectomies. Patients with multiple endocrine tumor 2 (MEN2) or von Hippel–Lindau disease (VHL) syndrome can benefit from cortical-preserving adrenalectomy in order to preserve and to maximize the adrenal function and to avoid chronic glucocorticoids replacement. Furthermore, cortical sparing technique can reduce the risk of Addisonian disease [17].

4. Laparoscopic technique

4.1 Elements of surgical technique and tactics

The operating table must benefit from adequate mobility in order to allow an adequate angulation in order to optimally open the anatomical space from the costal rim to the iliac crest. The operating surgeon and the cameraman are positioned in front of the patient and the assistant on the opposite side. The patient can be placed on the operating table in a lateral decubitus with a 90-degree angle position to ensure the full retraction of the spleen and a partial retraction of the liver by the gravity force.

At the time of pneumoperitoneum installation, the patient is already lying on his side. The Veress needle will be inserted through the abdominal flank, being warned of the risk of visceral (liver or colon on the right side) or vascular (epigastric pedicle branches) injuries. Classic, there are three subcostal ports that can be positioned on the left and one epigastric port that is localized at the inferior margin of the liver. It is not unusual for the first trocar (corresponding to the left mid-clavicular line) to be inserted just a little bit slower than the other three subcostal trocars in order to offer a comprehensive view of the operative field and to identify the entire trajectory of the left colonic flexure (to facilitate the dissection of the colonic ligament for a lower positioning of the colon and to offer a better view over the left adrenal lodge).

For the left adrenalectomy, the spleen can be mobilized till the gastric fundus appears in the visual field, this can allow the spleen to retract more medially. This maneuvers can develop the plane between the spleen and the pancreas' tail, up to the left adrenal gland. The first maneuver is the incision made at the later splenic peritoneum. Further dissection is performed in a relatively avascular plane that is located close to the retropancreatic and anterior to the adrenal and renal capsule. Through this conjunctive structure's transparency, the adrenal tissue specific aspect is easily distinguished as having a specific yellowish color.

Sometimes, it is mandatory to cut the conjunctive tissue between the left colonic flexure (at its highest point) to the abdominal wall and to re-positioning the colon down below the level of the inferior pole of the spleen. After that, a broad view of this area is noticed. More than that, an easy discovery of the kidney superior left pole is possible, and this should be the start to identify (especially on obese patients) the groove between the left kidney and the pancreas – the normal localization of the left adrenal gland. For a pheochromocytoma dissection, the surgical gestures should be delicate, precise, and firm – a proper instrument of dissection should be used (sealing-cutting device, ultrasound device – electrocautery hook is to be avoided by the beginners and is a time-consuming device for an experienced surgeon).

The essential vascular anatomical elements that will be treated in left adrenalectomy are the central vascular pedicle and the upper vascular pedicle. The left central vein (LCV) goes into the left renal vein, most commonly into the common trunk with the lower-left diaphragmatic vein (LLDV), from which it should be disected before injuring or clipping. The sectioning of this common

trunk interpreted as LCV will result in the cranial interception of LLDV; a vascular element misinterpreted as an accessory left central vein. The LCV must be double-clipped to the renal vein, for security reasons, and then sectioned with sharp surgical instrument – the latest surgical devices (like a sealing-cutting instrument with a computerized chip for measuring the impedance and secure the ligation) can be safely used with no clips (depending on surgeon's experience). The left middle adrenal artery comes from the aorta and will be highlighted later. It can be treated by titanium clip or bipolar electrosurgery. By following the upper margin of the adrenal gland, the upper adrenal pedicle branches will be highlighted and treated using an electrocoagulation procedure.

The complete disection of the entire adrenal gland is done by posterior dissection, in a very loose anatomical space, after witch is then separated from the upper renal pole and the muscular abdominal wall (up to the left quadratus lumborum muscle). The final steps of left laparoscopic adrenalectomy are made by the hemostasis, surgery gland extraction and local drainage.

Thoroughly attention should be given to the dissection of the superior part of the adrenal gland near the pancreas' inferior edge because important vessels are lying over there – including end-parts of the splenic vein and the veins' and arteries' network around the pancreatic tail. Finally, pancreatic parenchyma should be carefully avoided to be damaged during dissection to skip a postoperative pancreatic leakage.

For laparoscopic right adrenalectomy, four working trocars (3 of 10 mm and one of 5 mm) are required, arranged on a line parallel to the costal margin, developed between the sub-xiphoid region and the right anatomical flank (below the tip of the right tenth rib). Near the right kidney's upper pole covered by the right hepatic lobe can be found the the right adrenal gland, lying on the diaphragm, in close contact with the IVC. The right triangular ligament is disected, and the right liver lobe is then retracted with the instrument through the epigastric trocar. Displacemant of the right hepatic lobe depends a lot on obtaining a good and comfortable access in the adrenal gland's dissection space. The lifting of the hepatic love is performed by an atraumatic instument, of "snake" type or with atraumatic blades, inserted in the sub-xiphoid trocar. In the particular situation of a highly developed right hepatic lobe, additional maneuvers or additional tools are required to obtain a suitable elevation. A slightly reverse-Trendelenburg position also obtains a better position of the patient on the operating table. These exposure gestures are critical to prevent the application of excessive forces intended to widen the operating field. These traumatic maneuvers can lead to damage to the Glisson capsule and tears of the liver parenchyma. Consecutive bleeding significantly alters the dissection conditions, reducing the surgeon's ability to distinguish the specific appearance of the gland. The crimson-yellow specific gland color is easy to recognise under proper conditions of dissection. The anterior plane of the gland can be exposed by performing a blunt dissection or with the electrocautery. This can be performed in an extracapsular plane, anatomical space occupied by many loose and avascular lax fibrous tissue. The disection plane found between IVC and the right adrenal gland can be exposed. This will be the starting point of the surgical excision of a pheochromocytoma – the surgeon should prioritize the "attack" of the central vein expecially for the right adrenal gland. The arterial sources that approach the gland are anastomosing each other in the next presented way: first the central artery that arises from the aorta, second, the superior arterial pedicle that arises from the right inferior diaphragmatic artery and not the last, the inferior arterial pedicle from the right renal artery. Venous blood can be collected by the homonymous satellite veins, represented by the central vein that is collected directly into the IVC that should be well identified before any maneuver on the adrenal vessels. Any bloody source can

be solved by IVC partial clamping only if it is exposed and have a good control. It is mandatory for a safe treatment of the vascular pedicles and for the achievement of complete glandular removal to have a complete exposure of the entire medial and superior margin of the gland [4, 5].

The central vein can be clipped twice at the inferior vena cava margin and with a single clip to the margin of the gland. In approximately 20% of patients, there can be found a central accessory vein, sometimes this is the cause of difficult to control hemorrhage. Due to the lateral decubitus position, after dissecting the central vein, the IVC is mobilized to the medial, and the retro-IVC extension of the gland can be much easily dissected. The central artery can be dissected and sectioned by the branches with electrocautery. Modern means of electrosurgery (sealing-cutting devices or ultrasonic scalpel) offers additional operating comfort and efficiency, but the need to continuously follow the correct anatomical plans must be emphasized.

A complete mobilization of the gland is achieved by posterior dissection, to or from the side, in a loose fibrous anatomical space which is interposed between the renal upper pole and diaphragm until the aspect of the right quadratus lumborum muscle appears in the operating field. It is mandatory not to touch the adrenal tissue, especially the pheochromocytoma tumor, to avoid spillage the tumor cells in the peritoneal cavity. The piece will be placed in a bag and is extracted by widening one of the access wall brackets (usually the one on the right anterior axillary line). After a thorough control of the hemostasis, a drainage tube beneath the right hepatic lobe is placed for 24–48 hours [4].

For situations in which bilateral excision is required in the same operating session, the patient's position will be changed after removing one of the glands, the entire device is reset to perform the contralateral adrenalectomy.

Although this direction is time-consuming, involves the anesthetic-surgical team's synchronized effort, determines an increased consumption of materials by reorganizing the operating field, the benefit offered by the advantages of the transperitoneal lateral approach is entirely found in operating comfort [6, 7].

For cortical sparing/preservation technique, once the supraadrenal glands are exposed by the mobilization and dissection of the triangular hepatic ligament on the right side and the spleen on the left side, a mass can be seen in the retroperitoneum. Using the best imaging by ultrasound technique to identify the necessary anatomy, surgeons should try to preserve the adrenal veins to allow proper function of the adrenal remnants. It is recomanded to perform an ultrasound examination to assess relationship between the tumor and the adrenal veins and determin whether there are more nodules in patients with genetic predisposition. If there is only one nodule, a harmonic scalpel can be used to remove the nodule. Since the blood vessels of the adrenal gland are highly vigorous, harmonic activation is performed while the jaws are opened, and the adrenal tissue is slowly compressed to provide excellent hemostasis [4].

Do not use any device to grab the nodule or adrenal gland in any position. Grasping the nodule or the adrenal glands with any device may cause a rupture that lead to pheochromocytomatosis. Grasping a portion of adipose tissue located near the adrenal glands or attached to it, or using gentle retraction will give enucleation appropriate exposure. After the nodule is removed, the remaining adrenal glands should be checked for hemostasis. For multiple nodules suitable for removal, the surgeon should consider proceed as before. However, if there are multiple nodules and the restant gland is less than 30% of the total gland, the surgeon should consider total adrenalectomy. The remaining glands may lose function, and the patient may benefit from total adrenalectomy to avoid the need for reoperation of relapse. After the tumor is removed, put the specimen in the bag and take it out [4–7].

Laparoscopic adrenalectomy has been found to reduce the need for hospitalization, blood transfusion, postoperative analgesia and recovery. Laparoscopic adrenalectomy is more difficult to perform on the right side because of the exposure problems, the proximity of the gland to the IVC and the short right adrenal vein. Although there are more and more reports of laparoscopic resection of pheochromocytoma, but it should not be considered for malignant pheochromocytomas or tumors greater than 8 cm [2].

4.2 Posterior retroperitoneal laparoscopic approach

Place the patient in a jack-knife position and place a 1.5–2 cm transverse incision under the terlfth rib to access the retroperitoneum space. Digital palpation can be used to develop and disecting spaces. Guided by the surgeon's index finger, place another trocar along the lateral border of the paraspinous muscle. Similarly, place a side needle under the eleventh rib. Insert another 12 mm blunt balloon trocar into the first incision. When pneumoperitoneum is established, carbon dioxide needs to be injected and kept at 20–24 mmHg. The working space of superior border of the kidney is developed by dissecting the retroperitoneal areolar tissue and Gerota's fascia. After identifying the adrenal veins, dissect the upper adrenal glands laterally and inferiorly, and finally dissect the upper and mid-medial glands. Identify, dissect and remove the adrenal veins between the clamps. The adrenal gland is firstly dissected laterally and inferiorly and secondly the superior and medial adesions are dissected with the evidentiation of the adrenal vein. The adrenal vein is identified, dissected, and resected between clips. The next step is the dissection of the upper attachment, and then put the specimen into the Endo bag device and removed it from the abdomen [2].

4.3 Open techniques

Multiple incisions can be used to exposure the anatomy, including subcostal, midline, and the Makuuchi incision. The aim is to use subcostal incision two to three cm below the costal margin. This incision provides excellent liver and adrenal bed exposure. If a lymph node dissection is planned, the subcostal incision will provide the space betwen aorta and inferior vena cava and between the lymph nodes around the hilum. As with the laparoscopic technique, the triangular ligament on the right is also cut, and the spleen on the left is moved into the retroperitoneal cavity. Very important anatomical landmarks such as inferior vena cava, must be marked on the right, and the tail of the pancreas and the loose plane between the tail and the left adrenal gland on the left must be visualized. For boths sides, the adrenal veins must be identified and cut. Split all remaining attachments and remove the gland. The open transabdominal or thoracoabdominal approaches give the best exposure for resecting extensive tumors, for bilateral adrenalectomy or for metastatic disease [3].

5. Perioperative/postoperative management

Following surgical approach of pheochromocytoma, 80% of patients are suspected to be again normotensive. Persistent postoperative hypertension can be caused by the residual tumor, intraoperative injury to the kidney's renal artery or metastatic disease.

Intraoperative hypotension may be caused by (1) hemorrhage during surgery (2) insufficient hormone replacement after left and right adrenal excision (3) vascular

compliance changes and immediate reduction of catecholamine levels after tumor removal, (4) myocardial infarction (5) long-term residual effects of prolonged α-blockers before surgery. As shown, hypotension can be effectively controlled by replacing volume and blood transfusion. Use vasopressors only when hypotension fails to respond to sufficient volume replacement [16].

Postoperatively, the majority of patients that had an uneventful intraoperative course with or without hemodynamic instability do not necessitate intensive care supervision. In the first postoperative period, the patients that have pheochromocytoma have also a greater risk of hypoglycemia and hypotension [5]. After catecholamines are suddenly stopped, due to the relative increase in insulin sensitivity, hypoglecemia may occur. Therefore, blood glucose must be supervised every hour for the first three or four hours postoerative. When a total adrenalectomy is planned, glucocorticoid preparations can be taken before surgery, specifically for the patients that have bilateral tumors or a familial pheochromocytoma syndrome. After surgery,incidence of hypoglycemia dropped from 15% to 4.2%. Independent predictors related to postoperative hypoglycemia include prolonged operation time and increased urine adrenaline in 24-hour period before surgery. Therefore, glicemia must be checked regularly in the first day after surgery. Isolated episodes of hypotension are very common and can be attribueted to the preoperative alpha blockade residual values, hypovolemia that can be due to intraoperative blood loss or/and preoperative volume contract,. Treatment must be aggressive in terms of IV perfusions and vasopressors [3].

5.1 Postoperative outcomes

The rate of morbidity in untreated pheochromocytoma is very high and difficult to determin. 71% of patients can die from cardiovascular causes: myocardial infarction, hypertensive heart insuiciency, or hemodynamic instability occurring during different procedures [18].

Postoperative good outcomes for cortical-sparing adrenalectomy is focused on preventing a steroid dependency. The benefit of not having a steroid necesity must be compared to the risk of recurrence in time. The necessity of extensive adrenalectomy depends on the genetic or familial predisposition. The patients that have familial syndromes such as MEN 2B, VHL or/and MEN 2A are the ideal candidates for cortical sparing adrenalectomies. Patients with MEN 2A or 2B syndroms who suffered cortical sparing adrenalectomy have a recurrence risk about 51.8% at ten years. The steroid dependency rate of patients who underwent unilateral or/and bilateral cortical sparing technique was 43%. Cortical sparing adrenalectomy is the elective method for patients with VHL syndrome [19].

Patients with different type of pheochromocytomas should have a whole life follow-up program to avoid possible recurrence or the development of metastatic disease, which can occur up to 40 years after resectioning the tumor [17].

6. Particular situations

6.1 Malignant pheochromocytoma

As we all know, about 10% of adrenal pheochromocytomas tumors are malignant, and about 30% of any extra-adrenal tumors are are more commonly malignant. Malignant pheochromocytoma is less frequent in children than in elderly and is mainly at extra-adrenal glands. Pheochromocytomas that are associated with some familial syndromes usually have an early diagnoses and are less malignant than

the sporadic forms. The histological criteria that are used to distinguish benign and malignant forms of the tumors are not very accurate, as it happens in others endocrine or glandular tumors. Malignant tumors depend on the clinical tumoral manifestations and are accurantly diagnosed when there is infiltration of adjacent organs, distant metastasis or recurrence. The most common metastasis occur in bones, local LN, peritoneum, lungs and liver. Malignant tumors are commonly much bigger, with a higher frequency of vascular and capsule infiltration. They are usually characterized by DNA tetraploidy or aneuploidy, increased mitosis, angiogenesis, higher serum levels of neuropeptide Y, tumor necrosis, c-myc expression and higher neuron-specific enolase levels. Most malignant pheochromocytomas show increased uptake of metaiodo-benzylguanidine (MIBG). The survival rate at 5 years, for malignant pheochromocytomas is about 44%. In cases of extra-adrenal localization of pheochromocytomas the prognosis is worse than in adrenal tumors. Patients that have associated pulmonary metastasis have a much worse prognosis [18].

6.2 Pheochromocytoma in pregnancy

There are very common undiagnosed pheochromocytomas during pregnancy, and their maternal and infant mortality rates are very high, up to 58% and 56%. If the diagnosis is madein time, during the pregnancy period, the mortality and morbidity rate can reach below 11%. When the diagnosis is made at the time of delivery, the maternal mortality rate is still high, about 40%. In case of pregnant women the diagnosis of pheochromocytoma can be suspected in case of severe forms of hypertension in the first two months of pregnancy. If hypertension is not controlled in the second trimester, or is related to orthostatic hypotension, or if unexplainable shock occurs suddenly befor delivery, the diagnosis should be focused. The diagnosis as been confirmed by biochemical testing. MRI is the preferred local imaging tehnique to avoid radiation risk. In these cases, the freguently used irritation test is contraindicated, but in some specific cases, the clonidine inhibition test can be used. If the diagnosis is made in first trimester of pregnancy, it is recommended to remove the tumor after proper control of hypertension. In the last trimester of pregnancy, it is recommended to combine pregnancy with selective cesarean C-section intervention and immediate tumor removal under the same anesthesia through medical management. Due to the increased risk of fetal complication and hypertension, spontaneous and vaginal natural delivery methods should be avoided [19].

7. Conclusions/summary

The surgical methods for pheochromocytomas approach must have in priority list the assesment of the best imaging, the identifying any germline genetic mutations, and of course the utilization of any minimally invasive techniques when feasible and indicated. Biochemical diagnosis and precise tumor localization are necessary.

The minimally invasive technique of the abdominal or retroperitoneal approach is the standard surgical method. For large tumors with risk of rupture and potential malignancy, open surgery is recomanded. The results after surgical resection have a real potential to reduce the incidence of cardiovascular disease. Complete surgical resection is the ultimate treatment for benign and malignant pheochromocytoma that have low morbidity and mortality rates.

Special cases of malignant pheochromocytoma or this pathology's occurrence in pregnancy must be suppervised and treated with the utmost care. There are not any very accurate of uniform histological criteria so far, to distinguish malignancy in these cases, which depends on the tumor's clinical behavior.

Conflict of interest

The authors declare no conflict of interest.

Author details

Radu Mihail Mirica[1*] and Sorin Paun[2]

1 Emergency Clinical Hospital 'Saint John', University of Medicine and Pharmacy 'Carol Davila', Bucharest, Romania

2 Emergency Clinical Hospital Bucharest, University of Medicine and Pharmacy 'Carol Davila', Bucharest, Romania

*Address all correspondence to: mirica_rm@yahoo.com

IntechOpen

References

[1] Mirica RM, Ginghina O, Zugravu G, Iosifescu R, Ionescu M. Retroperitoneal Functioning Paraganglioma - A Rare Case of Secondary Diabetes. 2016;(2).

[2] Dhaval Patel Surgical approach to patients with pheochromocytoma Gland Surg. 2020 Feb; 9(1): 32-42. doi: 10.21037/gs.2019.10.20

[3] Hanna NN, Kenady DE. Pheochromocytoma. In: Holzheimer RG, Mannick JA, editors. Surgical Treatment: Evidence-Based and Problem-Oriented. Munich: Zuckschwerdt; 2001.

[4] C. Copãescu Suprarenalectomia laparoscopicã Revista chirurgia 2008. 134:25-29

[5] Laparoscopic bilateral cortical-sparing adrenalectomy for pheochromocytoma. Biteman BR, Randall JA, Brody F.Surg Endosc. 2016 Dec;30(12):5622-5623. doi: 10.1007/s00464-016-4919-5. Epub 2016 May 13th.PMID: 27177950

[6] Lenders JW, Eisenhofer G, Mannelli M, et al. Phaeochromocytoma. Lancet 2005; 366:665-675.

[7] Omura M, Saito J, Yamaguchi K, et al. Prospective study on the prevalence of secondary hypertension among hypertensive patients visiting a general outpatient clinic in Japan. Hypertens Res 2004; 27:193-202.

[8] Babic B, Aufforth R, Patel D, Pediatric patients with pheochromocytoma and paraganglioma should have routine preoperative genetic testing for common susceptibility genes in addition to imaging to detect extra-adrenal and metastatic tumors. Surgery 2017;161:220-227.

[9] Kercher KW, Novitsky YW, Park A, et al. Laparoscopic curative resection of pheochromocytomas. Ann Surg 2005; 241:919-926; discussion 926-8.

[10] Kinney MA, Warner ME, vanHeerden JA, et al. Perianesthetic risks and outcomes of pheochromocytoma and paraganglioma resection. Anesth Analg 2000;91:1118-1123.

[11] Goldstein RE, O'Neill JA Jr, Holcomb GW 3rd, et al. Clinical experience over 48 years with pheochromocytoma. Ann Surg 1999;229:755-764; discussion 764-6.

[12] Brunaud L, Boutami M, Nguyen-Thi PL. Both preoperative alpha and calcium channel blockade impact intraoperative hemodynamic stability similarly in the management of pheochromocytoma.Surgery 2014; 156:1410-1417;

[13] Steinsapir J, Carr AA, Prisant LM. Metyrosine and pheochromocytoma. Arch Intern Med 1997; 157:901-6.

[14] Chen Y, Hodin RA, Pandolfi C. Hypoglycemia after resection of pheochromocytoma. Surgery 2014; 156:1404-1408;

[15] Taskin HE, Berber E. Robotic adrenalectomy. J Surg Oncol 2012;106:622-625.

[16] Gagner M, Lacroix A, Bolte E. Laparoscopic adrenalectomy in Cushing's syndrome and pheochromocytoma.NEnglJMed 1992; 327: 1033.

[17] Go H, Takeda M, Takahashi H, Imai T, Tsutsui T, Mizusawa T, Nishiyama T, Morishita H, Nakajima Y, Sato S Laparoscopic Adrenalectomy for Primary Aldosteronism: A New Operative Method. J Laparoendosc Surg. 1993 Oct; 3(5):455-459.

[18] The role of chromogranin a in adrenal tumors A Mirica, IA Badarau, AM Stefanescu, R Mirica, S Paun, DAC Stefan,Revista de Chimie 69, 678-681

[19] A rare case of a patient with MEN 4 phenotype and associated pheochromocytoma A Mirica, R Petris, R Mirica, S Paun, DL Paun19th European Congress of Endocrinology 49

Section 3

Neuroblastoma

Primary Central Nervous System Neuroblastoma: An Enigmatic Entity

Rakesh Mishra and Amit Agrawal

Abstract

Neuroblastoma is one of the most common solid tumour in the paediatric age group. Central nervous system (CNS) involvement in neuroblastoma is commonly due to metastasis from the extracranial primary. Primary CNS Neuroblastoma (PCNS-NB) is a rare entity and highlights errors in development of neural crest cells and CNS. A lot has been published since the first description of PCNS-NB four decades ago. Over the years, neuroscientists, geneticists, and clinicians have improved the understanding of PCNS-NB. PCNS-NB is an enigmatic entity with variable presentation, epidemiology, clinical features and outcomes. Recent update in knowledge is seen in 2016 WHO classification of CNS tumours with reclassification of CNS neuroblastoma. It further subclassified different histological variants of PCNS-NB and its molecular correlates. Most common histological subtype of PCNS-NB is neuroblastoma followed by ganglioneuroblastoma. Studies support the view that younger age group, less number of lesions, ganglioneuroblastoma histology subtype and surgical management are good prognostic indicators. This chapter provides an updated overview of epidemiology, clinical features, histological and molecular diagnosis, and outcomes of PCNS-NB in addition to the role of adjuvant therapy.

Keywords: Primary central nervous system neuroblastoma, Ganglioneuroblastoma, CNS PNET, CNS Neuroblastoma with FOX-R2, CNS embryonal tumours

1. Introduction

1.1 Background

Neuroblastoma is one of the most common solid extracranial tumour in the paediatric age group. Key characteristics of neuroblastoma include onset at an early age, aggressive behaviour, tendency to metastasize, regress spontaneously in infancy, and variable presentation [1, 2]. Neuroblastoma is associated with grim prognosis with 60% of patients at presentation having only 5–15% chance of long term survival [3]. Most of the cases of central nervous system neuroblastoma are due to metastasis from the extracranial site. Primary central nervous system neuroblastoma (PCNS-NB) is uncommon as metastatic intracranial neuroblastoma (MIC-NB). It is essentialto understand that the manifestation of neuroblastoma varies with the site of origin [4, 5]. Therefore, a PCNS-NB has different epidemiology, clinical features, and outcomes compared to the MIC-NB. There is emerging evidence on various molecular and genetic profiling of neuroblastoma which dominates the clinical

picture. At the end of this chapter, the readers will acquire updated information on the PCNS-NB, various modes of presentation, and treatment outcomes in light of current evidence. Recent research areas, molecular and genetic findings, and areas with gaps of knowledge are also highlights of this chapter.

1.2 History

Horten, and Rubinstein provided the earliest large scale description of 35 cases of PCNS-NB in 1976 [6]. Their description includes the gross description of the tumour, clinical features and management, but lacks the description of the evolution of these tumours. They described three variants of PCNS-NB based on connective tissue stroma and cells with ganglionic differentiation. The classic variant is similar to the peripheral neuroblastoma with relatively high proportions of cells with ganglionic differentiation and high frequency of Homer Wright rosettes. A desmoplastic variant consists of tumours composed of intense connective tissue stroma. A transitional variant consists of tumours with both classical and desmoplastic features [6]. They found 40% to have metastasis along the craniospinal axis at autopsy and reported PCNS-NB to be similar to cerebellar medulloblastoma [6]. Overall three years survival is reported to be 60% and five years survival at 30% [7]. Most of these studies have probably clubbed other tumour types (Medulloblastoma, undifferentiated ependymoma, and sarcoma) in the expectedstandard category of CNS neuroblastoma; hence, they do not provide a precise analysis of this rare entity. Further, most studies on PCNS-NB have variable reporting on the treatment modalities, surgical options, extent of resection, adjuvant chemoradiation and long term outcomes. Therefore PCNS-NB is still one of the least understood neoplasms of the CNS.

1.3 Definition

In 2016 WHO classification of CNS tumours, CNS neuroblastoma is classified under neuronal and paraneuronal tumours with ICD 0 code of 9500/3 [8]. The first four digits of the ICD 0 code indicates the specific histologic term and the fifth digit after/indicates the nature of the tumour with 3 indicating malignant behaviour. Primary central nervous system neuroblastoma (PCNS-NB) is defined as an embryonal tumour with poorly differentiated neuroepithelial cells, groups of neurolytic cells and variable neuropil rich stroma [8]. These tumours carrier grave prognosis and usually portrays aggressive behaviour [4]. Ganglioneuroblastoma is a subtype of neuroblastoma and defined by the International Neuroblastoma Pathology Classification framework based on the Shimada system [9, 10].

1.4 Epidemiology

Neuroblastoma is primarily a neoplastic disease of the peripheral nervous system. Oncologists often describe neuroblastoma as enigmatic heterogenous neoplasia due to its unique features and biological properties of spontaneous regression, aggressive progression and maturation [2, 11, 12]. These variable factors serves as the prognostic factors in the cure and outcome of neuroblastoma [12, 13]. Epidemiology of PCNS-NB differs from the heterogeneous group of neuroblastoma [2]. In general, neuroblastoma is diagnosed most commonly in the first year of life with a median age of diagnosis at 18 months, with 90% of children with neuroblastoma presenting under ten years of age at an estimated prevalence of 25–50 cases per million individuals [14, 15]. However, only cases reports and case series of few patients exist for PCNS-NB. To understand the epidemiology and natural history of PCNS-NB, Lu et al. [16] conducted a population-based study using the SEER

(Surveillance, Epidemiology and End Results) program. The annual incidence of PCNS-NB has shown a downward trend from 1973 to 2013, probably because many of these tumours were earlier labelled as medulloblastoma, undifferentiated ependymoma or sarcoma due to inferior diagnostic methods [16]. As per the SEER program, the annual age-adjusted incidence rate was 0.12 per 1,000,000 persons in 2013 and the incidence decreased with age with peak incidence occurring in infants [16, 17]. No gender or racial variation has been reported for the occurrence of PCNS-NB. In the study by Lu et al. [16], 40.7% of patients belonged to the age group 1–9 years and only 8.2% were of age ≥ 40 years. Mean age of patients in reported literature of PCNS-NB is around five years with slight female preponderance.

1.5 Tumour characteristics

Histologically most common histology of the PCNS-NB is neuroblastoma, followed by ganglioneuroblastoma. In a large population-based study brain (53.6%) was found to be the most common site of PCNS-NB, followed by other nervous system tumours (46.4%). Tumours at sites in the nervous system other than the brain tend to occur in a much younger age group, extensive and more aggressive [16].

1.6 Etiopathogenesis

Neuroblastoma arises from the primitive elements of the neural crest and therefore predominantly affects the neural crest derivatives, i.e. adrenals and sympathetic ganglia. The central nervous system (CNS) can be involved in the form of primary CNS neuroblastoma, CNS metastasis secondary to occult primary, primary intraorbital neuroblastoma from the ciliary ganglion, metastatic neuroblastoma to the orbit, primary intraspinal neuroblastoma originating from dorsal root ganglion, metastatic spinal neuroblastoma and remote paraneoplastic effects such as myoclonic encephalopathy. WHO classification of CNS tumours (2007) enlist CNS-PNET-NOS (not otherwise specified) and four variants of CNS PNET which can be differentiated based on molecular characteristics as CNS neuroblastoma, CNS ganglioneuroblastoma, medulloepithelioma and ependymoblastoma [8]. According to the 2016 WHO classification of CNS tumours, CNS neuroblastoma is classified as an embryonal tumour [8]. CNS-PNET was not found to be a separate entity after the DNA methylation profile of most of the PNET tumours. However, when most well-defined CNS tumours with similar DNA methylation profiles were excluded, there were few unknown tumours, one of which is CNS neuroblastoma [18]. This new molecular entity after DNA methylation was designated as "CNS neuroblastoma with *FOX-R2* activation" (CNS NB-*FOXR2*) [18]. Various studies have elucidated the mechanism for development of CNS disease in a patient of neuroblastoma. Odeone-Filho hypothesised that meningeal surface can act as potential direct pathway for entry of neuroblastoma cells in the CNS, based on a case with CNS neuroblastma in completely controlled systemic disease.

The development of PCNS-NB does not follow two-hit models usually suggested in neuro-oncology. Instead, it results from the persistence of embryonic cell, which should have differentiated or undergone apoptosis during the ordinary course of CNS development. Bcl-2 family of genes regulate apoptosis, and its continued expression appears to play a significant role in the pathogenesis of neuroblastoma and its resistance to chemotherapeutic drugs. Other genetic factors implicated in neuroblastoma development include cytogenetic aberrations in neuro crest development, partial monosomy for the short arm of chromosome 1, and long arms chromosomes 11 and 14. Shimada system of classification of neuroblastoma

Type	Description
I	Neuroblastoma (Schwannoma stroma-poor)
II	Ganglioneuroblastoma, intermixed (Schwannoma stroma-rich)
III	Ganglioneuroma (Schwannoma stroma-dominant)
IV	Ganglioneuroblastoma, nodular (composite schwannoma stroma-rich/stroma-dominant and stroma-poor)
V	NT, unclassifiable

Table 1.
The international neuroblastoma pathology classification of neuroblastoma (Shimada system) [1].

Stage 1	Complete gross excision of localised tumour, with or without positive microscopic margins	Negative ipsilateral non-adherent lymph node(s) (lymph node(s) attached to and removed with the primary tumour may be positive)
Stage 2A	Incomplete gross excision of localised tumour	Negative ipsilateral non-adherent lymph node(s) (lymph node(s) attached to and removed with the primary tumour may be positive)
Stage 2B	Complete or incomplete gross excision of localised tumour	Positive ipsilateral non-adherent lymph node(s); contralateral lymph node(s) negative for tumour
Stage 3	a. Unresectable unilateral tumour infiltrating across the midline OR b. Localised unilateral tumour OR c. Unresectable midline tumour with bilateral extension	a. Positive or negative regional lymph node(s) OR b. Contralateral positive regional lymph node(s) OR c. May be "unresectable" due to positive bilateral lymph node(s)
Stage 4	Any primary tumour with involvement of distant lymph nodes, bone, bone marrow, liver, skin, and/or other organs (except 4S)	
Stage 4S	Any localised primary tumour with involvement of skin, liver, and/or less than 10% of bone marrow cellularity (ONLY applies to children less than 1 year of age)	

Source: [9].

Table 2.
International neuroblastoma staging system.

and International Neuroblastoma Staging System is illustrated in **Tables 1** and **2**, respectively. There are even reports of neuroblastoma occurring post-radiation in children and adults [19–22].

1.7 Clinical features

Patients usually present with features of intracranial mass lesion and raised intra-cranial pressure. Secondary neuroblastoma is mainly extra-axial pathology. It presents as a bony lesion involving the calvaria and extradural mass lesion. However, the lesion can produce haemorrhagic deposits in the parenchyma and increase intracranial

pressure and altered neurological status. Presentation with seizures is not very common. Extra-axial deposits of neuroblastoma present with neurological deficits due to compression of eloquent brain parenchyma. These lesions can also have sutural diastasis due to epidural deposits along the sutures and do not indicate raised intracranial pressure. The status of venous sinuses should be evaluated with CT and MR imaging in patients with sutural diastasis as increased intracranial pressure will show compression of venous sinuses, which will be absent in sutural diastasis due to neuroblastoma deposits [23]. PCNS-NB being intra-axial pathology presents headaches, vomiting, ill localised features, localising features based on cerebral location, and raised intracranial pressure and seizures. Many of these patients present with clinical features on intraventricular mass lesions and hydrocephalus. There can be sudden worsening in the neurological status in the event of a haemorrhage within the lesion.

2. Imaging and histopathology

2.1 Imaging

A typical CT picture of PCNS-NB shows a large intra-axial lesion with calcifications, cystic degeneration and areas of haemorrhage [24]. Perilesional oedema may be limited as compared to the size of the lesion [24]. On post-contrast CT images, uniform enhancement is seen in solid masses, and heterogeneous contrast enhancement is seen in lesions with cystic degeneration and extensive calcifications. Additionally, intraventricular lesions can demonstrate subependymal masses and help in differentiating these lesion from other differential diagnoses of intraventricular mass lesions. MR imaging of these tumours shows inhomogenous intensities on both T1 and T2-weighted images [24]. Areas of calcification and flow voids can be challenging to identify in classical MRI and can be seen well in susceptibility-weighted images (SWI). Different duration of haemorrhage within the lesion can be appreciated well on MR images. On gadolinium-enhanced T1-weighted MR imaging, tumour mass shows inhomogeneous contrast enhancement. Contrast MRI further helps in identifying subependymal enhancement, recurrence around previously operated sites and leptomeningeal spread. Imaging also helps to assess ventricular size as these tumours grow towards the ventricles and many patients develop secondary hydrocephalus. As there are no pathognomonic image findings of PCNS-NB, it should be kept in the differential diagnosis of any patients with the clinical possibility of PCNS-NB and intra-axial, intraventricular or periventricular mass lesion [24]. Primary CNS neuroblastoma is usually intra-axial and spread through CSF pathways, whereas secondary neuroblastoma is mainly extra-axial but can have haemorrhagic deposits in the parenchyma and sutural diastasis on CT due to epidural deposits [23].

2.2 Histopathology

Grossly PCNS-NB tumours are massive, discrete, firm, and cystic in appearance. Histopathology of a newly designated group of tumours as CNS neuroblastoma which were earlier designated as CNS neuroblastoma or CNS ganglioneuroblastoma in 2007 WHO classification scheme [8] showed distinct characteristics. CNS NB-FOXR2 showed an embryonal architecture with small cells and areas of differentiation in neuropil, neurocytic cells and ganglion cells with uniform expression of OLIG2 and neuronal antigen synaptophysin (**Figure 1**) [13, 18]. Histologically ganglioneuroblastoma consists of ganglion cells with different degrees of differentiation, Nerve sheath, glial fibres, and malignant neuroblastoma cells [9, 25–27]. Common pathological picture of ganglioneuroblastoma includes
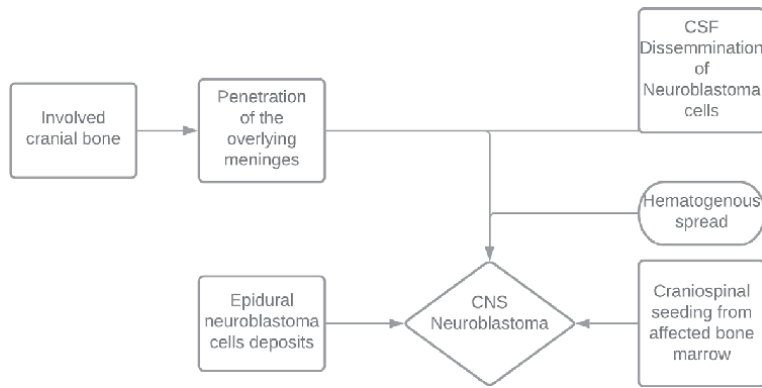
Figure 1.
Various routes for entry of neuroblastoma cells, and its spread to and within CNS.

ganglion cells with a double nucleus, highly infiltrated and proliferated cells with dense chromatin [28, 29]. Further ganglioneuroblastomata have two histological subtypes: undifferentiated type has a small round to oval cells with hyperchromatic nuclei, and poorly differentiated type has a large round to oval spindle-shaped cells with pale staining nuclei [30, 31].

2.3 Discussion

Neuroblastoma is an enigmatic and one of the most common malignant solid tumour of the paediatric age group. Neuroblastoma is a disease with a grim prognosis, and the outcome has not changed significantly in the past two decades. Neuroblastoma teaches us essential aspects of CNS and neural crest development. Primary CNS Neuroblastoma (PCNS-NB) is a rare subtype of neuroblastoma with variable classification. It includes CNS neuroblastoma and ganglioneuroblastoma. In 2016 WHO classification of CNS tumours, PCNS-NB is classified as embryonal tumours. Embryonal tumours with the exception of medulloblastoma has been reclassified based on molecular alterations, for example atypical teratoid rhabdoid tumour (AT/RT) characterised by SMARCB1 or SMARCA4 inactivation, C19MC altered and/or LIN28A expressing embryonal tumour with multi-layered rosettes (ETANTR) and CNS neuroblastoma/Ganglioneuroblastoma without specific histological features or molecular alterations [8]. Based on global transcriptional and methylation profiling four tumour entities have been proposed: CNS neuroblastoma with FOXR2 activation (NB-FOX-R2), High grade neuroepithelial tumour with MN1 alteration (HGNET-MN1), high grade neuroepithelial tumour with BCOR alteration (HGNET-BCOR), and Ewing sarcoma family tumour with CIC alteration (EFT-CIC) [18]. CNS neuroblastoma rarely contains GFAP positive cells which are usually reactive astrocytes and most of the NB-FOX-R2 tumours are neuroblastic differentiation and contains neurocytic cells with poorly differentiated neuropil rich stroma and embryonal architecture [32]. However, there are reports of CNS neuroblastoma with GFAP positive tumour cells demonstrating both neuronal and glial nature, though the clinical significance of such entity is unknown [32]. Since, PCNS-NB is a rare entity and usually present in younger age group, little is known about its treatment protocols, prognostic factors and patient risk stratification. Review of literature suggests that PCNS-NB preferentially occurs in the supratentorial space with involvement of frontal and parietal region [4]. Clinical presentation of PCNS-NB is usually as per the most common site of involvement. Since, most of the PCNS-NB prefers supratentorial location preferably in the frontal and parietal region, patients

usually manifest with focal neurological deficits, bony lesions, irritative symptoms in form of seizures and symptoms of raised intracranial pressure due to mass effect. These effects of raised intracranial pressure and mass effect are less pronounced in infancy in younger children because of compensatory and adaptive mechanism of surrounding brain structures. Metastatic presentation of PCNS-NB is reported only in couple of cases via cervical lymph nodes and cerebrospinal fluid [33]. Therefore in evaluation of PCNS-NB complete screening neuroimaging of whole cranio-spinal neuroaxis should be performed to rule out any metastatic spread through the CSF. In general, PCNS-NB appears like other solid CNS tumours in brain MRI. They can be purely solid or solid-cystic. Solid component of tumours are T1 and T2 hypointense with mild hyperintensity on DWI sequences and inhomogenous contrast enhancement and increased relative cerebral blood volume (rCBV) on perfusion images. Cystic component of tumour appears hyperintense due to hyperproteieic content. MRS sequences show increase in choline peak and inversion of choline/NAA ratio, but none of these imaging parameters are unique to the PCNS-NB. It is essential to understand that there are no tumour markers or radiological markers which can reliably differentiate PCNS-NB from other tumours. Two essential criteria for defining PCNS-NB is presence of classical histology and absence of systemic neuroblastoma.

The outcome of PCNS-NB depends on age, the tumour's aggressiveness, tumour subtype, locations, histology and extension. Surgery is the treatment of choice, and adjuvant radiotherapy improves survival. Safety and outcome of radiotherapy are not well established in infants and younger population but need to be viewed in light of improved survival obtained by adjuvant radiotherapy.

3. Summary and perspectives

3.1 Prognostic factors

Younger age group, a limited number of lesions, ganglioneuroblastoma subtype and surgical management, are found to be positive prognostic factors in PCNS-NB. Neuroblastoma has complex heterogeneous nature with varied prognosis, infants <1 year of age tend to have maximum overall survival with the tumour spontaneously regressing in some infants on the one hand and having widespread metastasis on the other hand [2, 12]. Studies have found best overall survival in infants <1 year of age and relatively less short term adverse events in age > 40 years with a 1-year survival of 57.2% [16].

3.2 Management options

In the population-based studies, patients with extensive disease, multiple lesions, and metastasis were more often offered conservative management as surgical excision was not feasible [16]. Surgical excision is often referred to as the first line of management in the treatment of PCNS-NB, whenever feasible [4]. Differentiation in ganglioneuroblastoma lies in between malignant neuroblastoma and benign ganglioneuroma. Ganglioneuroblastoma subtype is found to be associated with a good prognosis. Studies show that the ganglioneuroblastoma subtype rarely infiltrates and tends to be localised with less incidence of metastatic deposits [16, 34]. This explains that patients with this subtype are likely to be offered surgery and benefit from surgical excision with overall better survival. Ganglioneuroblastoma typically has a high invasive behaviour but slower multiplication rate and the asymptomatic period of up to 60 months has been reported after surgical excision [35, 36].

3.3 Adjuvant radiotherapy

Adjuvant radiotherapy of the primary site is the standard of care in high-risk neuroblastoma patients to reduce the risk of recurrence [6, 37]. Bennett et al. [7] suggested prophylactic irradiation craniospinal axis due to high propensity of CSF metastasis and recurrence of PCNS-NB [6]. However, the role of radiotherapy in PCNS-NB is not well elucidated. This is because the side effects of radiotherapy in the younger age group of radionecrosis and cognitive decline limit its applicability. Lu et al. [16] found a variable practice pattern of adjuvant radiotherapy and reported better survival and no significant side effects of radiotherapy, contrary to other studies.

Author details

Rakesh Mishra[1] and Amit Agrawal[2*]

1 Department of Neurosurgery, Institute of Medical Sciences, Banaras Hindu University, Varanasi, India

2 Department of Neurosurgery, All India Institute of Medical Sciences, Bhopal, Madhya Pradesh, India

*Address all correspondence to: dramitagrawal@gmail.com

IntechOpen

References

[1] Matthay KK, Maris JM, Schleiermacher G, et al. Neuroblastoma. Nat Rev Dis Primers. 2016;2: 16078. https://doi.org/10.1038/nrdp.2016.78.

[2] Maris JM. Recent Advances in Neuroblastoma. New England Journal of Medicine. 2010;362(23): 2202-2211. https://doi.org/10.1056/NEJMra0804577.

[3] Bonilla MA, Cheung NK. Clinical progress in neuroblastoma. Cancer Invest. 1994;12(6): 644-653. https://doi.org/10.3109/07357909409023049.

[4] Bianchi F, Tamburrini G, Gessi M, Frassanito P, Massimi L, Caldarelli M. Central nervous system (CNS) neuroblastoma. A case-based update. Child's Nervous System. 2018;34(5): 817-823. https://doi.org/10.1007/s00381-018-3764-3.

[5] Vo KT, Matthay KK, Neuhaus J, et al. Clinical, biologic, and prognostic differences on the basis of primary tumor site in neuroblastoma: a report from the international neuroblastoma risk group project. J Clin Oncol. 2014;32(28): 3169-3176. https://doi.org/10.1200/jco.2014.56.1621.

[6] Horten BC, Rubinstein LJ. Primary cerebral neuroblastoma. A clinicopathological study of 35 cases. Brain. 1976; 99(4): 735-756. https://doi.org/10.1093/brain/99.4.735.

[7] Bennett Jr JP, Rubinstein LJ. The biological behavior of primary cerebral neuroblastoma: A reappraisal of the clincal course in a series of 70 cases. Annals of Neurology. 1984;16(1): 21-27. https://doi.org/https://doi.org/10.1002/ana.410160106.

[8] Louis DN, Perry A, Reifenberger G, et al. The 2016 World Health Organization Classification of Tumors of the Central Nervous System: a summary. Acta Neuropathologica.

2016;131(6): 803-820. https://doi.org/10.1007/s00401-016-1545-1.

[9] Shimada H, Ambros IM, Dehner LP, et al. The International Neuroblastoma Pathology Classification (the Shimada system). Cancer. 1999;86(2): 364-372.

[10] Hsiao CC, Huang CC, Sheen JM, et al. Differential expression of delta-like gene and protein in neuroblastoma, ganglioneuroblastoma and ganglioneuroma. Mod Pathol. 2005;18(5): 656-662. https://doi.org/10.1038/modpathol.3800335.

[11] Brodeur G, Castleberry R. Principles and Practice of Pediatric Oncology Pizzo PA and Poplack DG. Lippincott-Raven: Philadelphia; 1997.

[12] Nuchtern JG, London WB, Barnewolt CE, et al. A prospective study of expectant observation as primary therapy for neuroblastoma in young infants: a Children's Oncology Group study. Ann Surg. 2012;256(4): 573-580. https://doi.org/10.1097/SLA.0b013e31826cbbbd.

[13] Carlsen NL, Christensen IJ, Schroeder H, et al. Prognostic factors in neuroblastomas treated in Denmark from 1943 to 1980. A statistical estimate of prognosis based on 253 cases. Cancer. 1986;58(12): 2726-2735. https://doi.org/10.1002/1097-0142(19861215)58:12<2726::aid-cncr2820581229>3.0.co;2-m.

[14] Stiller C, Parkin D. International variations in the incidence of neuroblastoma. International journal of cancer. 1992;52(4): 538-543.

[15] London W, Castleberry R, Matthay K, et al. Evidence for an age cutoff greater than 365 days for neuroblastoma risk group stratification in the Children's Oncology Group. Journal of clinical oncology. 2005;23(27): 6459-6465.

[16] Lu X, Zhang X, Deng X, et al. Incidence, Treatment, and Survival in Primary Central Nervous System Neuroblastoma. World Neurosurg. 2020;140: e61-e72. https://doi.org/10.1016/j.wneu.2020.04.145.

[17] Georgakis MK, Dessypris N, Baka M, et al. Neuroblastoma among children in Southern and Eastern European cancer registries: Variations in incidence and temporal trends compared to US. International Journal of Cancer. 2018;142(10): 1977-1985. https://doi.org/ https://doi.org/10.1002/ijc.31222.

[18] Sturm D, Orr BA, Toprak UH, et al. New Brain Tumor Entities Emerge from Molecular Classification of CNS-PNETs. Cell. 2016;164(5): 1060-1072. https://doi.org/10.1016/j.cell.2016.01.015.

[19] Perez Garcia V, Martinez Izquierdo Mde L. Radiation-induced olfactory neuroblastoma: a new etiology is possible. Oral Maxillofac Surg. 2011;15(2): 71-77. https://doi.org/10.1007/s10006-010-0234-9.

[20] Tamase A, Nakada M, Hasegawa M, Shima H, Yamashita J. Recurrent intracranial esthesioneuroblastoma outside the initial field of radiation with progressive dural and intra-orbital invasion. Acta Neurochir (Wien). 2004;146(2): 179-182. https://doi.org/10.1007/s00701-003-0179-y.

[21] Park KJ, Kang SH, Lee HG, Chung YG. Olfactory neuroblastoma following treatment for pituitary adenoma. J Neurooncol. 2008;90(2): 237-241. https://doi.org/10.1007/s11060-008-9657-7.

[22] McVey GP, Power DG, Aherne NJ, Gibbons D, Carney DN. Post irradiation olfactory neuroblastoma (esthesio-neuroblastoma): a case report and up to date review. Acta Oncol. 2009;48(6): 937-940. https://doi.org/10.1080/02841860902759709.

[23] Zimmerman RA, Bilaniuk LT. CT of primary and secondary craniocerebral neuroblastoma. American Journal of Roentgenology. 1980;135(6): 1239-1242. https://doi.org/10.2214/ajr.135.6.1239.

[24] Davis PC, Wichman RD, Takei Y, Hoffman JC. Primary cerebral neuroblastoma: CT and MR findings in 12 cases. American Journal of Roentgenology. 1990;154(4): 831-836. https://doi.org/10.2214/ajr.154.4.2107684.

[25] Shimada H, Ambros IM, Dehner LP, Hata J, Joshi VV, Roald B. Terminology and morphologic criteria of neuroblastic tumors: recommendations by the International Neuroblastoma Pathology Committee. Cancer. 1999;86(2): 349-363.

[26] Peuchmaur M, d'Amore ES, Joshi VV, et al. Revision of the International Neuroblastoma Pathology Classification: confirmation of favorable and unfavorable prognostic subsets in ganglioneuroblastoma, nodular. Cancer. 2003;98(10): 2274-2281. https://doi.org/10.1002/cncr.11773.

[27] Umehara S, Nakagawa A, Matthay KK, et al. Histopathology defines prognostic subsets of ganglio-neuroblastoma, nodular. Cancer. 2000;89(5): 1150-1161.

[28] Yokoyama M, Okada K, Tokue A, Takayasu H, Yamada R. Ultrastructural and biochemical study of neuroblastoma and ganglioneuroblastoma. Invest Urol. 1971;9(2): 156-164.

[29] Ryu KH, Woo SY, Lee MY, et al. Morphological and biochemical changes induced by arsenic trioxide in neuroblastoma cell lines. Pediatr Hematol Oncol. 2005;22(7): 609-621. https://doi.org/10.1080/08880010500198897.

[30] Taxy JB. Electron microscopy in the diagnosis of neuroblastoma. Arch Pathol Lab Med. 1980;104(7): 355-360.

[31] Fatimi SH, Bawany SA, Ashfaq A. Ganglioneuroblastoma of the posterior mediastinum: a case report. J Med Case Rep. 2011;5: 322. https://doi.org/ 10.1186/1752-1947-5-322.

[32] Furuta T, Moritsubo M, Muta H, et al. Central nervous system neuroblastic tumor with FOXR2 activation presenting both neuronal and glial differentiation: a case report. Brain Tumor Pathol. 2020;37(3): 100-104. https://doi. org/10.1007/s10014-020-00370-2.

[33] Ahdevaara P, Kalimo H, Törmä T, Haltia M. Differentiating intracerebral neuroblastoma: report of a case and review of the literature. Cancer. 1977;40(2): 784-788. https://doi. org/10.1002/1097-0142(197708)40:2< 784::aid-cncr2820400228>3.0.co;2-8.

[34] Yao P-S, Chen G-R, Shang-Guan H-C, et al. Adult hippocampal ganglioneuroblastoma: Case report and literature review. Medicine. 2017;96(51): e8894. https://doi.org/10.1097/ md.0000000000008894.

[35] Kratimenos GP, Crockard HA. Cavernous sinus neuroblastoma. Br J Neurosurg. 1993;7(6): 691-696. https:// doi.org/10.3109/02688699308995101.

[36] Gasparetto EL, Rosemberg S, Matushita H, Leite Cda C. Ganglio-neuroblastoma of the cerebellum: neuroimaging and pathological features of a case. Arq Neuropsiquiatr. 2007; 65(2A): 338-340. https://doi.org/10.1590/ s0004-282x2007000200029.

[37] Mazloom A, Louis CU, Nuchtern J, et al. Radiation Therapy to the Primary and Postinduction Chemotherapy MIBG-Avid Sites in High-Risk Neuroblastoma. *International Journal of Radiation Oncology*Biology*Physics.* 2014;90(4): 858-862. https://doi.org/https://doi. org/10.1016/j.ijrobp.2014.07.019.

Chapter 6

The Scaffold Protein p140Cap as a Molecular Hub for Limiting Cancer Progression: A New Paradigm in Neuroblastoma

Giorgia Centonze, Jennifer Chapelle, Costanza Angelini,
Dora Natalini, Davide Cangelosi, Vincenzo Salemme,
Alessandro Morellato, Emilia Turco and Paola Defilippi

Abstract

Neuroblastoma, the most common extra-cranial pediatric solid tumor, is responsible for 9–15% of all pediatric cancer deaths. Its intrinsic heterogeneity makes it difficult to successfully treat, resulting in overall survival of 50% for half of the patients. Here we analyze the role in neuroblastoma of the adaptor protein p140Cap, encoded by the *SRCIN1* gene. RNA-Seq profiles of a large cohort of neuroblastoma patients show that *SRCIN1* mRNA levels are an independent risk factor inversely correlated to disease aggressiveness. In high-risk patients, *SRCIN1* was frequently altered by hemizygous deletion, copy-neutral loss of heterozygosity, or disruption. Functional assays demonstrated that p140Cap is causal in dampening both Src and Jak2 kinase activation and STAT3 phosphorylation. Moreover, p140Cap expression decreases *in vitro* migration and anchorage-independent cell growth, and impairs *in vivo* tumor progression, in terms of tumor volume and number of spontaneous lung metastasis. p140Cap also contributes to an increased sensitivity of neuroblastoma cells to chemotherapy drugs and to the combined usage of doxorubicin and etoposide with Src inhibitors. Overall, we provide the first evidence that *SRCIN1*/p140Cap is a new independent prognostic marker for patient outcome and treatment, with a causal role in curbing the aggressiveness of neuroblastoma. We highlight the potential clinical impact of *SRCIN1*/p140Cap expression in neuroblastoma tumors, in terms of reducing cytotoxic effects of chemotherapy, one of the main issues for pediatric tumor treatment.

Keywords: p140Cap, *SRCIN1* gene, Src kinase, Signal transducer and activator of transcription 3, chemotherapy, neuroblastoma, Src inhibitors

1. Introduction

Neuroblastoma (NB) is the most frequent embryonic malignancy among children particularly before 5 years of age [1]. It originates from primitive sympathetic neural precursor cells of the peripheral nervous system [2]. The majority of these tumors develop in the adrenal medulla; however, NB can arise anywhere along the

sympathetic nervous system (neck, chest, abdomen or pelvis). Primary tumors in the neck or upper chest can cause Horner's syndrome (ptosis, miosis, and anhidrosis). Tumors arising along the spinal column can expand through the intraforaminal spaces and cause cord compression, with resulting paralysis [3].

NB is a complex disease with different outcomes, going from metastasis to one or more distant sites [4] to spontaneous regression or differentiation, even in the absence of any specific treatment [5]. Given the high heterogeneous features of NB, the International Neuroblastoma Staging System (INSS), considers a plethora of criteria to rank patients. Namely, the degree of surgical excision of primary tumor, lymph node involvement, dissemination to distant organs, degree of bone marrow involvement and the age of infant [6]. Accordingly, stages 1, 2A and 2B include patients with localized tumor, without propagation to lymph nodes. Stage 3 and stage 4 comprehends patients with metastatic disease. Stage 4S specifies a metastatic disease in children under the age of one year, which may undergo spontaneous regression, usually associated with 90% survival rate at 5 years [7].

The genetic etiology of NB includes some established markers such as the presence of segmental chromosome abnormalities (chromosomes 1p, 3p, 4p, 11q loss and of 1q, 2p, 17q gains) [8] and DNA ploidy [9]. At the molecular level, the Anaplastic Lymphoma Kinase (*ALK*) oncogene is the most frequently mutated gene in hereditary familial NB, where it is amplified or constitutively activated in its tyrosine kinase domain [10, 11]. Amplification of the *N-MYC* oncogene (*MYCN*) occurs in 20% of NB, representing a poor prognostic factor for this embryonic malignancy [12, 13]. Tropomyosin receptor kinase B (*TrkB*) and Brain-Derived Neurotrophic Factor (*BDNF)* are both expressed in aggressive NB with *MYCN* amplification [14]. In addition, driver mutations in the lin-28 homolog B (*LIN28B*) [15] and in the Paired-like Homeobox 2b (*PHOX2B*) [16] genes have been reported.

NB therapeutic standard of care worldwide is based on multi-modality therapy including chemotherapy, surgery, radiation therapy, myeloablative therapy with stem cell transplant, immunotherapy and differentiation therapy [17–19]. However, a more accurate stratification of patients based on newly identified prognostic markers would allow the development of additional therapeutic strategies with increased effectiveness and reduced toxicity.

p140Cap (Cas-associated protein), also known as SNIP (Snap25-interacting protein) [20], is a scaffold protein codified by the gene *SRCIN1*. It is highly expressed in the brain, testis and epithelial rich tissue [21]. In human cancer patients, p140Cap/*SRCIN1* is a new favorable prognostic marker in HER2-related breast cancer, where p140Cap expression is associated with good prognosis [22]. At the molecular level, p140Cap impairs breast cancer growth and metastatic progression, interfering with both Src kinase [23] and Rac1 GTPases [22] activation.

More recently we have investigated p140Cap/*SRCIN1* relevance in NB. This chapter aims to present data supporting p140Cap/*SRCIN1* as a key biological determinant of NB outcome, representing a new independent prognostic marker for patient outcome and treatment. We highlight the potential clinical impact of *SRCIN1*/p140Cap expression in NB tumors in terms of reducing cytotoxic effects of chemotherapy, one of the main issues for pediatric tumor treatment.

2. The p140Cap adaptor protein

The human *SRCIN1* gene, located on chromosome 17q12, includes 27 exons, and it is highly conserved in vertebrates and mammals [24]. The genomic region immediately bordering *SRCIN1* contains several genes involved in breast cancer onset and progression such as *ERBB2* (17q12), *BRCA1* (17q21), retinoic acid receptor-α
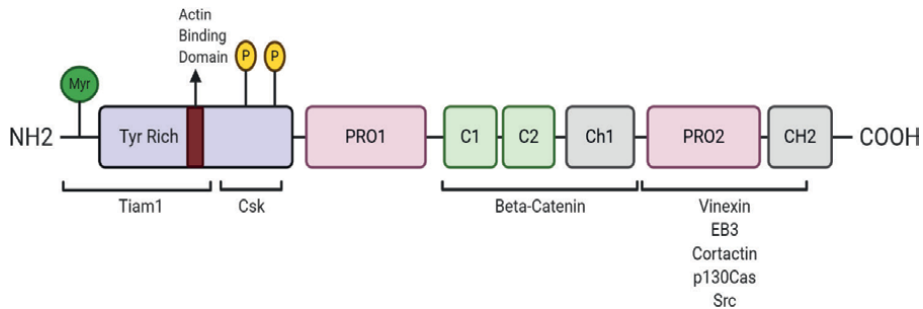
Figure 1.
The structure of the adaptor protein p140Cap. p140Cap protein analysis reveals the presence of a putative N-terminal myristoylation site, a tyrosine-rich region (Tyr-rich), an actin-binding domain (ABD), a proline rich domain (Pro1), a coil-coiled region (C1-C2), two domains rich in charged amino acids (CH1, CH2) and a C-terminal proline-rich domain (Pro2). Tyrosine phosphorylation (PY) EPLYA and EGLYA are shown. The interactors Tiam1, Csk, β-catenin, Vinexin, EB3, Cortactin, p130Cas and Src are associated with specific domains.

(*RARA*; 17q21) and signal transducer and activator of transcription 3 (*STAT3*; 17q21). These genes often undergo a gain of function role in human tumors [25]. Moreover, the 17q gain occurs in 50–70% of all high stage NB and is associated with poor prognosis as an independent marker of adverse outcome [26–29].

p140Cap shares different Intrinsically Disordered Regions (IDRs) that classify p140Cap as "Intrinsic Disorder Protein" (IDP) [30, 31]. The IDP features of p140Cap could allow the interaction with several partners and promote protein–protein interactions that are the elected functions for a scaffold protein. The p140Cap protein can interact with multiple partners [30] (**Figure 1**). In particular, p140Cap associates with the tyrosine kinases Csk and Src. This macromolecular complex triggers Csk activity to phosphorylate Src on its inhibitory tyrosine, resulting in Src inactivation and in the suppression of downstream pathways regulating motility and invasion of cancer cells [23]. Indeed, at the structural level, p140Cap contains a tyrosine rich domain, important for the interaction with Csk [32], two coiled coil regions, that can mediate the binding with beta-catenin [10] and two different proline rich domains responsible for the association with the microtubule associated protein EB3 [33], Cortactin [34] and Vimentin [35].

The physiologic role of p140Cap has been mainly investigated in the brain [35], where it is expressed in neurons both in the presynapse [10, 36] and in the postsynapse [10, 37–41]. In differentiated neurons, it controls synaptic plasticity [33, 40], and regulates GABAergic synaptogenesis and development of hippocampal inhibitory circuits [36]. In particular, p140Cap enters and accumulates in the dendritic spine (DS) through EB3 binding [33]. In this compartment p140Cap acts as hub interacting with Cortactin, a protein that regulates actin branching and new filament polymerization [42] and with Citron-N [40] resulting in mature DS stabilization. In both the pre- and post-synaptic regions, p140Cap is involved in a network of protein–protein interactions as confirmed by its interactome in synaptosomes. p140Cap interactors converge on key synaptic processes, including transmission across chemical synapses, actin cytoskeleton remodeling and cell–cell junction organization [41].

3. *SRCIN1* mRNA expression is an independent prognostic marker for NB

To address the involvement of p140Cap in NB patients, we first investigated the relationship between *SRCIN1* mRNA levels and patient outcomes, by using the R2 genomics analysis and visualization platform (R2: Genomics analysis and

Visualization Platform (http://r2.amc.nl)). The bioinformatics analysis performed on a dataset containing clinical and gene expression data of 498 NB patients revealed that *SRCIN1* positively impacts on patients' outcome. In fact, the Kaplan–Meier analysis showed that high expression of *SRCIN1* is associated with good prognosis in 403 patients, whereas low expression is observed in 95 poor prognosis patients (**Figure 2A**). Furthermore, high *SRCIN1* expression was significantly
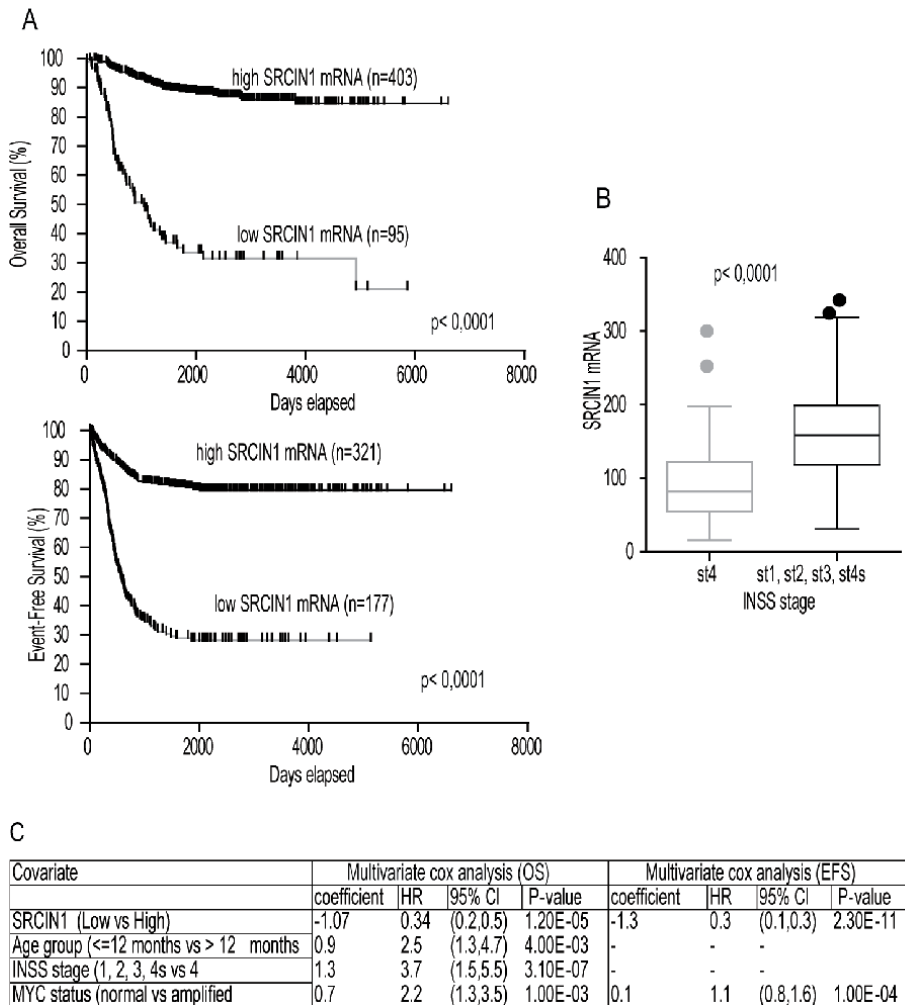

C

Covariate	Multivariate cox analysis (OS)				Multivariate cox analysis (EFS)			
	coefficient	HR	95% CI	P-value	coefficient	HR	95% CI	P-value
SRCIN1 (Low vs High)	-1.07	0.34	(0.2,0.5)	1.20E-05	-1.3	0.3	(0.1,0.3)	2.30E-11
Age group (<=12 months vs > 12 months	0.9	2.5	(1.3,4.7)	4.00E-03	-	-	-	
INSS stage (1, 2, 3, 4s vs 4	1.3	3.7	(1.5,5.5)	3.10E-07	-	-	-	
MYC status (normal vs amplified	0.7	2.2	(1.3,3.5)	1.00E-03	0.1	1.1	(0.8,1.6)	1.00E-04

Figure 2.
Stratification by SRCIN1 mRNA expression in primary NB patients and SRCIN1 gene status. A) Kaplan–Meier curves for overall (upper panel) and event-free (bottom panel) survival stratified by SRCIN1 expression in a cohort of 498 NB patients. Cut off for high or low SRCIN1 expression was chosen by Kaplan–Meier scan method. Survival curves were compared by log-rank test. P-values were corrected for multiple hypotheses testing by Bonferroni method. Each plot reports the corrected P-value (P). Corrected P-values lower than 0.05 were considered statistically significant. The number of patients with high or low expression of SRCIN1 mRNA is reported in every curve. B) Box and whisker plot for the expression of SRCIN1 mRNA in the two risk groups defined by INSS stages (st1, st2, st3, st4s vs. st4). The significance of the mean expression was measured by unpaired student t-test. A P-value lower than 0.05 was considered significant. C) Multivariate cox regression analysis for overall survival (OS) and event-free survival (EFS). The prognostic value of SRCIN1 mRNA expression (high and low) was tested in the context of known risk factors: Age at diagnosis (>12 months vs. <12 months) MYCN amplification (normal vs. amplified) INSS stages (st1, st2, st3, st4s vs. st4). Cut off for high or low SRCIN1 expression was chosen by Kaplan–Meier scan method. Cox regression coefficient (coefficient), hazard ratio (HR), 95% of confidence interval (95% CI) and P-value are shown for each variable in the OS and EFS panel. Significant P-values are lower than 0.05 (OS: HR 0.34 95% CI 0.2–0.5 P < 0.0001; EFS: HR 0.27 95% CI 0.1–0.4, P < 0.0001).

NB patients	*SRCIN1* gene status	CHROMOSOMAL COORDINATES
Case 1	disrupted in the breakpoint	Chr17: 36696338–81029941 Cytoband: 17q12-q25.3 Size: 44.33 Mb
Case 2	disrupted in the breakpoint	Chr17: 36694901–80943345 Cytoband: 17q12-q25.3 Size: 44.24 Mb
Case 3	loss	Chr17: 25311574–36777884 Cytoband: 17q11.1-q12 Size: 11.46 Mb
Case 4	disrupted in the breakpoint	Chr17: 36696338–80969424 Cytoband: 17q12-q25.3 Size: 44.27 Mb
Case 5	disrupted in the breakpoint	Chr17: 36696279–81029941 Cytoband: 17q12-q25.3 Size: 44.33 Mb
Case 6	copy neutral LOH	Chr17: 25569094–42949451 Cytoband: 17q11.1-q21.31 Size: 17.38 Mb
Case 7	copy neutral LOH	Chr17: 29149425–45297941 Cytoband: 17q11.1-q21.31 Size: 16.14 Mb
Case 8	copy neutral LOH	Chr17: 31571877–40588363 Cytoband: 17q11.2-q21.2 Size: 9.01 Mb
Case 9	loss	Chr17: 25278114–37876263 Cytoband: 17q11.1-q12 Size: 12.59 Mb
Case 10	loss	Chr17: 25278114–68301170 Cytoband: 17q11.1-q24.3 Size: 43.02 Mb
Case 11	disrupted in the breakpoint	Chr17: 36696279–81029941 Cytoband: 17q12-q25.3 Size: 44.33 Mb
Case 12	disrupted in the breakpoint	Chr17: 36696338–81029941 Cytoband: 17q12-q25.3 Size: 44.33 Mb
Case 13	disrupted in the breakpoint	Chr17: 36740844–80943189 Cytoband: 17q12-q25.3 Size: 44.20 Mb
Case 14	disrupted in the breakpoint	Chr17: 36740903–80993001 Cytoband: 17q12-q25.3 Size: 44.25 Mb
Case 15	loss	Chr17: 25278114–81029941 Cytoband: 17q11.1-q25.3 Size: 55.75 Mb
Case 16	disrupted in the breakpoint	Chr17: 36672992–77470237 Cytoband: 17q12-q25.3 Size: 40.79 Mb
Case 17	disrupted in the breakpoint	Chr17: 36694044–81099040 Cytoband: 17q12-q25.3 Size: 44.40 Mb

Table 1.
SRCIN1 loss/cn-LOH or disruption in the breakpoint on 17 NB patients.

associated with event-free survival (EFS) (321 patients) whereas a low expression was significantly associated with reduced metastatic recurrence (177 patients) (**Figure 2B**). *SRCIN1* mRNA expression was a favorable prognostic factor, both in terms of overall survival (OS) and EFS, regardless of the other known risk factors, including *MYCN* amplification, INSS stage, and age at diagnosis (**Figure 2C**).

To date, p140Cap expression by immunohistochemistry (IHC) on NB samples has not been studied owing to the lack of available cancer tissues, but *SRCIN1* mRNA expression correlates with a good outcome and is an independent prognostic marker for NB.

The *SRCIN1* gene is located on chromosome 17q12, a genomic region frequently involved in genetic abnormalities in NB. Therefore, a large cohort of 225 NB patients of all stages with 17q gain with poor prognosis, was analyzed by high-resolution oligonucleotide array-Comparative Genomic Hybridization (a-CGH) and Single Nucleotide Polymorphism - array (SNP-array). *SRCIN1* was hemizygously deleted in four NB tumors and it was subjected to copy-neutral Loss Of Heterozygosity (cn-LOH) in three specimens. Moreover, ten tumors displayed *SRCIN1* loss due to a breakpoint involved in the generation of 17q gain [43] (**Table 1**). However, because of the limited number of analyzed cases, survival differences between patients harboring these alterations did not reach statistical significance. Similar results come out in NB cell lines, as shown in SK-N-SH cells, where cn-LOH (8.72 Mb) that included *SRCIN1* gene, correlates with weak protein expression, suggesting an effective partial knockout of gene expression, originally proving that in NB patients the *SRCIN1* gene status may affect p140Cap expression, affecting prognosis.

4. p140Cap negatively affects tumorigenic features

The data obtained in NB patients support the hypothesis that p140Cap may curb the intrinsic biological aggressiveness of NB tumors. NB originates from the developing sympathetic nervous system, with a preferential localization in sympathetic ganglia and adrenal glands. Interestingly, we found that p140Cap is expressed in the main site of origin of NB tumors, in the medulla of normal human neonatal adrenal glands (**Figure 3A**). p140Cap is also expressed in a board panel of human NB cell lines which represent valid surrogate models for NB research [44]. Among these cell lines, p140Cap level was highly detected in HTLA-230, IMR-5, IMR-32, LAN-1 and SH-SY-5Y cell lines, weakly in SK-N-SH cells and undetectable in ACN cell line, a neuroblast-like cell line derived from bone marrow metastasis [45] (**Figure 3B**). According to the protein level analysis, the genomic profiling revealed a wide spectrum of *SRCIN1* gene abnormalities. Indeed, the *SRCIN1* gene was lost in ACN, while a single copy was found in SH-SY-5Y, IMR-32, and HTLA-230 cell lines. Moreover, a genomic gain was observed in the LAN-1 cell line, whereas SK-N-SH cells displayed a cn-LOH.

The absence of p140Cap protein renders the ACN cell line a suitable tool for the generation of a p140Cap-expressing NB cell line via retroviral infection that might be leveraged for further functional investigations (**Figure 3C**). It is well established that p140Cap inhibits breast cancer cell features such as migration and proliferation [22]. Consistently, p140Cap-overexpressing ACN (p140Cap-ACN) cells exhibited decreased migration properties in a Wound Healing assay, and impaired anchorage-independent growth of NB cells, one of the main hallmarks of cancer. Cancer cells are known to avoid apoptosis by increasing or decreasing the expression of apoptotic and anti-apoptotic genes, respectively [46]. A specific type of apoptotic process, called anoikis, occurs in cells in response to loss of adhesion to the extracellular matrix.
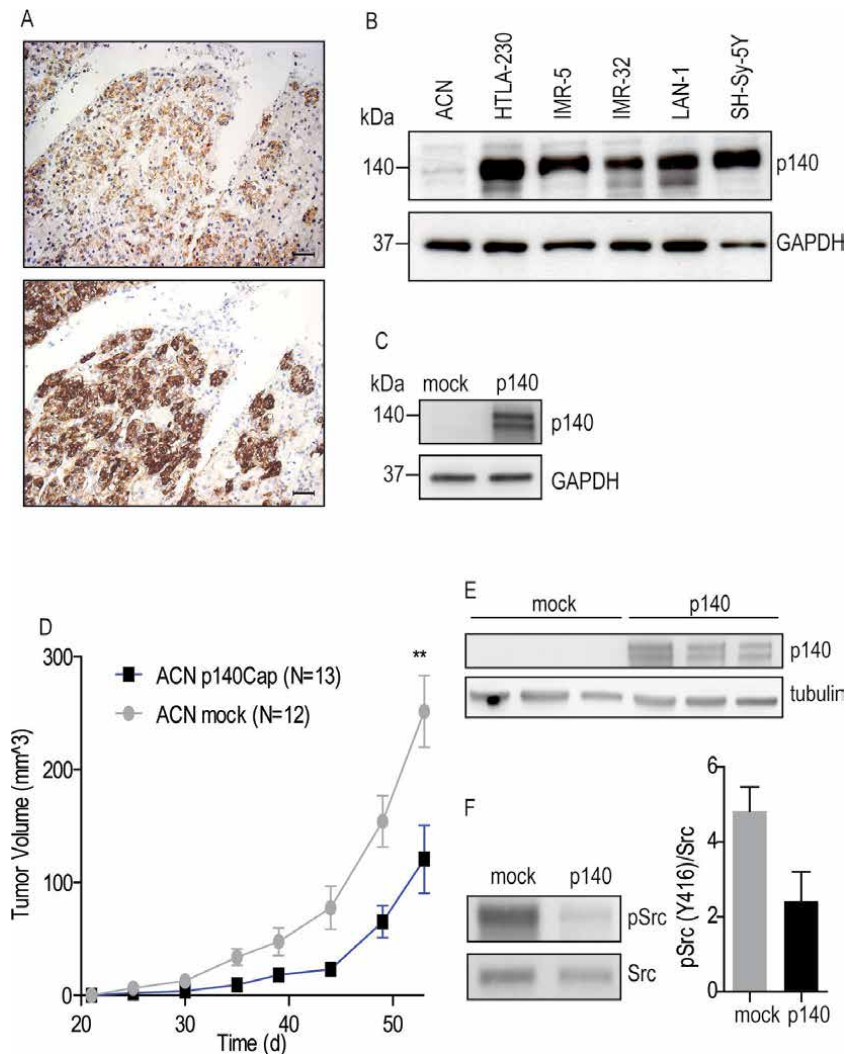
Figure 3.
In vitro expression and in vivo role of p140Cap. (A) p140Cap staining is visible in the chromaffin cells of the adrenal medulla (upper panel), as confirmed by the chromogranin a staining (lower panel). Scale bar: 50 μM; (B) p140Cap expression in NB cell lines, by western blot of equal amounts of proteins from the indicated cell lines; (C) p140Cap expression in a pool of clones of ACN cells upon viral infection; (D) p140Cap limits in vivo tumor growth. Mock and p140 cells (2 × 10⁵ cells in 0.2 ml of PBS) were subcutaneously injected into the dorsal region of male NSG mice. Average tumor volume. The size of the tumors was evaluated twice a week using digital calipers in blind experiments and significance was quantified by unpaired t-test (**P < 0.01); (E) WB analysis of p140Cap expression on explanted tumors by SDS-PAGE. Antibodies to p140Cap and tubulin (as loading control) were used; (F) Src kinase activation in tumor extracts. Tyr 416 phosphorylation (Y416) and Src protein level is shown. Quantification on the right is the ratio between phosphorylated Src and total Src protein in 5 tumors per group, as mean ± SEM (right) (unpaired t-test **P < 0.01).

Upon anoikis, p140Cap-ACN cells showed both a lower upregulation of the anti-apoptotic protein Bcl-2 compared to mock cells, and a significantly higher percentage of apoptotic cells detected by annexin V labeling. Overall, p140Cap can limit anchorage-independent growth, migration and apoptosis of NB cells, suggesting a causal involvement of this protein in curbing NB cancer cell properties.

To date, the *in vivo* models commonly used for NB research and drug efficacy studies ranges from genetically engineered mouse models to xenograft murine systems [47] and from syngeneic mice to zebrafish and chick embryo chorioallantoic membrane [48, 49]. Each animal model has its own strengths and limitations, and

provides insights to specific biological questions. Immunodeficient mouse models such as the NOD Scid Gamma (NSG) mice represent a valuable tool for the study of engrafted human cell lines and PDX tumors [50]. In particular, NSG mice exhibit a complete deficiency in the adaptive immunity and a severe deficiency in the innate immunity as a consequence of mutations in the IL2-receptor common gamma chain, the *Prkdc* gene, which determines the so-called "scid" mutation, and the Rag1 or Rag2 null mutation [50]. Therefore, the NSG preclinical model was a suitable candidate to investigate the *in vivo* tumor-suppressing role of p140Cap. Upon subcutaneous injection into the dorsal region of the NSG mice, p140Cap cells gave origin to smaller tumors, compared to mock cells. p140Cap tumors were also extensively poorly proliferative, in terms of proliferation marker KI67 (**Figure 3D, E**).

In NB, angiogenesis has a prominent role in determining tumor phenotype. A study published by Meitar D *et al.* demonstrated that higher vascularity in NB correlates with metastasis, unfavorable histology, and poor outcome [51]. p140Cap tumors showed a slight but significant lower number of vessels positive for CD31 and CD105 endothelial cell markers compared to control. Histological sections were also stained for AML and NG2 markers of mature or young pericytes, respectively, in order to evaluate the pericyte coverage of vessels. In line with the idea that p140Cap limits the angiogenic activity of cancer cells leading to the formation of larger and more stable vessels, p140Cap tumors exhibited higher pericyte coverage of the endothelium compared to control.

As already mentioned, p140Cap has been widely demonstrated to limit breast cancer cells growth and metastasis formation [22, 23]. The ability of p140Cap to inhibit cancer cell adhesion, migration and proliferation may contribute to the overall reduced occurrence of metastatic events. p140Cap tumors gave rise to a significantly reduced number of lung metastases compared to control. Overall, p140Cap impairs NB tumor growth and spontaneous metastasis *in vivo*, with a significant decrease in proliferation markers and an increase in tumor vessel pericyte coverage. These results are in line with those obtained in HER2 positive breast cancer patients and preclinical models [22], where p140Cap dampens the aggressiveness of these highly aggressive tumors.

Further evidence supporting the biological relevance of p140Cap in curbing NB aggressiveness was provided by the recent work of Yuan XL *et al*. [52]. Yuan XL *et al*. demonstrated that *SRCIN1* is a direct target of the microRNA-373 (miR-373) and that their expression has a negative correlation in both NB human samples and cell lines. miR-373 functions as an oncomiRNA promoting proliferation, migration and invasion of NB cells. Inhibition of miR-373 by using a specific anti-miRNA in SK-N-BE(2) cells led to a significant decrease of tumor growth in a mouse xenograft model that was paralleled with increased p140Cap mRNA and protein levels in the resected tumors. Silencing of *SRCIN1* partially abrogated the inhibitory effect of antimiR-373 in NB cell proliferation, migration and invasion.

The molecular mechanisms underpinning the tumor-suppressive properties of p140Cap in NB may rely on the modulation of specific intracellular signaling pathways that will be dissected in the next sections.

5. Molecular mechanisms and therapeutic targets in neuroblastoma

Over the last years, genomic analysis, exome and whole-genome sequencing, genome-wide association studies, transcriptomics and drug screenings have shed light on NB biology [53]. The ongoing phase relies on translating NB biology and genetics into improved prognostic stratification and precision medicine. New druggable targets could come out from the identification of predictors for response and

outcome as well as from the discovery of molecular aberrations in the tumors (for a recent review see [53]). Of the genetic aberrations described in NB only *MYCN* overexpression and activating mutations of the tyrosine kinase receptor (RTK) *ALK* have been proven to be de novo oncogenic drivers as mutation or overexpression of these molecules give rise to NB in genetically engineered mouse models [54, 55]. The oncogenic transcription factor *MYCN* is a hallmark of poor prognosis in NB patients [56]. However, the compounds that can interfere with *MYCN* interaction with its partner MAX as a way to block its transcriptional action, were not efficient *in vivo* [57], dampening their development in clinical testing. Strategies to exploit *MYCN* as a tumor-associated antigen for immunotherapy deserve further functional validation [58]. The *ALK* gene is altered by gain-of-function point mutations in around 14% of high-risk NB and represents an ideal therapeutic target given its low or absent expression in healthy tissue postnatally [59]. ALK signaling can be blocked in ALK-mutant NB cell lines and mouse models by different means, including RNA interference and small-molecule inhibitors. Moreover, the STAT3, PI3K/AKT and Ras/MAPK are the main pathways involved in full-length ALK signaling [60]. In particular, Mass Spectrometry-based phosphotyrosine profiling of signaling events associated with the full-length ALK receptor, showed robust activation of STAT3 on Tyr705 in a number of independent NB cell lines. STAT3 silencing reduces *MYCN* protein levels downstream of ALK signaling, together with inhibition of NB cell growth in the presence of STAT3 inhibitors. Overall these data suggest that activation of STAT3 is important for ALK signaling activity in NB [61]. On the other hand, ERK5 can mediate ALK-induced transcription of *MYCN* and proliferation of NB, suggesting that targeting both ERK5 and ALK may be beneficial in NB patients [62].

In addition to ALK, signaling through the EGFR and ERBB2 RTK, both found to be non-mutational activated in subsets of NB, converge at MAPK, with increased MAPK signaling. Further, MAPK/ERK kinase (MEK) inhibitors have been shown to inhibit the growth of NB cells *in vitro* [63] and *in vivo*, alone or in synergy with the CDK4/6 inhibitor, ribociclib to suppress tumor growth in a panel of murine xenograft models of NB [64]. However, a recent preclinical study advises against trametinib as monotherapy in ALK-addicted NB due to increased feedback activation of other signaling pathways including PI3K/AKT in both cell lines and mice xenografts [65].

Interestingly, high-risk NBs without *MYCN* amplification may deregulate *MYC* and other oncogenic genes via altered beta-catenin signaling providing a potential candidate pathway for therapeutic inhibition [66]. XAV939, a tankyrase 1 inhibitor, promotes cell apoptosis in NB cell lines by inhibiting Wnt/beta-catenin signaling pathway, by reducing the expression of anti-apoptotic markers and decreasing colony formation *in vitro* [67]. O6-methylguanine-DNA methyltransferase (MGMT) is commonly overexpressed in cancers and is implicated in the development of chemoresistance. A significant correlation between Wnt signaling and MGMT expression was found in several cancers, including NB. Further, immunofluorescence analysis on human tumor tissues showed co-localization of nuclear beta-catenin and MGMT in subtypes of NB. Pharmacological or genetic inhibition of Wnt activity downregulates MGMT expression and restores chemosensitivity of DNA-alkylating drugs [68].

6. p140Cap impairs the Src/p130Cas and the STAT3/Jak2 signaling pathways

Focal adhesion kinase (FAK) and Src are two non-receptor intracellular kinases highly expressed in a number of human tumors including NB, and together regulate both cellular adhesion and survival. Both FAK and Src play a role in protecting NB

cells from apoptosis, and dual inhibition of these kinases may be important when designing therapeutic interventions for this tumor [69]. Immunohistochemical staining showed FAK to be present in 73% of human NB specimens examined. In addition, p125FAK staining was significantly increased in stage IV tumors with amplification of the *MYCN*. Src expression in NB patients has been associated with poor outcomes [70, 71]. Indeed, Src family kinases promote cell survival/ proliferation and reduce cell aggregation of NBs. Conversely, its inhibition results in decreased proliferation and enhanced apoptosis in NB cells [72, 73], suggesting that Src family kinase inhibitors may be good candidates for molecular targeted therapy [74]. Of note, dasatinib, a well-known Src kinase inhibitor, is a potent inhibitor of NB cell viability with an IC(50) in the submicromolar range. As a consequence, dasatinib decreased anchorage-independent growth, affecting senescence and apoptosis. Interestingly, in the HTLA-230 NB model, dasatinib decreased c-Kit and Src activation together with a strong MAPK and Akt impairment. Dasatinib was also tested *in vivo* in a murine orthotopic model, where NB cells were injected directly in the adrenal gland in a microenvironment that closely mimics the human tumors conditions. HTLA-230 tumors were reduced in size and cellularity, with proliferation disease. Drug treatment in the orthotopic model utilizing HTLA-230 cells produced a significant reduction of tumor burden. Nevertheless, dasatinib activity *in vivo* was also significantly inhibited, but complete tumor eradication was not achieved [75]. Recently, the scaffold protein PAG1 was involved in the regulation of Src family kinase (SFK) signaling in NB. The NB cell line expressing PAG1™⁻ lacks the membrane-spanning domain of PAG1 and is located in the cytoplasm. PAG1™⁻ cells exhibited higher amounts of active SFKs and increased growth rate. Under differentiation conditions, PAG1™⁻ cells continued to proliferate and did not undergo differentiation. Activated FYN was sequestered in PAG1™⁻ cells, suggesting that disruption of FYN localization led to the observed defects in differentiation. Overall, PAG1 is an additional example of how a scaffold protein may control SFK intracellular localization, impacting on their activity and signaling that induces differentiation events, that may be crucial in the control of NB aggressiveness [76].

IL-6-dependent activation of STAT3 [77] has already been reported in NB, where STAT3 is critical in mediating increased survival and drug resistance [78–80]. Interestingly, very recently, the antiapoptotic and prometastatic JAK-STAT3 pathway was activated in chemoresistant tumors, generated in the Th-*MYCN* [CPM32] model. This model derives from a multicycle treatment with cyclophosphamide of the Th-*MYCN* genetically engineered mice which develop rapidly progressive chemosensitive NB, but lack clinically relevant metastases. Copy number aberrations in these tumors reflect the genomic alterations typical of human *MYCN*-amplified NB, e.g. copy number gains at mouse chromosome 11, syntenic with gains on human chromosome 17q. The Th-*MYCN* [CPM32] model is characterized by chemoresistance and progression in spontaneous bone marrow metastatic events. NB tumors show a huge remodeling of the immune microenvironment, with augmented tumor-associated fibroblasts and stroma. Treatment with the JAK1/JAK2 inhibitor CYT387 reduced progression of chemoresistant tumors and increased survival, highlighting that under treatment conditions that mimic chemotherapy in human patients, Th-*MYCN* [CPM32] mice develop genomic, microenvironmental, and clinical features reminiscent of human chemorefractory disease, with dysregulation of signaling pathways such as JAK-STAT3 that could be targeted to improve treatment of aggressive disease [81].

Our recent data show that p140Cap expression in NB cells is sufficient to down-modulate the tyrosine phosphorylation of Src Tyr 416 (p-Src), a marker of active Src, as well as of p130Cas, a well-known Src substrate [82] (**Figure 4A, B**).
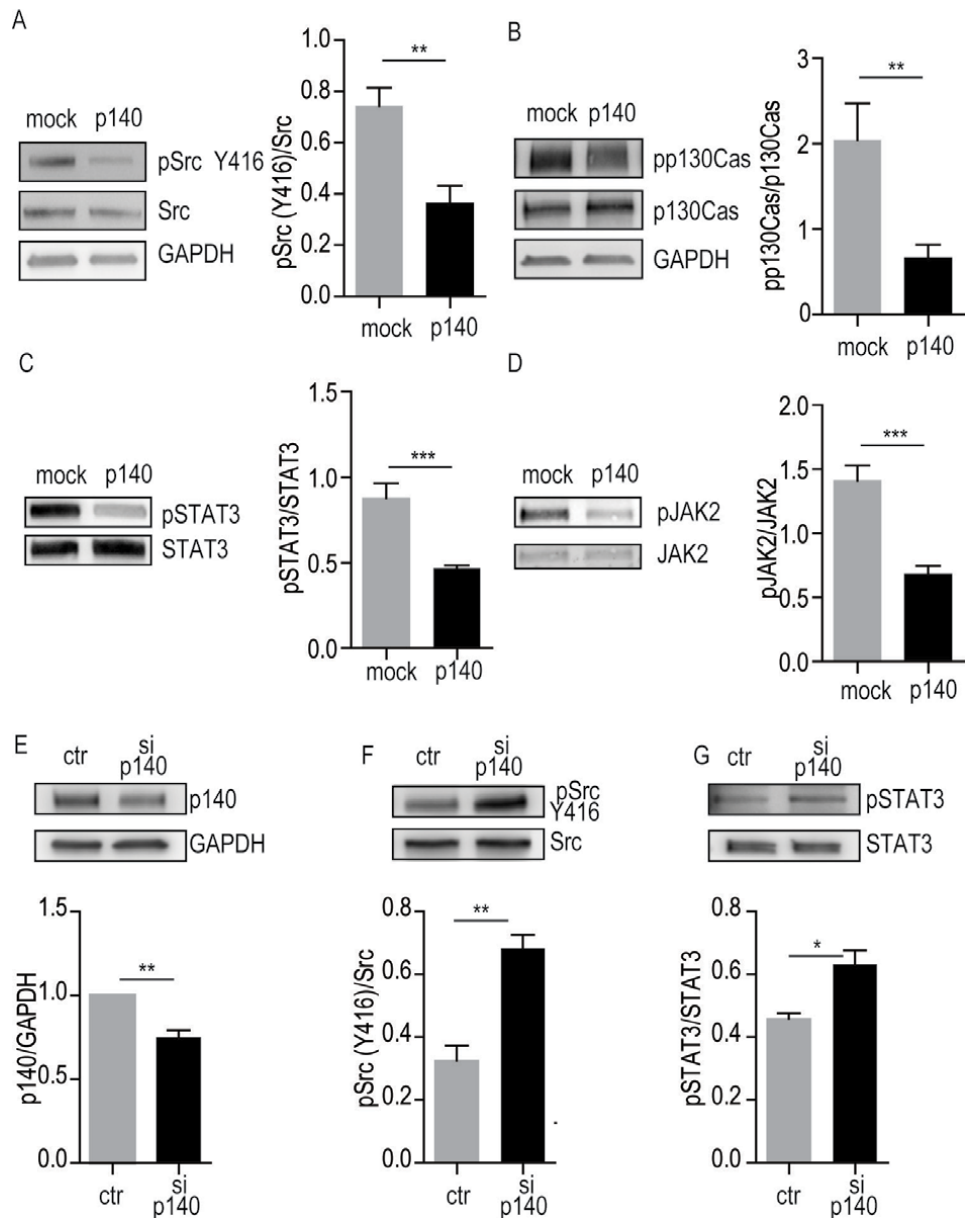
Figure 4.
p140Cap affects signaling pathways in NB cells. (A) Src activation was evaluated on mock and p140 ACN cells by WB analysis of Tyr 416 phosphorylation (Y416) and Src protein level as loading control. Antibodies to GAPDH (as loading control) were used. Quantification on the right is the ratio between phosphorylated Src and total Src protein; (B) p130Cas phosphorylation was evaluated with antibodies to phosphorylated p130Cas at Tyr 410, p130Cas and GAPDH antibodies for loading control. Quantification on the right is the ratio between phosphorylated p130Cas and total p130Cas; (C) STAT3 phosphorylation was evaluated with antibodies to phosphorylated STAT3 at Tyr705 and STAT3 antibodies for loading control. Quantification on the right is the ratio between phosphorylated STAT3 and total STAT3 protein from three independent experiment; (D) Jak2 activation was evaluated with antibodies to phosphorylated Jak2 at Tyr1007/1008 and Jak2 antibodies for loading control. Quantification on the right is the ratio between phosphorylated Jak2 and total Jak2 protein; in E-G p140Cap silenced cells were tested for p140Cap WB, and GAPDH as loading control (E), for Src activation at Tyr 416 phosphorylation (Y416) and Src protein level as loading control (F), and for phosphorylated STAT3 at Tyr 705 and STAT3 protein level as loading control (G). Quantification is shown on the left as the ratio between phosphorylated Src/STAT3 and total Src/STAT3 protein.

Moreover, we showed that STAT3 Tyr 705 (pSTAT3) is less phosphorylated, and JAK2 kinase is less active in p140Cap cells (**Figure 4C, D**). Consistent with these data, silencing of the endogenous p140Cap in SH-SY-5Y cells RNA [22] caused increased Src activation of STAT3 phosphorylation, confirming that p140Cap can regulate these two signaling pathways (**Figure 4E**-**G**). Overall, p140Cap ability to influence the Src/p130Cas and the JAK2/STAT3 pathways could be causal for the impairment of NB progression observed in patients [70, 72, 78–80, 83]. p140Cap also impairs Src kinase activity in breast cancer cells upon integrin-mediated adhesion or growth factor treatment stimulation [23, 84]. Overall, p140Cap may negatively regulate Src activity at least two tumor types, as a key event in dampening their migratory and invasive phenotype.

Based on the pro-survival role of STAT3 in NB, we also performed anoikis assays, showing that p140Cap-expressing cells were characterized by a significant decrease in the level of pSTAT3. Only the forced expression of the constitutive active STAT3C mutant is able to decrease p140Cap sensitivity to anoikis-dependent death. Overall, our data indicate that in NB cells, p140Cap expression may affect cell death, by impairing the pro apoptotic signaling sustained by the JAK2/STAT3-Bcl2 survival pathway.

7. p140Cap increases NB cell sensitivity to chemotherapeutic treatment

Despite advances in the molecular exploration of pediatric cancers, approximately 50% of children with high-risk NB lack effective treatment [85]. NB treatments are designed on the basis of a risk classification, which takes into account a subset of prognostic factors associated with a patient's outcome. Clinical features (for instance, the tumor stage or patient's age at diagnosis) and biological tumor properties (such as histology, genetic alteration and molecular markers) can be used as prognostic factors [9, 19] to classify NB patients in low risk, intermediate risk (IR) or high risk (HR) groups [19].

Non-high-risk represent slightly more than half of newly diagnosed patients. Outcomes are generally excellent for these children, with variable treatment strategies including observation alone, surgical resection, or moderate doses of chemotherapy [86, 87]. On the other hand, high-risk NB are very difficult to treat and require multi-modal therapy. Intensification of therapy has vastly improved survival rates, and research is focused on novel treatments to further improve survival rates [88].

Children with an intermediate or high risk often receive chemotherapy, namely carboplatin, cyclophosphamide, doxorubicin, etoposide, busulfan, ifosfamide or vincristine [9]. However, the side effects of chemotherapy and the outcome depend on the individual and the dose used. In this context, we demonstrated that p140Cap correlates with an increased sensitivity to chemotherapy. Namely, we tested five chemotherapeutic drugs commonly used in NB patients (ciclophosphamide, carboplatin, doxorubicin, etoposide, and vincristine) in dose viability assays. NB cell lines overexpressing p140Cap showed significantly increased sensitivity to low doses (10 nM, 100 nM) of cyclophosphamide, vincristine, doxorubicin and etoposide (**Figure 5A**-**C**). Consistently, in SH-SY-5Y cells, p140Cap silencing resulted in increased viability to both doxorubicin and etoposide [43] (**Figure 5D**).

Both etoposide and doxorubicin prevent ligation of the DNA strands, stopping the process of replication. The number of foci/cells of phosphorylated histone H2AX (gamma H2AX), an established marker of DNA damage [89], was counted
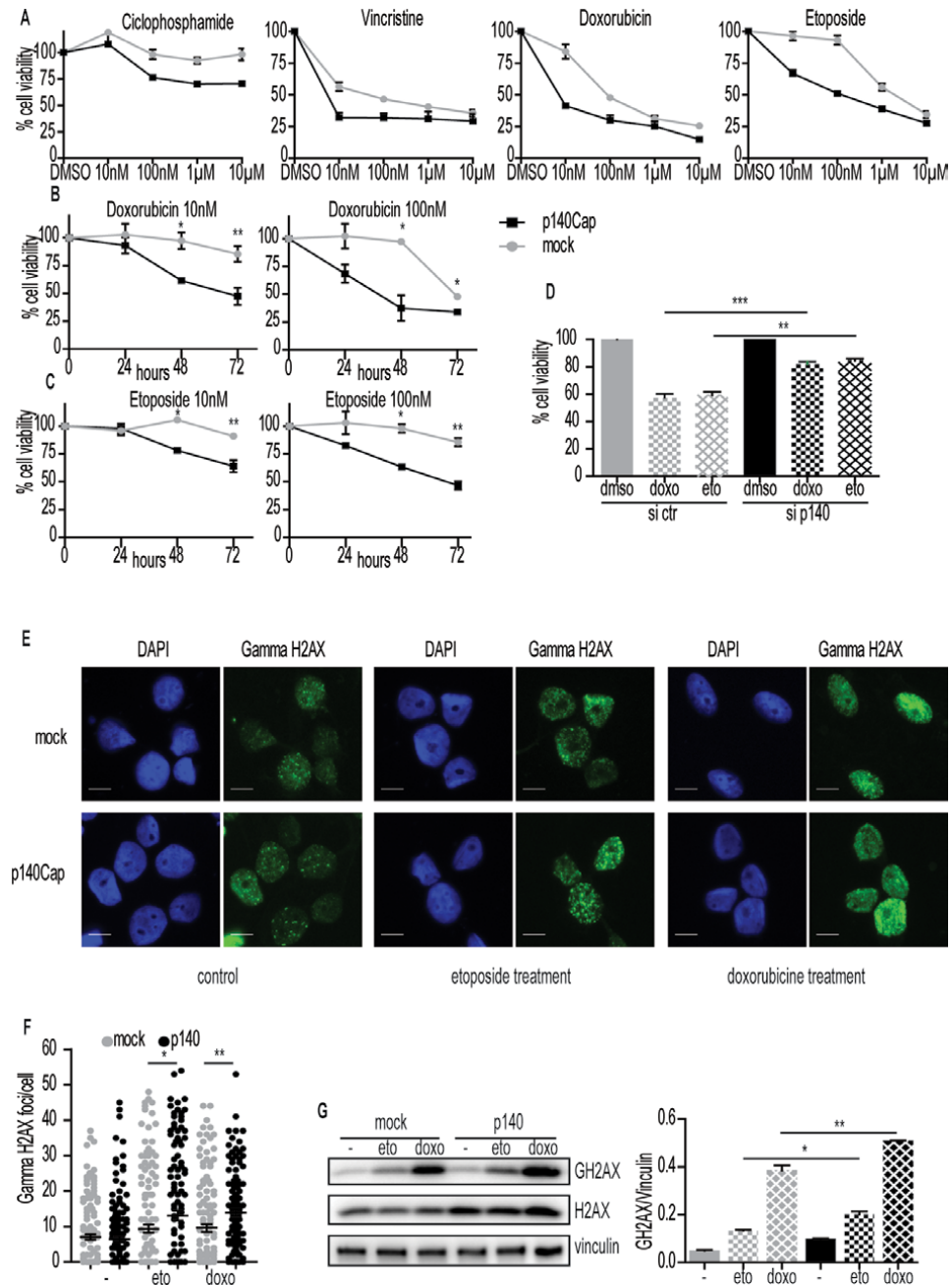
Figure 5.
p140Cap regulates cell viability to chemotherapeutic drugs. (A) Dose dependence viability to chemotherapy drugs. Mock and p140 cells were treated with the four indicated doses and cell viability was quantified at 72 h of treatment; (B-C) time dependent viability. Mock and p140 cells were processed as in (a); (D) cell viability in SH-5YSY cells silenced for p140Cap. Cells were transfected with appropriate siRNA and after 24 h treated with 1 μM etoposide or doxorubicin. Cell viability was quantified at 48 h; (E) visualization of nuclear foci for gamma H2AX histone as a marker of DNA damage. Mock and p140 cells on glass slides were treated for 6 h with 1 μM etoposide and doxorubicin. Green: Gamma H2AX foci; blue: DAPI for nuclear staining. Scale bar: 10 μm; (F) quantification of gamma H2AX foci/cell. Mock: Red; p140: Green. 50 nuclei were evaluated for each experiment; (G) gamma H2AX levels upon chemotherapy treatment. Mock and p140 cells were acutely treated with 1 μM etoposide or doxorubicin for 6 h. extracts were analyzed by western blot with antibodies to gamma-H2AX, H2AX and vinculin for loading controls. Quantification on the right is the ratio between gamma-H2AX and vinculin.

after an acute 6 h treatment with 1 μM etoposide and doxorubicin. p140Cap cells showed a significant increase in this marker over mock cells, indicating that the increased sensitivity of p140Cap cells to these drugs was associated with increased DNA lesions (**Figure 5E**-**G**). Overall, our study indicates that p140Cap NB cells display a significant decrease in cell viability upon drug treatment, with an increased sensitivity to drug-dependent DNA damage [43].

8. p140Cap increases NB cell sensitivity to Src kinase inhibitors

As already said above, Src family kinases are proto-oncogene tyrosine-protein kinases which are involved in tumor progression in several cancer types and are considered as a target for a low toxic anti-tumor treatment. High Src levels are generally associated with a poor prognosis and play an important role in the differentiation, cell-adhesion and survival of NB cells. Indeed, the inhibition of such kinase is an effective approach for NB treatment and several Src- inhibitors have been developed, holding a promising antiproliferative effect, cell cycle arrest, apoptosis induction and decreased adhesion/invasiveness [69, 72, 73].

Since active Src was significantly down-regulated in p140Cap tumors over mock tumors and p140Cap overexpressing cells showed lower levels of active Src (**Figure 3F** and **4A**), we hypothesized that Src activity may be involved in NB cell viability [89]. In mock cells, Src activity was highly sensitive to two well-known Src inhibitors, saracatinib (which also inhibits the Abl kinase [90] at 100 nM), and sugen (used in preclinical NB models [91] at 1 μM). At 72 h, in mock cells both inhibitors decreased cell viability of 20–25%. Interestingly, the same treatment in p140Cap cells leads to a reduction in viability of nearly 40%. Moreover, viability to Src inhibitors was increased in cells silenced for p140Cap compared to p140Cap overexpressing cells. However, the partially silenced cells were still more sensitive than mock cells, indicating that there is a direct correlation between p140Cap expression and the augmented sensitivity to Src inhibitors.

We observed a decreased viability in mock cells upon treating them with Src inhibitors coupled with drugs that induce a DNA damage (in particular, doxorubicin or etoposide have been used at a concentration of 10 nM and 100 nM in association with saracatinib and sugen).

The decreased viability of mock cells (approximately at 50%) in these conditions indicates that may Src inhibitors concur in increasing chemotherapy cytotoxic effect in those cells which do not express p140Cap.

In addition, the use of both genotoxic drugs and Src inhibitors in the same treatment confers to p140Cap overexpressing cells a lower viability, in particular in cells treated with doxorubicin. Taken together, our data suggest that a combined treatment with Src inhibitors could increase NB cells sensitivity to etoposide and doxorubicin.

Upon a treatment with augmented doses of etoposide and doxorubicin (in a range of 1 nM-1 mM) used alone or in association with the same concentrations of Src inhibitors, we observed that the combined experimental setting was synergistic in both the cell lines (mock and p140Cap overexpressing cells).

Indeed, the Combination Index (CI) values computed for the different combinations of drugs were < 1 in all the experimental settings [92]. The p140Cap overexpressing cells still showed an increased sensitivity to the Src inhibitors in the combined treatment, with a shift of the sensitivity to lower doses (**Figure 6**). Therefore, our data show that chemotherapy and Src inhibitors combination synergistically decreases NB cell viability and this effect can be further increased by p140Cap expression [43].

treatment	Cell line	CI	DRI50	r	Cell line	CI	DRI50	r
Doxo, Sug	mock	0.08838	Doxo -12.39; Sug -130.442	0.97494	p140	0.17652	Doxo -5.814; Sug -221.354	0.93442
Doxo, Sara	mock	0.1775	Doxo -9.021; Sara -14.904	0.98575	p140	0.3368	Doxo -3.219; Sara -38.115	0.95530
Eto, Sug	mock	0.277	Eto -5.606; Sug -10.041	0.99194	p140	0.07017	Eto -18.881; Sug -58.115	0.96845
Eto, Sara	mock	0.08899	Eto -28.921; Sara -18.377	0.97889	p140	0.07185	Eto -26.208; Sara -29.676	0.92729

Figure 6.
Synergistic analysis of combined treatments with chemotherapy drugs and Src inhibitors. The CI (combination index to reduce viable cells to 50%) and the DRI50 (the dose-reduction necessary to decrease viable cells to 50%, were calculated using the CalcuSyn software (www.biosoft.com/w/calcusyn.htm); r: Linear regression coefficient.

9. Conclusions

This chapter highlights the original involvement of *SRCIN1*/p140Cap in NB, providing evidence that *SRCIN1* gene expression may be exploited as a marker of good outcomes in NB (**Figure 7**). *SRCIN1* mRNA levels are clinically relevant in NB
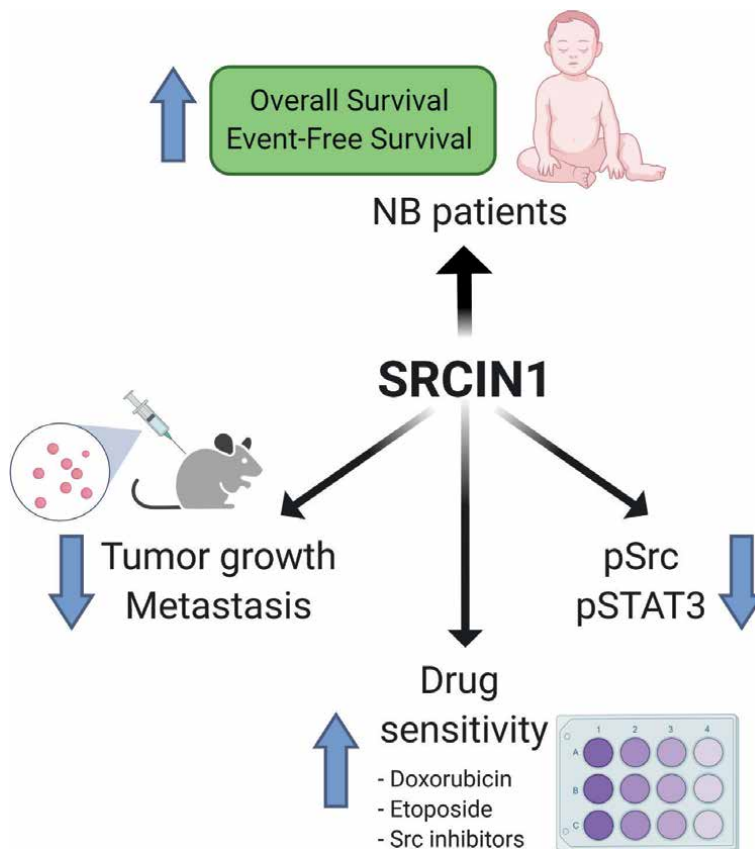
Figure 7.
Overview of SRCIN1 involvement in NB. The data reported here indicate a key causal role of SRCIN1/ p140Cap in dampening cell signaling, tumor growth, metastasis and drug sensitivity in NB cells, leading to a good outcome in NB patients.

patients, with high levels of expression positively correlating with good prognosis and high survival rate. Of note, *SRCIN1* mRNA behaves as an independent risk factor, thus providing evidence that *SRCIN1* is a useful, additional marker for better stratifying NB patient cohorts.

Overall, the protein p140Cap acts as a tumor suppressor gene in NB tumors, dampening tumor volume and decreasing progression towards distant metastasis. This might occur because of an increased ability to undergo apoptosis and a decreased capability of p140Cap NB cells to proliferate *in vivo*. Tumor microenvironment could also play a role, as shown by decreased permeability of p140Cap tumor vessels, likely due to the increased presence of pericytes, as shown by their specific marker NG2 [93].

An urgent need in NB is to increase the five-year OS rate of high-risk NB patients, which is still less than 40% [94]. Despite emerging new therapies, the impact of treatments is very heavy for affected children, which can have serious consequences for years to come [95]. The data showing that p140Cap expressing NB have significantly increased sensitivity to low doses (10 nM concentration) of doxorubicin and etoposide, two drugs used in first line NB treatment, open new perspectives. Further, the fact that a combo treatment with Src inhibitors and low doses doxorubicin or etoposide, sensitize mock cells, reducing cell viability to that of p140Cap cells treated with chemotherapy alone, is an encouraging result. Therefore, it would be interesting to set combinatorial approaches with low doses of both chemotherapy drugs and specific inhibitors, including also the Jak2 pathway, to quantify the additional/synergistic effects. Further, to increase the understanding of the mechanism of action of p140Cap on the sensitization to specific drugs, it would be very useful to identify the vital molecular signaling mechanisms involved. To achieve these results, both automated platforms for cell viability and genome-wide CRISPR-CAS9 technology are largely available. In conclusion, we believe that these data demonstrate the potential clinical impact of SRCIN1/p140Cap expression and of p140Cap-regulated pathways in NB tumors. These results pave the way to include *SRCIN1* mRNA in the NB patients' prognostic status, as a key marker for patient outcome.

Acknowledgements

Conflict of interest

There is no competing of interest to declare.

Rights and permissions

Abbreviations

Abl	Abelson Tyrosine-Protein Kinase
a-CGH	array - Comparative Genomic Hybridization
AKT	AKT serine/threonine kinase 1
ALK	Anaplastic Lymphoma Kinase
AML	Acute myeloid leukemia
Bcl-2	B-cell lymphoma 2
Bcl-2	B-cell lymphoma gene 2
BDNF	Brain-Derived Neurotrophic Factor
BRCA1	BRCA1 DNA repair associated
CAP	Cas-associated protein
CD105	endoglin
CD31	platelet and endothelial cell adhesion molecule 1
CDK4/6	cyclin D-cyclin-dependent kinase 4/6
CI	Combination Index
cn-LOH	copy-neutral Loss Of Heterozygosity
Csk	C-terminal Src kinase
DS	Dendritic spines
EB3	microtubule associated protein RP/EB family member 3
EFS	event free survival
ERBB2	erb-b2 receptor tyrosine kinase 2
ERK	extracellular signal-regulated kinase
ERK5	Extracellular signal-regulated kinase 5
FAK	focal adhesion kinase
FYN	FYN oncogene related to SRC, FGR, YES
H2AX	H2A histone family member X
IC50	the half maximal inhibitory concentration
IDP	Intrinsic Disorder Protein
IDR	Intrinsically Disordered Regions
IHC	Immunohistochemistry
IL-6	Interleukin 6
INSS	International Neuroblastoma Staging System
JAK	Janus kinase
Ki67	marker of proliferation Ki-67
LIN28B	lin-28 homolog B
MAPK	mitogen-activated protein kinase
MAX	myc-associated factor X
MGMT	O(6)-Methylguanine-DNA methyltransferase
MYCN	MYCN proto-oncogene
NB	Neuroblastoma

NG2	Neural/glial antigen 2
NSG	NOD Scid Gamma mice
OS	Overall survival
PAG1TM-	PAG1 fragment that lacks the membrane spanning domain
PDX	patient derived xenograft
PHOX2B	Paired-like Homeobox 2b
PI3K	Phosphoinositide 3-kinase
Prkdc	protein kinase, DNA-activated, catalytic subunit
Rag-1 and 2	Recombinant activating 1,2
RARA	retinoic acid receptor-α
Ras	Ras-related C3 botulinum toxin substrate
RTK	tyrosine kinase receptor
SFK	Src family kinase
SNIP	SNAP25 Interacting Protein
SNP-array	Single Nucleotide Polymorphism – array
Src	proto-oncogene tyrosine-protein kinase Src
SRCIN1	SRC kinase signaling inhibitor 1
STAT3	Signal transducer and activator of transcription 3
TrkB	Tropomyosin receptor kinase B
Wnt	Wingless-related integration site

Author details

Giorgia Centonze[1†], Jennifer Chapelle[1†], Costanza Angelini[1†], Dora Natalini[1†], Davide Cangelosi[2], Vincenzo Salemme[1], Alessandro Morellato[1], Emilia Turco[1] and Paola Defilippi[1*]

1 Department of Molecular Biotechnology and Health Science, University of Torino, Torino, Italy

2 Laboratory of Molecular Biology, Giannina Gaslini Institute, Genova, Italy

*Address all correspondence to: paola.defilippi@unito.it

† These authors equally contribute to this work.

IntechOpen

References

[1] Gatta, G., et al., *Embryonal cancers in Europe.* Eur J Cancer, 2012. **48**(10): p. 1425-33.

[2] Maris, J.M., *Recent advances in neuroblastoma.* N Engl J Med, 2010. **362**(23): p. 2202-11.

[3] Farrell, P.A., A.L. Caston, and D. Rodd, *Changes in insulin response to glucose after exercise training in partially pancreatectomized rats.* J Appl Physiol (1985), 1991. **70**(4): p. 1563-8.

[4] DuBois, S.G., et al., *Metastatic sites in stage IV and IVS neuroblastoma correlate with age, tumor biology, and survival.* J Pediatr Hematol Oncol, 1999. **21**(3): p. 181-9.

[5] Brodeur, G.M. and R. Bagatell, *Mechanisms of neuroblastoma regression.* Nat Rev Clin Oncol, 2014. **11**(12): p. 704-13.

[6] Brodeur, G.M., et al., *Revisions of the international criteria for neuroblastoma diagnosis, staging, and response to treatment.* J Clin Oncol, 1993. **11**(8): p. 1466-77.

[7] Monclair, T., et al., *The International Neuroblastoma Risk Group (INRG) staging system: an INRG Task Force report.* J Clin Oncol, 2009. **27**(2): p. 298-303.

[8] Schleiermacher, G., et al., *Segmental chromosomal alterations have prognostic impact in neuroblastoma: a report from the INRG project.* Br J Cancer, 2012. **107**(8): p. 1418-22.

[9] Cohn, S.L., et al., *The International Neuroblastoma Risk Group (INRG) classification system: an INRG Task Force report.* J Clin Oncol, 2009. **27**(2): p. 289-97.

[10] Li, M.Y., et al., *A Critical Role of Presynaptic Cadherin/Catenin/p140Cap Complexes in Stabilizing Spines and Functional Synapses in the Neocortex.* Neuron, 2017. **94**(6): p. 1155-1172 e8.

[11] Ogawa, S., et al., *Oncogenic mutations of ALK in neuroblastoma.* Cancer Sci, 2011. **102**(2): p. 302-8.

[12] Zhu, S., et al., *Activated ALK collaborates with MYCN in neuroblastoma pathogenesis.* Cancer Cell, 2012. **21**(3): p. 362-73.

[13] Wang, L.L., et al., *Augmented expression of MYC and/or MYCN protein defines highly aggressive MYC-driven neuroblastoma: a Children's Oncology Group study.* Br J Cancer, 2015. **113**(1): p. 57-63.

[14] Nakagawara, A., et al., *Expression and function of TRK-B and BDNF in human neuroblastomas.* Mol Cell Biol, 1994. **14**(1): p. 759-67.

[15] Diskin, S.J., et al., *Common variation at 6q16 within HACE1 and LIN28B influences susceptibility to neuroblastoma.* Nat Genet, 2012. **44**(10): p. 1126-30.

[16] van Limpt, V., et al., *The Phox2B homeobox gene is mutated in sporadic neuroblastomas.* Oncogene, 2004. **23**(57): p. 9280-8.

[17] Owens, C. and M. Irwin, *Neuroblastoma: the impact of biology and cooperation leading to personalized treatments.* Crit Rev Clin Lab Sci, 2012. **49**(3): p. 85-115.

[18] Morgenstern, D.A., S. Baruchel, and M.S. Irwin, *Current and future strategies for relapsed neuroblastoma: challenges on the road to precision therapy.* J Pediatr Hematol Oncol, 2013. **35**(5): p. 337-47.

[19] Whittle, S.B., et al., *Overview and recent advances in the treatment of neuroblastoma.* Expert Rev Anticancer Ther, 2017. **17**(4): p. 369-386.

[20] Chin, L.S., et al., *SNIP, a novel SNAP-25-interacting protein implicated in regulated exocytosis.* J Biol Chem, 2000. **275**(2): p. 1191-200.

[21] Di Stefano, P., et al., *P130Cas-associated protein (p140Cap) as a new tyrosine-phosphorylated protein involved in cell spreading.* Mol Biol Cell, 2004. **15**(2): p. 787-800.

[22] Grasso, S., et al., *The scaffold protein p140Cap limits ERBB2-mediated breast cancer progression interfering with Rac GTPase-controlled circuitries.* Nat Commun, 2017. **8**: p. 14797.

[23] Di Stefano, P., et al., *p140Cap protein suppresses tumour cell properties, regulating Csk and Src kinase activity.* EMBO J, 2007. **26**(12): p. 2843-55.

[24] Di Stefano, P., et al., *The adaptor proteins p140CAP and p130CAS as molecular hubs in cell migration and invasion of cancer cells.* Am J Cancer Res, 2011. **1**(5): p. 663-73.

[25] Lamy, P.J., et al., *Quantification and clinical relevance of gene amplification at chromosome 17q12-q21 in human epidermal growth factor receptor 2-amplified breast cancers.* Breast Cancer Res, 2011. **13**(1): p. R15.

[26] Combaret, V., et al., *Determination of 17q gain in patients with neuroblastoma by analysis of circulating DNA.* Pediatr Blood Cancer, 2011. **56**(5): p. 757-61.

[27] Bown, N., et al., *Gain of chromosome arm 17q and adverse outcome in patients with neuroblastoma.* N Engl J Med, 1999. **340**(25): p. 1954-61.

[28] Vandesompele, J., et al., *Unequivocal delineation of clinicogenetic subgroups and development of a new model for improved outcome prediction in neuroblastoma.* J Clin Oncol, 2005. **23**(10): p. 2280-99.

[29] Lastowska, M., et al., *Comprehensive genetic and histopathologic study reveals three types of neuroblastoma tumors.* J Clin Oncol, 2001. **19**(12): p. 3080-90.

[30] Salemme, V., et al., *The p140Cap adaptor protein as a molecular hub to block cancer aggressiveness.* Cell Mol Life Sci, 2020.

[31] Wright, P.E. and H.J. Dyson, *Intrinsically disordered proteins in cellular signalling and regulation.* Nat Rev Mol Cell Biol, 2015. **16**(1): p. 18-29.

[32] Repetto, D., et al., *Mapping of p140Cap phosphorylation sites: the EPLYA and EGLYA motifs have a key role in tyrosine phosphorylation and Csk binding, and are substrates of the Abl kinase.* PLoS One, 2013. **8**(1): p. e54931.

[33] Jaworski, J., et al., *Dynamic microtubules regulate dendritic spine morphology and synaptic plasticity.* Neuron, 2009. **61**(1): p. 85-100.

[34] Damiano, L., et al., *p140Cap suppresses the invasive properties of highly metastatic MTLn3-EGFR cells via impaired cortactin phosphorylation.* Oncogene, 2012. **31**(5): p. 624-33.

[35] Ito, H., et al., *Characterization of a multidomain adaptor protein, p140Cap, as part of a pre-synaptic complex.* J Neurochem, 2008. **107**(1): p. 61-72.

[36] Russo, I., et al., *p140Cap Regulates GABAergic Synaptogenesis and Development of Hippocampal Inhibitory Circuits.* Cereb Cortex, 2019. **29**(1): p. 91-105.

[37] Tomasoni, R., et al., *SNAP-25 regulates spine formation through postsynaptic binding to p140Cap.* Nat Commun, 2013. **4**: p. 2136.

[38] Yang, Y., et al., *Endophilin A1 regulates dendritic spine morphogenesis and stability through interaction with p140Cap.* Cell Res, 2015. **25**(4): p. 496-516.

[39] Fossati, G., et al., *Reduced SNAP-25 increases PSD-95 mobility and impairs spine morphogenesis.* Cell Death Differ, 2015. **22**(9): p. 1425-36.

[40] Repetto, D., et al., *p140Cap regulates memory and synaptic plasticity through Src-mediated and citron-N-mediated actin reorganization.* J Neurosci, 2014. **34**(4): p. 1542-53.

[41] Alfieri, A., et al., *Synaptic Interactome Mining Reveals p140Cap as a New Hub for PSD Proteins Involved in Psychiatric and Neurological Disorders.* Front Mol Neurosci, 2017. **10**: p. 212.

[42] Blanchoin, L., T.D. Pollard, and R.D. Mullins, *Interactions of ADF/cofilin, Arp2/3 complex, capping protein and profilin in remodeling of branched actin filament networks.* Curr Biol, 2000. **10**(20): p. 1273-82.

[43] Grasso, S., et al., *The SRCIN1/ p140Cap adaptor protein negatively regulates the aggressiveness of neuroblastoma.* Cell Death Differ, 2020. **27**(2): p. 790-807.

[44] Harenza, J.L., et al., *Transcriptomic profiling of 39 commonly-used neuroblastoma cell lines.* Sci Data, 2017. **4**: p. 170033.

[45] Gross, N., et al., *New anti-GD2 monoclonal antibodies produced from gamma-interferon-treated neuroblastoma cells.* Int J Cancer, 1989. **43**(4): p. 665-71.

[46] Fernald, K. and M. Kurokawa, *Evading apoptosis in cancer.* Trends Cell Biol, 2013. **23**(12): p. 620-33.

[47] Kamili, A., et al., *Mouse models of high-risk neuroblastoma.* Cancer Metastasis Rev, 2020. **39**(1): p. 261-274.

[48] Corallo, D., et al., *The zebrafish as a model for studying neuroblastoma.* Cancer Cell Int, 2016. **16**: p. 82.

[49] Ribatti, D. and R. Tamma, *The chick embryo chorioallantoic membrane as an in vivo experimental model to study human neuroblastoma.* J Cell Physiol, 2018. **234**(1): p. 152-157.

[50] Shultz, L.D., et al., *Human cancer growth and therapy in immunodeficient mouse models.* Cold Spring Harb Protoc, 2014. **2014**(7): p. 694-708.

[51] Meitar, D., et al., *Tumor angiogenesis correlates with metastatic disease, N-myc amplification, and poor outcome in human neuroblastoma.* J Clin Oncol, 1996. **14**(2): p. 405-14.

[52] Yuan, X.L., et al., *miR-373 promotes neuroblastoma cell proliferation, migration, and invasion by targeting SRCIN1.* Onco Targets Ther, 2019. **12**: p. 4927-4936.

[53] Johnsen, J.I., et al., *Molecular mechanisms and therapeutic targets in neuroblastoma.* Pharmacol Res, 2018. **131**: p. 164-176.

[54] Weiss, W.A., et al., *Targeted expression of MYCN causes neuroblastoma in transgenic mice.* EMBO J, 1997. **16**(11): p. 2985-95.

[55] Heukamp, L.C., et al., *Targeted expression of mutated ALK induces neuroblastoma in transgenic mice.* Sci Transl Med, 2012. **4**(141): p. 141ra91.

[56] Goto, S., et al., *Histopathology (International Neuroblastoma Pathology Classification) and MYCN status in patients with peripheral neuroblastic tumors: a report from the Children's Cancer Group.* Cancer, 2001. **92**(10): p. 2699-708.

[57] Guo, J., et al., *Efficacy, pharmacokinetics, tisssue distribution, and metabolism of the Myc-Max disruptor, 10058-F4 [Z,E]-5-[4-ethylbenzylidine]-2-thioxothiazolidin-4-one, in mice.* Cancer Chemother Pharmacol, 2009. **63**(4): p. 615-25.

[58] Schramm, A. and H. Lode, *MYCN-targeting vaccines and*

immunotherapeutics. Hum Vaccin Immunother, 2016. **12**(9): p. 2257-8.

[59] Trigg, R.M. and S.D. Turner, *ALK in Neuroblastoma: Biological and Therapeutic Implications.* Cancers (Basel), 2018. **10**(4).

[60] Sattu, K., et al., *Phosphoproteomic analysis of anaplastic lymphoma kinase (ALK) downstream signaling pathways identifies signal transducer and activator of transcription 3 as a functional target of activated ALK in neuroblastoma cells.* FEBS J, 2013. **280**(21): p. 5269-82.

[61] Janoueix-Lerosey, I., et al., *Somatic and germline activating mutations of the ALK kinase receptor in neuroblastoma.* Nature, 2008. **455**(7215): p. 967-70.

[62] Schwartzseid, E.E., *Ethics as an important determinant of success of orthopaedic dental care for debilitated and elderly patients.* Gerodontology, 1989. **8**(3): p. 83-8.

[63] Tanaka, T., et al., *MEK inhibitors as a novel therapy for neuroblastoma: Their in vitro effects and predicting their efficacy.* J Pediatr Surg, 2016. **51**(12): p. 2074-2079.

[64] Hart, L.S., et al., *Preclinical Therapeutic Synergy of MEK1/2 and CDK4/6 Inhibition in Neuroblastoma.* Clin Cancer Res, 2017. **23**(7): p. 1785-1796.

[65] Fodor Becsky, A., J. Gonzalez Santander, and I. Schneider Keller, *[Statistical study of 1,010 cases of dento-alveolar injuries].* Odontol Chil, 1978. **26**(120): p. 87-91.

[66] Liu, X., et al., *Deregulated Wnt/beta-catenin program in high-risk neuroblastomas without MYCN amplification.* Oncogene, 2008. **27**(10): p. 1478-88.

[67] Tian, X.H., et al., *XAV939, a tankyrase 1 inhibitior, promotes cell apoptosis in neuroblastoma cell lines by inhibiting Wnt/beta-catenin signaling pathway.* J Exp Clin Cancer Res, 2013. **32**: p. 100.

[68] Wickstrom, M., et al., *Wnt/beta-catenin pathway regulates MGMT gene expression in cancer and inhibition of Wnt signalling prevents chemoresistance.* Nat Commun, 2015. **6**: p. 8904.

[69] Beierle, E.A., et al., *Inhibition of focal adhesion kinase and src increases detachment and apoptosis in human neuroblastoma cell lines.* Mol Carcinog, 2010. **49**(3): p. 224-34.

[70] Kratimenos, P., et al., *Multi-targeted molecular therapeutic approach in aggressive neuroblastoma: the effect of Focal Adhesion Kinase-Src-Paxillin system.* Expert Opin Ther Targets, 2014. **18**(12): p. 1395-406.

[71] Bjelfman, C., et al., *Expression of the neuronal form of pp60c-src in neuroblastoma in relation to clinical stage and prognosis.* Cancer Res, 1990. **50**(21): p. 6908-14.

[72] Navarra, M., et al., *Antiproliferative and pro-apoptotic effects afforded by novel Src-kinase inhibitors in human neuroblastoma cells.* BMC Cancer, 2010. **10**: p. 602.

[73] Radi, M., et al., *Identification of potent c-Src inhibitors strongly affecting the proliferation of human neuroblastoma cells.* Bioorg Med Chem Lett, 2011. **21**(19): p. 5928-33.

[74] Hishiki, T., et al., *Src kinase family inhibitor PP2 induces aggregation and detachment of neuroblastoma cells and inhibits cell growth in a PI3 kinase/Akt pathway-independent manner.* Pediatr Surg Int, 2011. **27**(2): p. 225-30.

[75] Vitali, R., et al., *Activity of tyrosine kinase inhibitor Dasatinib in neuroblastoma cells in vitro and in orthotopic mouse model.* Int J Cancer, 2009. **125**(11): p. 2547-55.

[76] Foltz, L., et al., *PAG1 directs SRC-family kinase intracellular localization to mediate receptor tyrosine kinase-induced differentiation.* Mol Biol Cell, 2020. **31**(20): p. 2269-2282.

[77] Avalle, L., et al., *STAT3 in cancer: A double edged sword.* Cytokine, 2017. **98**: p. 42-50.

[78] Ara, T., et al., *Critical role of STAT3 in IL-6-mediated drug resistance in human neuroblastoma.* Cancer Res, 2013. **73**(13): p. 3852-64.

[79] Borriello, L., et al., *More than the genes, the tumor microenvironment in neuroblastoma.* Cancer Lett, 2016. **380**(1): p. 304-14.

[80] Rebbaa, A., P.M. Chou, and B.L. Mirkin, *Factors secreted by human neuroblastoma mediated doxorubicin resistance by activating STAT3 and inhibiting apoptosis.* Mol Med, 2001. **7**(6): p. 393-400.

[81] Yogev, O., et al., *In Vivo Modeling of Chemoresistant Neuroblastoma Provides New Insights into Chemorefractory Disease and Metastasis.* Cancer Res, 2019. **79**(20): p. 5382-5393.

[82] Cabodi, S., et al., *Integrin signalling adaptors: not only figurants in the cancer story.* Nat Rev Cancer, 2010. **10**(12): p. 858-70.

[83] Odate, S., et al., *Inhibition of STAT3 with the Generation 2.5 Antisense Oligonucleotide, AZD9150, Decreases Neuroblastoma Tumorigenicity and Increases Chemosensitivity.* Clin Cancer Res, 2017. **23**(7): p. 1771-1784.

[84] Damiano, L., et al., *p140Cap dual regulation of E-cadherin/EGFR cross-talk and Ras signalling in tumour cell scatter and proliferation.* Oncogene, 2010. **29**(25): p. 3677-90.

[85] Almstedt, E., et al., *Integrative discovery of treatments for high-risk neuroblastoma.* Nat Commun, 2020. **11**(1): p. 71.

[86] Baker, D.L., et al., *Outcome after reduced chemotherapy for intermediate-risk neuroblastoma.* N Engl J Med, 2010. **363**(14): p. 1313-23.

[87] Strother, D.R., et al., *Outcome after surgery alone or with restricted use of chemotherapy for patients with low-risk neuroblastoma: results of Children's Oncology Group study P9641.* J Clin Oncol, 2012. **30**(15): p. 1842-8.

[88] Smith, V. and J. Foster, *High-Risk Neuroblastoma Treatment Review.* Children (Basel), 2018. **5**(9).

[89] Turinetto, V. and C. Giachino, *Multiple facets of histone variant H2AX: a DNA double-strand-break marker with several biological functions.* Nucleic Acids Res, 2015. **43**(5): p. 2489-98.

[90] Musumeci, F., et al., *An update on dual Src/Abl inhibitors.* Future Med Chem, 2012. **4**(6): p. 799-822.

[91] Backman, U. and R. Christofferson, *The selective class III/V receptor tyrosine kinase inhibitor SU11657 inhibits tumor growth and angiogenesis in experimental neuroblastomas grown in mice.* Pediatr Res, 2005. **57**(5 Pt 1): p. 690-5.

[92] Chou, T.C., *Drug combination studies and their synergy quantification using the Chou-Talalay method.* Cancer Res, 2010. **70**(2): p. 440-6.

[93] Carmeliet, P. and R.K. Jain, *Principles and mechanisms of vessel normalization for cancer and other angiogenic diseases.* Nat Rev Drug Discov, 2011. **10**(6): p. 417-27.

[94] Seeger, R.C., *Immunology and immunotherapy of neuroblastoma.* Semin Cancer Biol, 2011. **21**(4): p. 229-37.

[95] Maris, J.M., et al., *Neuroblastoma.* Lancet, 2007. **369**(9579): p. 2106-20.

Targeting MYC and HDAC8 with a Combination of siRNAs Inhibits Neuroblastoma Cells Proliferation In Vitro and In Vivo Xenograft Tumor Growth

Nagindra Prashad

Abstract

HDAC8, c MYC and MYCN are involved in the tumorigenesis of neuroblastoma. A mouse Neuroblastoma (NB) tumor model was used to understand the role of miRNA, miR-665 in NB tumorigenesis and cellular differentiation. During cellular differentiation of NB cells there is an up regulated miRNA-665. We found that HDAC 8, c MYC and MYCN are the direct targets of mimic miR-665 which was validated by luciferase reporter plasmid with 3' UTR and ELISA. Mimic miR-665 inhibited cell proliferation, arrested cells in G1 stage and decreased S Phase in cell cycle. miR-665 increased the acetylation of histones and activated Caspase 3. This is the first report to recognize miRNA 665 as a suppressor miRNA of NB. The effects of miR-665 were confirmed with the transfection of siRNA for HDAC8 and siRNA for MYC. Individual siRNA- HDAC8 or siRNA-MYC inhibited 40–50% of cell proliferation in vitro, however, the treatment with the combination of both siRNA-MYC + siRNA- HDAC8 inhibited 86% of cell proliferation. Indicating that both the targets c MYC and HDAC 8 should be reduced to obtain a significant inhibition of cell proliferation. Intratumoral treatment of xenograft tumors in mice with the combination of siRNA-MYC + siRNA- HDAC8 reduced the levels of target c-MYC protein by 64% and target HDAC 8 protein by 85% and the average tumor growth reduced by 80% compared to control tumors treated with NC-siRNA. Our results suggest the potential therapeutic effect of suppressor miR-665 and the combination of siRNA-MYC + siRNA-HDAC8 for neuroblastoma treatment.

Keywords: neuroblastoma, miRNA, siRNA, MYC, HDAC8

1. Introduction

Neuroblastoma is the most frequently diagnosed extracranial solid tumor in children. About 90% of cases occur in children less than 5 years old and it is rare in adults. Of cancer deaths in children, about 15% are due to neuroblastoma [1]. Chances of long-term survival, however, are less than 40% despite aggressive treatment [2].

MYC is an oncogenic transcription factor that is overexpressed in many types of cancer. MYC has been shown to directly upregulate a protumorigenic group of miRNAs and represses several suppressor miRNAs, thus contributing to tumorigenesis [3]. For example, MYC overexpression can upregulate the oncogenic miR-17-92 cluster, that are directly activated in lymphoma [4], and can also repress several suppressor miRNAs [3]. The MYC gene is amplified in various human cancers, including in lung carcinoma, breast carcinoma, and colon carcinoma [5].

Histone deacetylases affect gene expression by altering the histone acetylation status, and that as a consequence, HDAC overexpression contribute to tumorigenesis by affecting the expression of key mRNAs and miRNAs. HDACs are overexpressed in most cancers, leading to histone deacetylation, inhibition of growth- suppressive genes, and increased cell proliferation [6]. HDAC8 overexpression correlates with advanced neuroblastoma in patient tumor samples, and HDAC8 inhibition reduced cell proliferation and induced neuroblastoma cell differentiation [7]. HDAC inhibitors reduced the proliferation and induced the apoptosis of neuroblastoma cells in vitro and in vivo in mice [8, 9].

Given that both MYC and HDACs play an important role in the maintenance of the normal cellular physiological functions and that their overexpression is linked to neuroblastoma tumorigenesis, we asked whether the levels of both MYC and HDAC8 should be reduced to obtain significant inhibition of cell proliferation.

Our results demonstrate that miR-665 targets c-MYC and HDAC8 m RNA, miR-665 treatment also increased the percentage of cells in G1 phase and reduced the percentage of cells in S phase of the cell cycle. This is the first report to show that miR-665 is a suppressor miRNA directly targeting the 3'-UTR of c-MYC and HDAC8 in neuroblastoma [10].

We investigated the effects of small interfering RNAs (siRNAs) targeting HDAC8 and MYC in murine neuroblastoma cells. RNA interference is a process of posttranscriptional gene silencing in which a double stranded RNA inhibits gene expression in a sequence-dependent manner via degradation of the corresponding mRNA. siRNAs can be used as potent and specific tools for gene knockdown. Several laboratories have reported siRNA targeting of gene expression in cancer cells and the inhibition of cell proliferation *in vitro* and tumor growth *in vivo* [11–14].

We reported that *in vitro*, single-agent siRNA HDAC8 or siRNA-MYC inhibited cell proliferation by 40–50%; however, treatment with the combination of siRNA MYC + siRNA-HDAC8 inhibited cell proliferation by 86% [10]. To further confirm these findings in an animal model, we set out to verify if tumor growth can be inhibited in a neuroblastoma xenograft mouse model when tumors are treated with a combination of siRNA-MYC and siRNA HDAC8. Our findings from this study show that the tumor growth was reduced by 80% following intratumoral delivery of a combination of siRNAs targeting both MYC and HDAC8 simultaneously [15].

2. Materials and methods

2.1 Reagents

Cell culture media, DMEM with high glucose (D6429), essential and non-essential amino acids (M5550, m7145), Bt2c AMP (D0627), the colorimetric Caspase 3 kit (Code CASP-3-C), and propidium iodide (P4170) were purchased from Sigma Aldrich, St. Louis. Fetal bovine serum (FBS) was purchased from Phenix Research Products, Candler, NC, USA. BD-Falcon tissue culture 96-well plates (353072) were purchased from BD Biosciences. The RNA extraction miR-Neasy kit (Cat No. 217084) was purchased from Qiagen, Germantown, MD, USA.

The MTS Cell. Titer 96 Aqueous One Solution (Cat # G3580) cell proliferation assay was purchased from Promega Biotechnology, Madison,WI, USA. The HDAC Kit (#K331–100) was purchased from BioVision, Inc. Co rning. 96-well EIA/RIA plates (CLS3369) were used for ELISA. Antibodies for HDAC 8, H-145 (sc11405), C MYC, C-19 (SC-786), acetylated Histones, Ac- H2B, Lys 5/12/15/20 (SC-8652), Ac-H3, lys9 (sc-8655), Ac-H4, lys16 (sc-8662), and siRNA for c-MYC (pool of 4 different siRNA duplexes, sc-29227) were purchased from Santa Cruz Biotechnology, Dallas, TX, USA. Negative control #2 siRNA (#4390846), siRNA-HDAC 8 (S88696) and Lipofectamine RNAi Max (#13778075) were purchased from Life Technologies/ Ambion/ Invitrogen. Negative control miRNA Cel-miR-67 (#CN-001000) sequences based on *C. elegans* miRNA, mimic hsa-miR-665 (#C 301246–01), and transfection reagent Dharmafect Duo (#T2010–01) were purchased from Dharmacon. Luciferase expression plasmids with the 3'-UTR for HDAC8 (#S804229), C-MYC (#S804638), MYCN (Product No S807230), or empty vector without 3'-UTR (#S890005), and the LightSwitch luciferase assay kit (#32031, LS010) were purchased from Active Motif, CA, USA.

2.2 Cells and cell culture

Mouse neuroblastoma cholinergic clonal cells (S20) were obtained from Dr. Marshall Nirenberg of The US National Institutes of Health (NIH). Cells were grown in monolayers in DMEM supplemented with essential and nonessential amino acids, penicillin/streptomycin, and 10% FBS at 37°C with 5% CO_2 and humidity.

Neuroblastoma cells were plated in 96-well plates at $12x10^3$ cells per well and After 48–72 h, cell viability was measured colorimetrically using the MTS Cell Titer 96 Aqueous One Solution. Samples were incubated at 37°C for 3–4 h and samples were read at 490 nm in a plate reader according to the manufacturer's instructions.

For cell cycle analysis, $1x10^6$ cells were plated in T25 flasks. After 48 h, cells were trypsinized, treated with 75% ethanol and 100ug/ml RNAse A, and then stained with propodium iodide (PI). Untreated and (20,000 cells/ sample) were analyzed for cell cycle distribution via flow cytometry at the Core lab of Children's Cancer Center Hospital, Houston, TX, USA.

2.3 Transfections

The effects of miR-665 or siRNA on cell proliferation were determined using reverse transfection. First, 100 nM negative control miRNA, miR-665, negative control siRNA, C-MYC siRNA, or HDAC8 siRNA was mixed with Lipofectamine RNAimax. This mixture was added to $12x10^3$ cells, which were then plated in 96-well plates. After 48–72 h, cell viability was measured using MTS Cell Titer 96 Aqueous One Solution and incubated at 37°C for 3–4 h. Samples were read at 490 nm according to manufacturer's instructions.

miRNA effects on the cell cycle were assessed using reverse transfection of cells with 100 nM negative control miRNA or miR-665 mimic plus Lipofectamine RNAimax. The transfection mixture was added to $1x10^6$ cells, which were then plated in a T25 flask. After 48 h, cells were trypsinized, treated with 75% ethanol and 100ug/ml RNAse A, and then stained with PI. For cell cycle analysis, 20,000 cells/sample were analyzed via flow cytometry in the Core lab of Children's Cancer Center Hospital, Houston, TX.

2.4 Whole cell extracts

Cell extracts were prepared from untreated,, and miRNA transfected cells for target assays. miRNA-transfected cells were reverse transfected with 100 nM

negative control miRNA, miR-665, negative control siRNA, c-MYC siRNA, or HDAC8 siRNA plus Lipofectamine RNAimax. Transfected cells were plated in T25 flasks. After 48–72 h, cell extracts were prepared in assay buffer as described by Khandelia, *et al.* [16]. Assay buffer consisted of 20 mM Tris–HCL pH 7.5, 150 mM NaCl, 5 mM EDTA, 10% glycerol, 1% Nonidet P40, and protease inhibitor cocktail from Sigma (P8340). Protein concentrations were determined using Pierce's BCA Assay as per the manufacturer's instructions.

miR-665 inhibit cell growth compared to untreated cells and cells treated with negative control miRNA. Assays were normalized using equal concentrations of protein (50–100 ug) from untreated, negative control miRNA-, and miR-665-treated cells in assessing total HDAC and Caspase 3 activity, and HDAC8 and c-MYC levels via ELISA.

2.5 Quantitation of miR-665 in transfected cells

Mouse neuroblastoma cells were transfected with 100 nM miR-665 mimic and negative control cel-miR-67. 48 h post-transfection, total RNA was extracted from three biological replicates per treatment using the Qiagen RNEasy mini kit. miR-665 was quantitated via realtime qPCR by Arraystar, Inc. (Rockville, MD, USA).

Real-time PCR was performed for each RNA sample to quantify miR-665 and the housekeeping gene, U6. According to the standard curve, mRNA concentrations in each sample are determined directly using Rotor-Gene Real-Time Analysis software v.6.0 and the $2^{\Delta\Delta Ct}$ method.

2.6 Total HDAC activity

Total HDAC activity was measured in 50–75ug of protein from cell extracts prepared from untreated, or negative control miRNA- or miR 665-transfected cells using the Biovision kit (#K331–100). Acetylated HDAC substrate and other reagents were added according to the manufacturer's instructions and the final deacetylated product was read at 405 nm in a plate reader.

2.7 HDAC8 and c-MYC protein quantitaion via ELISA

HDAC8 and c-MYC proteins were quantitated using cell extracts prepared from untreated or 1 mM Bt2cAMP treated cells, or negative control miRNA- or miR-665- transfected cells via ELISA. 100ug protein per sample was mixed with 0.02 M carbonate coating buffer (pH 9.5) and added to 96-well BD-Falcon ELISA plates.

Samples were incubated at 4°C for 15 h. Wells were blocked with 10% FBS in PBS, treated with antibodies (diluted 1:30) specific for HDAC8 (SC11405) or c-MYC (SC-798), and incubated at 37°C for 2 h. Samples were washed with PBS + 0.05% Tween, treated with goat anti-rabbit IgG.

HRP secondary antibody (diluted 1:500), and incubated at 37°C for 1 h. Wells were washed and treated with substrate TMB and incubated at room temperature for 30 min, and then the reaction was stopped with 2 N H_2SO_4. Samples were read at 450 nm in a plate reader.

2.8 Caspase 3 activity

Caspase 3 activity was measured in 50ug protein from untreated, Bt2cAMP-treated, or miR-665-transfected cells using Sigma Aldrich's colorimeter kit (Code

CASP3-C). 50ug protein was mixed with the peptide substrate, Ac-DEVD-pNA (p-nitroanilide), in the presence of 10 mM DTT. Caspase 3 hydrolyzes the substrate, releasing p-nitroaniline, which is read at 405 nm. The specificity of caspase 3 activity was determined in the presence of the inhibitor, Ac-DEVD- CHO.

2.9 Target validation using luciferase expression plasmids

HepG2 cells were used for miR-665 target validation, because miR-665 does not inhibit the growth of these cells. When mouse neuroblastoma cells were used for target validation, the negative control luciferase vector plasmid without any target 3'-UTR showed a 50% decrease in luciferase activity when co-transfected with miR-665 compared to negative control miRNA. This decrease in luciferase activity was non-specific and was caused by cell growth inhibition due to miR-665 transfection.

To validate miR-665 targets, HepG2 cells were grown for 24 h in a 96-well plate. Cells were then co transfected with 100 ng luciferase expression plasmids containing the 3'-UTR for HDAC8, c-MYC, or MYCN, or the empty vector without any target 3'UTR, plus 100 nM negative control miRNA or miR-665 with Dharmafect Duo transfection agent. After 48 h of cotransfection, luciferase activity was measured using the Active Motifs LightSwitch luciferase assay kit. Luminescence was read on a Molecular Devices Soft Max Pro5 luminometer.

2.10 Histone acetylation

Histone acetylation was quantified via ELISA in cell extracts prepared from cells transfected with negative control miRNA, miR-665, negative control siRNA, or HDAC8 siRNA. 100ug protein was mixed with 0.02 M carbonate coating buffer (pH 9.5), added to 96-well BD Falcon ELISA plates, and incubated at 4°C for 15 h. Wells were blocked with 10% FBS in PBS, treated with acetylated antibodies (diluted 1:30) for Ac H2B (Lys 5/12/15/20), Ac-H3 (lys9), or Ac-H4 (lys16), and incubated at 37°C for 2 h. Samples were washed with PBS + 0.05% Tween, treated with an appropriate HRP-conjugated secondary antibody (diluted 1:500), and incubated at 37°C for 1 h. Wells were washed and treated with substrate TMB and incubated at room temperature for 30 min, and then the reaction was stopped using 2 N H_2SO_4. Samples were read at 450 nm in a plate reader.

2.11 Neuroblastoma tumor model

Mice experiments were performed with the approval of the institutional Animal Care and Use Committee, IACUC at Nanospectra Biosciences Inc. Houston, Texas.

A/J female mice six weeks old were purchased from Jackson Laboratory, Bar Harbor, Maine, USA. Murine neuroblastoma cells, 1x106 cells in DMEM media with 50% matrigel in 100 ul without fetal bovine serum and without antibiotics were subcutaneously injected on the right flanks. After 12 days, tumor growth can be seen and tumors were measured with a caliper.

When tumors reached 100 mm3 in size, mice were divided into two groups with 8–10 mice in each group.

Intratumoral delivery of siRNA.

siRNA-HDAC8 (S88696), Sense Sequence: (5′----3′).

CGACGGAAAUUUGACCGUAtt.

Antisense Sequence:

UACGGUCAAAUUUCCGUCGca.

siRNA-MYC (S70224), Sense Sequence: (5′------3′).

AGGUAGUGAUCCUCAAAAAtt.

Antisense Sequence: UUUUUGAGGAUCACUACCUtg.

Negative control #2 siRNA (#4390846), and Lipofectamine RNAi Max (#13778075) were purchased from Life Technologies/Ambion.

A total of 3 nmol Negative control siRNA or 3 nmol combinations of siRNA-MYC + siRNA-HDAC8 were mixed with Lipofectamine RNAi max (Liposome) in DMEM media without fetal bovine serum and without antibiotic. siRNA complexed with Lipofectamine in a volume of 30 ul was delivered into tumors by intratumoral injection every third day. Tumors were measured every second day with a caliper and mice were weighed every third day. Tumor volume was calculator with a formula, V = Length X width2/2. Experiment was stopped when the control tumors treated with negative control siRNA reached a tumor burden volume of 1200 mm3. Mice were euthanized by CO_2 inhalation 2 days after last treatment with siRNA. Tumors were removed and weighed. Tumors were frozen in liquid nitrogen and stored at -80o C freezers until used for preparation of tumor extracts for ELISA.

2.12 Tumor extract preparation

Tumors treated with NC-siRNA or with combined siRNA-HDAC8 + siRNA-MYC were cut into small pieces and homogenized in assay buffer in a glass homogenizer. Assay buffer as described by Khandelia et al. [16], consisted of 20 mM Tris–HCL pH 7.5, 150 mM NaCl, 5 mM EDTA, 10% glycerol, 1% Nonidet P40, and protease inhibitor cocktail from Sigma (P8340). Protein concentrations were determined using Pierce's BCA Assay as per the manufacturer's instructions.

2.13 Statistical analysis

Error bars represent standard error of the mean (SEM) from 2 to 3 biological replicates from 3 to 5 independent experiments. P-values were calculated using T.Test (2 tailed, 3 samples, unequal variance) and $p < 0.05$ was considered statistically significant.

3. Results

3.1 miR-665 inhibits cell proliferation

NB cells transfected with miR-665 show changes in cell morphology, lost the normal spindle shape and cells grew in clumps without processes compared to cells transfected with negative control miRNA (**Figure 1A** and **B**). Cell cycle analysis results show that miR-665 treated cells show an increase of 16% of cells in G1 phase of cell cycle and the cell number decreased by 18% in S phase compared to negative control miRNA transfected cells. miR-665 treatment did not affect the cells in G2 phase (**Figure 1C**). Cell viability decreased proportionally with the increasing concentration of miR-665, represented by black bars (**Figure 1D**)**.**

3.2 miR-665 targets HDAC 8, c MYC and MYCN

Computational algorithm prediction site TargetScan and miRanda (microRNA. org) predicts mRNA targets for Mirna. *miranda* predicted hsa-miR-665 targets 3' UTR of HDAC 8 and the sequence alignment is presented in **Figure 2A**. *miranda*, also predicts that hsa-miR-665 targets MYCN 3' UTR and the sequence alignment is presented in **Figure 2B**.
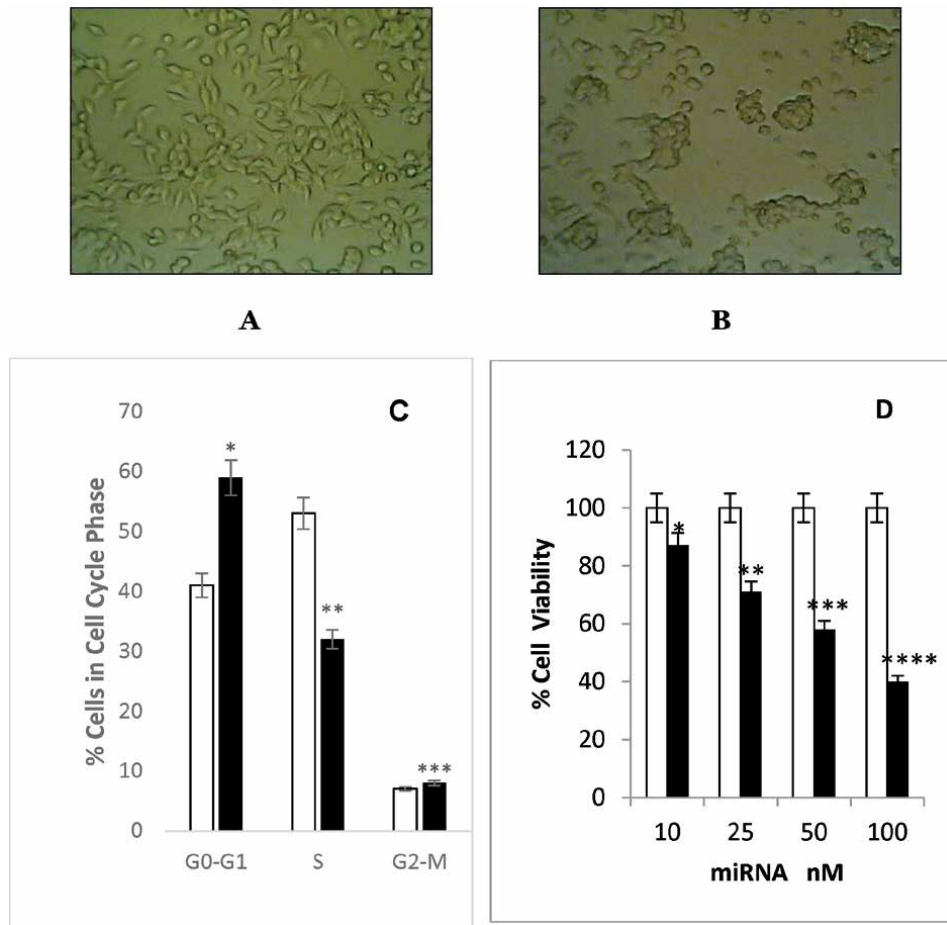
Figure 1.
miR-665 effects on cell proliferation (A) cells treated with 100 nM negative control miRNA and miR-665 (B) for 72 hr. were prepared for cell cycle distribution analysis. Propidium iodide stained cells were analyzed by FLOW cytometry (C) Several concentration of miR-665 effect on cell viability (D) STDEV was used for +/− standard error bar; data is from 2 independent experiments with 3 biological replicates for each experiment was used. (figures were printed from published article in "Oncotarget", N.Prashad Vol 9, 33186–33201, 2018).

MYC is overexpressed in 30% of all human cancers and frequently predicts for a poor clinical outcome, and deregulated expression of MYC is a hallmark feature of cancer [3] miRanda and Targetscan did not include 3' UTR of C MYC as miR-665 target. Therefore, Complimentary sequences between miR-665 and 3' UTR of C MYC were compared at online pairwise sequence alignment site www.ebi.ac.uk. Results show two complementary binding sites for miR-665 in the 3' UTR of c MYC (**Figure 2C**).

First we measured total HDAC activity in the cell extracts prepared from negative control miRNA and miR-665 transfected cells in the presence of acetylated HDAC substrate Ac-Lys (Ac)-p NA and deacetylated end product was measured colorimetrically. HDAC 8 and c MYC proteins were measured with antibody in ELISA. The results show that total Pan HDAC activity was decreased by 40%, and HDAC 8 and c MYC proteins were decreased by 40% in miR-665 transfected cells compared to negative control miRNA treated cells (**Figure 3A–C**).

Next, we tested whether HDAC 8, c MYC and MYCN genes are the direct target of miR-665. In these experiments HepG2 cells were used because miR-665 does not affect the growth of these cells (our unpublished results). Luciferase reporter
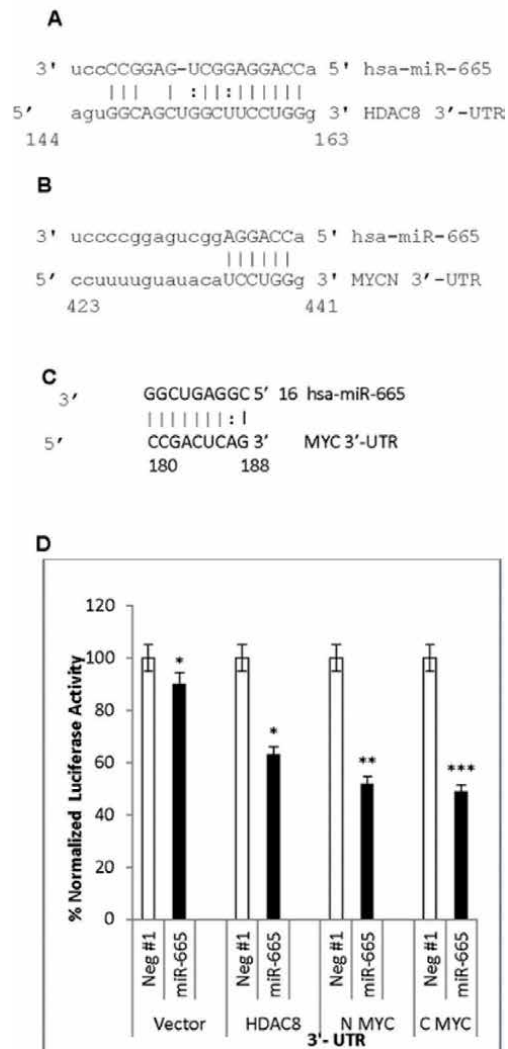
Figure 2.
Predicted binding sites for miR-665 in targets HDAC 8, c MYC and MYCN 3' UTR. Computational prediction site miRanda (microRNA.org) predicted hsa-miR-665 targets 3' UTR of HDAC 8 and the sequence alignment is presented in (A). miranda*, also predicts that hsa-miR-665 targets MYCN 3' UTR and the sequence alignment is presented in (B).* miranda *and Targetscan did not include 3' UTR of C MYC as miR-665 target. Therefore, complimentary sequences between miR-665 and 3' UTR of C MYC were compared at online pairwise sequence alignment site www.ebi.ac.uk. Sequence alignment is presented in (C). (D) miR-665 targets were validated by co transfection of 100 ng luciferase expression plasmids with 3'-UTR and 100 nM negative control miRNA and miR-665 into HepG2 cells. Empty vector without 3' UTR was used as a control. After 48 hr., luciferase activity was measured and normalized luciferase activity is presented. Data is presented from 2 independent experiments with 3 biological replicates were used. STDEV was used for +/− standard error bar. (figures were printed from published article in "Oncotarget", N.Prashad Vol 9, 33186–33201, 2018).*

plasmids with 3' UTR were cotransfected with negative control miRNA and miR-665 in HepG2 cells and after 48 hr. luciferase activity were measured in cell extracts. Results show a 40% decrease in luciferase activity of HDAC 8 3' UTR, a 51% decrease in luciferase activity of c MYC 3' UTR and a 50% decrease in luciferase activity of MYCN 3'UTR from the cells co transfected with miR-665 compared to the co transfection with negative control miRNA (**Figure 2D**). These results validate that m RNAs of HDAC 8, c MYC and MYCN are the direct targets of suppressor miR-665.
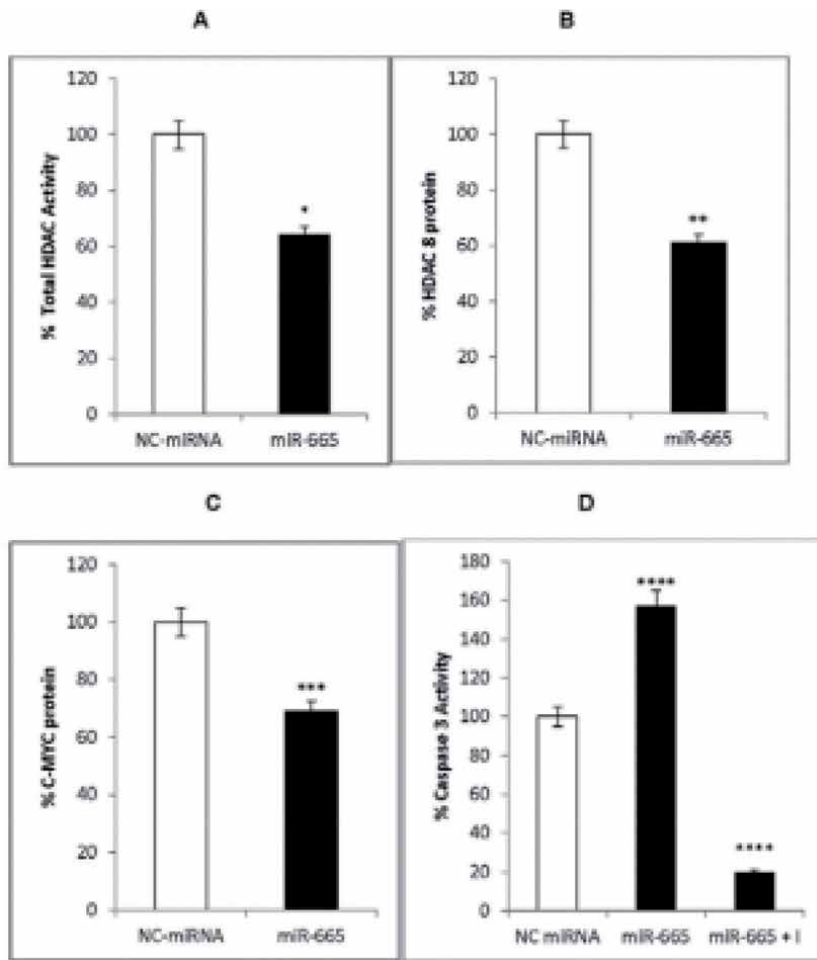
Figure 3.
miR-665 effect on target HDAC 8, c MYC and MYCN cell extracts from100nM negative control miRNA and miR-665 transfected cells were used for the quantitation of; (A) total HDAC activity, (B) HDAC8 protein by ELISA, (C) c MYC protein by ELISA and (D) caspase 3 activity and specificity of caspase 3 enzyme activity was determined in the presence of inhibitor. Data is presented from 2 independent experiments with 3 biological replicates were used. STDEV was used for +/− standard error bar. (figures were printed from published article in "Oncotarget", N.Prashad Vol 9, 33186–33201, 2018).

3.3 MiR-665 induced activation of caspase 3

HDAC inhibitors induce the caspase 3-dependent apoptosis [8] Suppressor miR-34a increased the activation of caspase 3 and caused caspase dependent apoptosis in neuroblastoma cells [17, 18]. Caspase 3 is a critical part of apoptosis, and is required for the DNA fragmentation and for the typical morphological changes of cells undergoing apoptosis. We investigated the effect of miR-665 on the activation of caspase 3 and activity was measured by the hydrolysis of the peptide substrate attached to p-nitroanilid. Caspase 3 activity was measured in cell extracts prepared from cells transfected with negative control miRNA and miR-665. Results show that caspase 3 activity was increased by 2.5-fold in miR-665 transfected cells compared to negative control miRNA (**Figure 3D**). Specificity of the caspase 3 was determined by the addition of caspase 3 inhibitor TSA before the addition of substrate in the assay. The results show that inhibitor binds to caspase 3 and inhibited 90% of miR-665 activated caspase 3 activity **(Figure 3D)**. These

results show that mimic miR-665 activated caspase 3 in neuroblastoma cells, suggesting that miR-665 can inhibit cell growth and reduced viable cells by caspase 3 dependent apoptosis.

3.4 miR-665 levels following transfection

miR-665 levles were quantitated in neuroblastoma cells transfected with negative control miRNA and miR 665 using real time qPCR. Mouse neuroblastoma cells have very low levels of endogenous miR-665 (**Figure 4A**); however, miR-665 expression increased 848-fold in cells transfected with mimic miR-665 compared to cells transfected with the negative control miRNA, cel miR-67 (**Figure 4A** and **B**). miRNA levels reportedly increased by over 1000-fold in cells transfected with miR 200a [19]. Our results strongly indicate that miR-665 upregulation decreased MYC and HDAC8 expression, thus inhibiting proliferation and inducing apoptosis in mouse neuroblastoma cells.
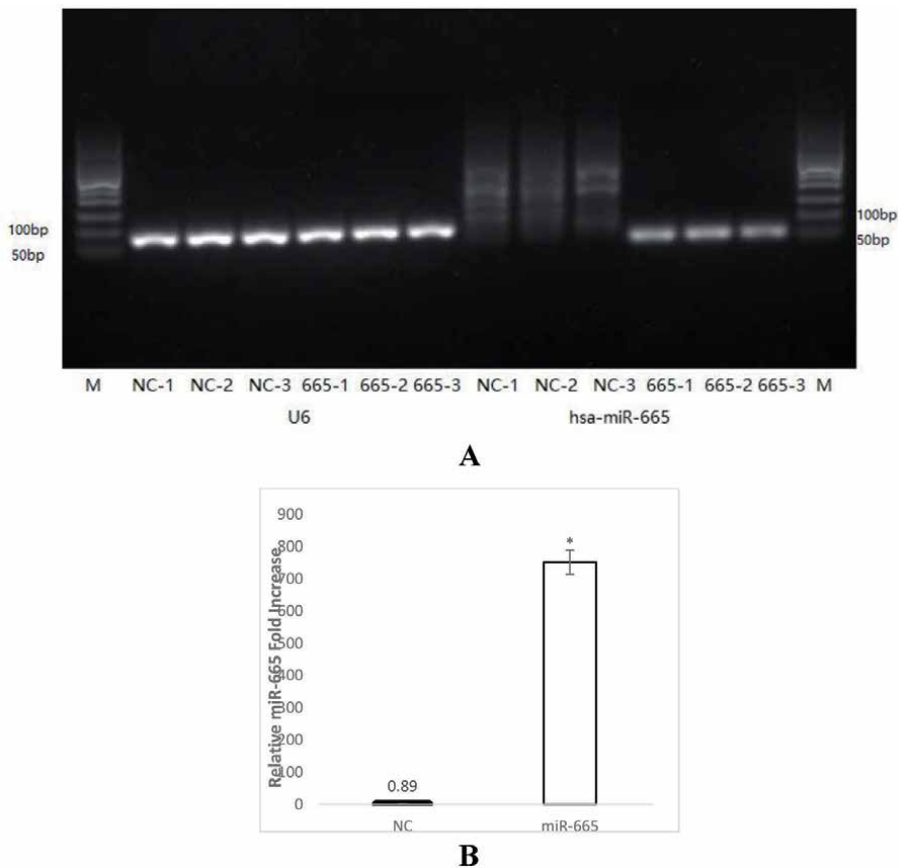
Figure 4.
*Quantitation of miR-665 in transfected cells. miR-665 was quantitated via real-time qPCR normalized to the U6 gene from three biological replicates 48 h after transfection with negative control miRNA (cel-miR-67) or miR-665. From left, lane 1 and 14 (M), show DNA molecular weight ladder (A) lanes 2–7 (NC-1–NC3 and 665–1–665-3) show the U6 gene. Lanes 8–10 (NC-1–NC3) show miR-665 levels from cells transfected with negative control miRNA. Lanes 11–13 (665–1–665-3) show miR-665 levels from cells transfected with miR-665. The miR-665 fold increase in miR-665-transfected cells was quantitated using the 2-ΔΔCt method (B) miR665 levels are shown in cells transfected with negative control miRNA (black bar) and in miR-665-transfected cells (white). Error bars were calculated from the standard deviation from three biological replicates. *P < 0.54x10–6. (figures were printed from published article in "Oncotarget", N.Prashad Vol 9, 33186–33201, 2018).*

3.5 siRNA effect on mouse neuroblastoma cells

miRNA targets hundreds of m RNAs and suppresses their expression, however, siRNA targets a specific m RNA. In these experiments, siRNA for HDAC 8 (siRNA-HDAC 8) and siRNA for MYC (siRNA-c MYC) were used to substantiate the effects of miR-665 on neuroblastoma cells.

3.6 SiRNA effect on cell proliferation

NB cells were transfected with negative control siRNA, siRNA-HDAC 8, siRNA-c MYC and the combination of siRNA-HDAC 8 + siRNA-c MYC. After 48 hr. of growth, cell viability was determined with CellTiter assay (Promega). SiRNA-HDAC8 inhibited 42% and siRNA-c MYC inhibited 55% of cell proliferation, however, the combination of both siRNAs inhibited 86% of the growth of the cells (**Figure 5A**). Therefore, the combination of siRNA-HDAC8 plus siRNA-c MYC was more targeted towards mRNA of HDAC8 and c MYC and caused more effective apoptosis and loss of cells. These results show that HDAC 8 and MYC are critical targets and inhibition of both targets is required for the inhibition of neuroblastoma.

3.7 SiRNA effect on HDAC 8 and C MYC

HDAC 8 and c MYC proteins were quantitated by antibody in ELISA in cell extracts prepared from the cells transfected with negative control siRNA and siRNA-HDAC 8. The results show that siRNA-HDAC 8 transfection inhibited 40% of HDAC 8 proteins (**Figure 5B**) as well as inhibited 35% of MYC protein. Inhibition of MYC may be indirect effect of HDAC 8 inhibition. HDAC8 inhibition increases acetylation of histones and alters gene expression, thus decreasing MYC expression. Therefore, miR-665 represses the expression of c MYC both at the transcription and at the post transcription levels. siRNA-HDAC 8 and siRNA-c MYC substantiated the effects of miR-665 on neuroblastoma cells.

3.8 siRNA activates caspase 3

Caspase 3 activity was measured in the cell extracts prepared from cells transfected with negative control siRNA, siRNA-HDAC8 and siRNA-c MYC. The results show that siRNA-HADC8 increased the activity of caspase 3 by 1.8-fold and siRNA –c MYC increased the activity of caspase 3 by 2.5-fold compared to negative control siRNA (**Figure 5C**). Therefore, the results of siRNA effects substantiate the effects of miR-665 on the activation of caspase 3.

3.9 Effect of miR-665 and siRNAs on histone acetylation

Our results show that miR-665 and siRNA-HADC8, decreased total HDAC activity and decrease HDAC 8 protein, therefore, we measured the acetylation of histones in the cell extracts and the results were compared among all treatments. MiR-665 transfected cells show increases in the acetylation of histones Ac-H2B by 25%, Ac-H3 by 40% and Ac-H4 by 50% compared to negative control miRNA transfected cells (**Figure 6A**). miR-665 acetylates predominantly H3 and H4 histones.

Likewise, Si RNA-HDAC8 treated cells also show increases in the acetylation of histones Ac-H2B by 38%, acetylation of Ac-H3 by 58% and show higher acetylation of Ac-H4 by 2-fold (200%) compared to negative control siRNA treated cells
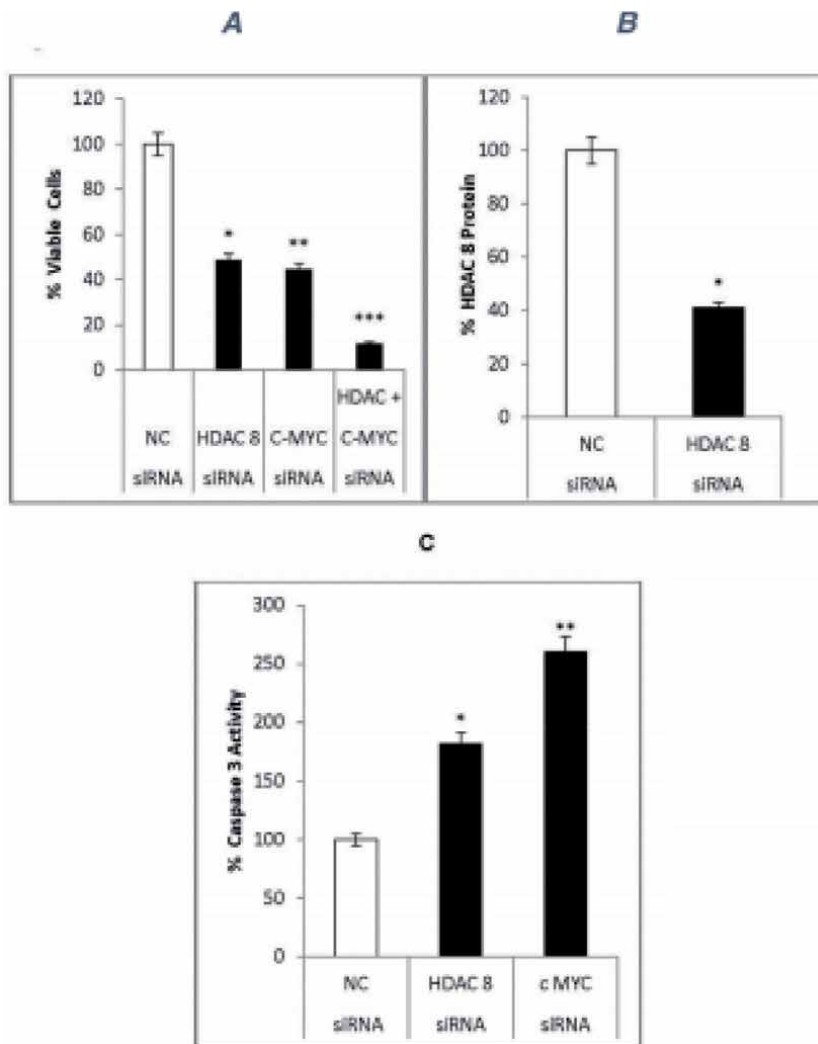
Figure 5.
siRNA effects on neuroblastoma cells. siRNA specific for HDAC8 (siRNA-HDAC8) or c-MYC (siRNA-c-MYC, a mixture of 4 siRNAs) were used to confirm the effects of miR665 in neuroblastoma cells. (A) siRNA effect on cell proliferation. Neuroblastoma cells were transfected with 50 nM siRNA-HDAC8, 100 nM siRNA-c-MYC, or both siRNAs together. Cell viability was measured via MTS assay. SEM bars represent the standard deviation from two independent experiments with three biological replicates each. *P < 0.005, **P < 0.001, ***P = 6.8x10–5. (B) Cell extracts from negative control siRNA- or siRNA-HDAC8-treated cells were used to quantify HDAC8 levels via ELISA. HDAC8 was down regulated in HDAC8-siRNA-transfected cells *P < 0.04. (C) Caspase 3 activity was quantified in cell extracts via Casp-3 kit. Caspase 3 activity increased in siRNA-HDAC8- and siRNA-c-MYC-transfected cells. SEM bars represent the standard deviation from two independent experiments with two biological replicates each. *P < 0.01, **P < 0.004. (figures were printed from published article in "Oncotarget", N.Prashad Vol 9, 33186–33201, 2018).

(**Figure 6B**). siRNA-HDAC8 acetylated predominately AC-H4 and correlate with the results of miR-665.

3.10 miR-665 targets c-MYC and HDAC8

Taken together, our results indicate that miR-665 targets c-MYC and HDAC8, decreasing their expression, increasing histone acetylation, and modulating expression of cell proliferation related genes. We propose a model (**Figure 7**)
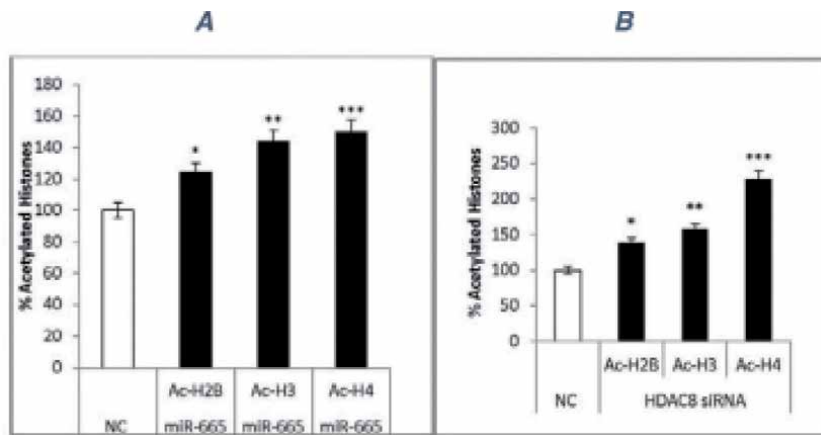
Figure 6.
Histone acetylation. Cell extracts from negative control miRNA-, miR-665-, negative control siRNA-, or siRNA-HDAC8 treated cells were used to quantitate histone acetylation via ELISA. Data represent standard deviations from two independent experiments. Negative control miRNA (white) and miR-665 transfection increased histone acetylation (black) (A) *P < 0.01, **P < 0.01, ***P < 0.04. Negative control siRNA (white) and siRNA-HDAC8 increased histone acetylation (black) (B) *P < 0.008, **P < 0.04, ***P < 0.001.
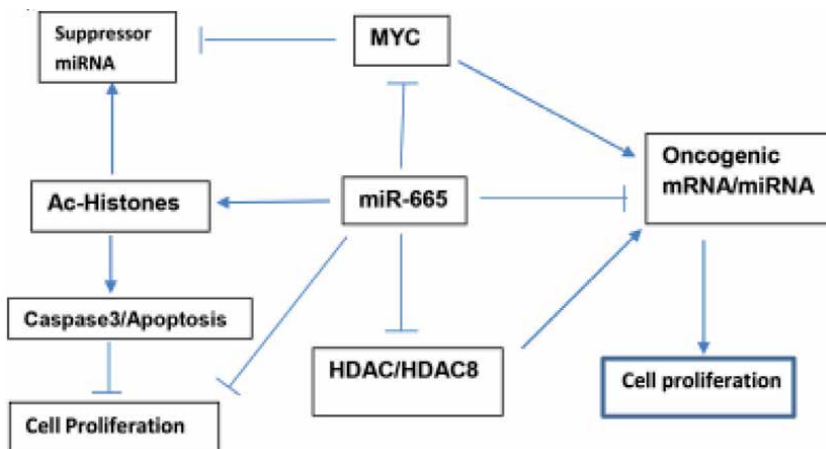
Figure 7.
Proposed model illustrating how suppressor miR-665 targets c-MYC and HDAC8 to inhibit neuroblastoma cell proliferation and maintain cellular homeostasis. (figures were printed from published article in "Oncotarget", N.Prashad Vol 9, 33186–33201, 2018).

illustrating suppressor miR-665 involvement in the inhibition of neuroblastoma cell proliferation [10].

3.11 Effects of combination of siRNA-HDAC 8 ± siRNA-MYC on neuroblastoma cells in vitro

When cells were treated with the combination of siRNA HDAC 8 + siRNA-MYC, cell proliferation was inhibited by 86% [10]. Therefore, HDAC 8 and MYC are critical targets and effective blockade of both targets is required to ensure a maximum inhibition of neuroblastoma cell proliferation.

On the basis of these results, we hypothesized that neuroblastoma tumor xenograft growth in mice can be inhibited when treated with the combination of siRNA-MYC + siRNA- HDAC8.

3.12 Neuroblastoma tumor treatment with the combination of siRNA-HDAC8 + siRNA-MYC

We explored the therapeutic effect of the combination of siRNA-HDAC8 + siRNA-MYC treatment on neuroblastoma tumor xenograft in mice. A total of 1x106 mouse neuroblastoma cells in 50% Matrigel were inoculated subcutaneously in 6 weeks old female A/J mice. Tumors were formed with an average
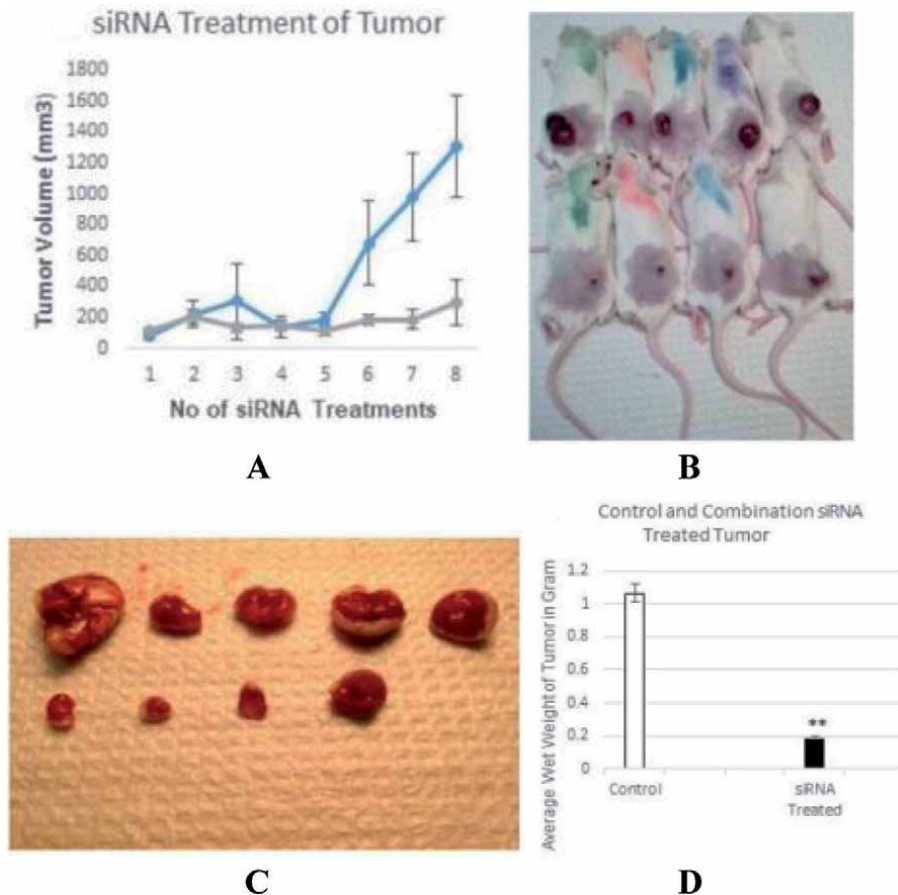

Figure 8.
(A) Effect of combination of siRNA on the growth of neuroblastoma tumor. Murine neuroblastoma cells, 1 × 106 cells in DMEM media with 50% matrigel in 100 ul were subcutaneously injected on the right flanks. After 12 days, tumor growth can be seen and tumors were measured with a caliper. When tumors reached 100 mm3 in size, mice were divided into two groups with 8 mice in each group. Negative control siRNA or combination of siRNA-MYC + siRNA-HDAC8 was mixed with Lipofectamine RNAi max (liposome) in DMEM media without fetal bovine serum and without antibiotic. siRNA complexed with Lipofectamine in a volume of 30 ul was delivered into tumors by intratumoral injection every third day. Tumors were measured every second day with a caliper and mice were weighed every third day. Tumor volume was calculator with a formula, V = length × width 2 /2. The numbers on X-axis show the number of siRNA treatments. Control tumor growth is shown by diamond (^) markers and the growth of tumors treated with siRNAs is shown by round (o) markers. SEM bars represent the standard deviation from 8 mice at each point P* < 0.031. (figure is printed from published article in "J. Cancer Biology and Therapeutics" N. Prashad V 6: 301–307 2020). (B) Mice with control and combination of siRNA treated tumors. Top row of mice with control tumors treated with NC siRNA and the bottom row of mice with tumors treated with the combination of siRNA-MYC + siRNA-HDAC. (C) Tumors from control and combination of siRNA treated mice. Top row representative control tumors treated with NC-siRNA and the bottom row representative tumors treated with the combination of siRNA-MYC + siRNA-HDAC8. (figure is printed from published article in "J. Cancer biology and therapeutics" N. Prashad V 6: 301–307 2020). (D) Weights of control and combination of siRNA treated tumors. Average of 8 control tumors was 1 gram and average of 8 tumors treated with combination of siRNA MYC + siRNA-HDAC8 was 0.186 gram. SEM bars represent the standard deviation from 8 tumors P** < 0.004.

volume of 100 mm3, 12 days after cells were inoculated. A 3 nmol negative control siRNA (NC-siRNA) or a 3 nmol combination of siRNA-HDAC + siRNA-MYC complexed with Lipofectamine RNAi max (Invitrogen) were inoculated into 10 tumors each by intratumoral injections every 3rd day. Tumor growth was measured every 2 days with a caliper and volume was calculated with the formula, length X width2/2. The growth of control tumors treated with NC-siRNA increased, however, the tumors treated with the combination of siRNA-HDAC8 + siRNA-MYC show inhibition of the growth of tumors (**Figure 8A**). The rates of tumor growth were significantly decreased when treated with combined siRNA-MYC + siRNA-HDAC8 compared to tumors treated with control negative siRNA.

All mice experiments were performed under IACUC approved animal study protocol.

Experiment was stopped when the control tumors reached an average volume of over 1200 mm3, then mice were euthanized by CO_2 and tumors were removed and weighed. Pictures of mice with tumors were taken before tumors were removed (**Figure 8B**) and pictures of tumors removed and weighed are shown in (**Figure 8C**). The average wet weight of 8 control tumors treated with NC-siRNA and tumors treated with combination of siRNA-HDAC + siRNA-MYC is presented in **Figure 8D**. The average weight of tumors treated with the combination of siRNA-HDAC8 + siRNA-MYC was decreased by 5-fold [0.186 g] compared to average weight of control tumors [1 g] treated with NC-siRNA. Tumor xenograft experiment was repeated twice with 10 mice treated with NC-siRNA and 10 mice treated with a combination of siRNA-HDAC8 + siRNA-MYC.

3.13 The quantitation of targets HDAC 8 and MYC in tumors

Tumor targets HDAC 8 and MYC proteins were quantitated by ELISA in extracts prepared from tumors treated with negative control siRNA and combination of siRNA-HDAC 8 + siRNA-MYC treated tumors. The results indicate that targets HDAC 8 and MYC were decreased by 85% and 65% in tumors treated with the
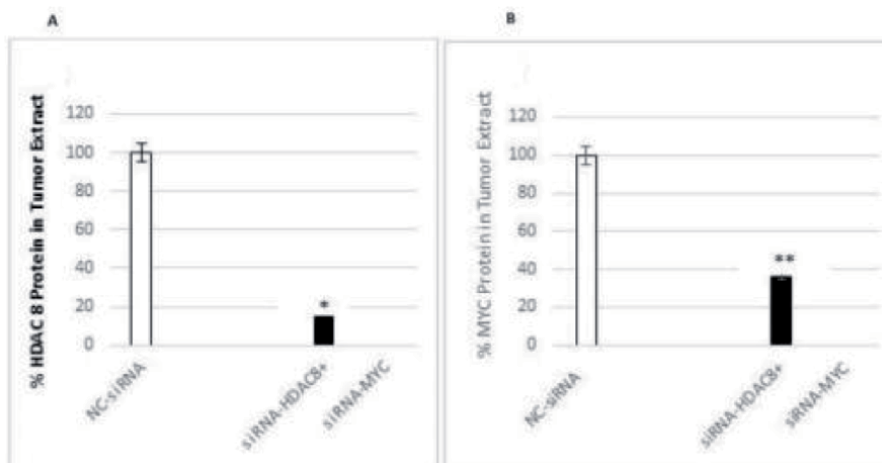

Figure 9.
(A, B) Quantitation of Myc and Hdac8 proteins from control and combination of siRNA treated tumors. Tumor targets Hdac8 and Myc proteins were quantitated by ELISA in extracts prepared from 3 tumors treated with negative control siRNA and 3 tumors treated with the combination of siRNA-HDAC 8 + siRNA-MYC. Average targets Hdac8 (A) and Myc (B) proteins were decreased by 85% and 65% in tumors treated with the combination of siRNA-HDAC8 + siRNA-MYC compared to tumors treated with NC-siRNA. SEM bars represent the standard deviation from 3 tumors (P* < 0.030, P** < 0.01). (figures printed from the article published in "J Cancer Biol Therap," N. Prashad 6(1): 301–307 (2020)).

combination of siRNA-HDAC8 + siRNA-MYC compared to tumors treated with NC-siRNA (**Figure 9A** and **B**).

The results indicate that a decrease in the tumor targets HDAC 8 and MYC caused the inhibition of the growth of tumors.

4. Discussion

miRNAs are both oncogenic and tumor suppressors. In normal cells homeostasis is maintained by keeping equilibrium between oncogenic and suppressor miRNA. If this equilibrium is disrupted that can cause dysfunction with increases in oncogenic miRNA and decreases in suppressor miRNA. A decrease in a specific suppressor miRNA can cause overexpression of HDCAs, c MYC and MYCN which can alter gene expression and cause cancer. However, when suppressor miRNAs are added exogenously to these cells then these cells restore normal properties and show growth arrest and apoptosis Therefore, suppressor miRNAs seem to be critical in the maintenance of cellular homeostasis.

A decrease in suppressor miRNA can over express genes like c MYC, MYCN and HDACs and cause cancers. Over expression of c MYC and MYCN cause the down regulation of suppressor miRNAs. HDACs indirectly effect gene expression by the deacetylation of histones, therefore, this process can also effect the expression of miRNA.

Transfection of miR-665 into murine NB cells caused growth inhibition, cell cycle arrest, decreased total HDAC activity, decreased HDAC8 and MYC protein expression, activated caspase 3 and increased the acetylation of histones. miR-665 targets HDAC8, c MYC and MYCN oncogene and decreases their expression. These targets are validated by the co- transfection of luciferase reporter with target 3' UTR and miRNA-665. Therefore, miRNA 665 directly targets HDAC 8, MYCN and c MYC in the inhibition of mouse neuroblastoma cells. This is the first report to show that miR-665 is a suppressor miRNA of mouse neuroblastoma.

In targeted therapy of cancer, critical genes and proteins involved in the tumorigenesis are identified and therapeutic agents' miRNA and siRNA are used to inhibit the expression of target genes to inhibit the growth of cells in vitro and in vivo. SiRNA-mediated gene knockdown is much more potent and specific with only one mRNA target, whereas miRNA has multiple mRNA targets. siRNA therapeutic approach was used in gene targeting overexpressed cancer proteins in inhibiting cancer cell growth in vitro and inhibited tumor growth in vivo in the following mouse models: breast cancer mouse model, Glioma cells tumor and colon cancer tumor. MYCN, c-MYC, and HDAC8 may each contribute to neuroblastoma tumorigenesis. We reported that transfection of mimic suppressor miR-665 inhibited the expression of c-MYC and HDAC 8 and increased caspase 3 involved in apoptosis and inhibited the growth of neuroblastoma cells in vitro [10].

Our data also indicate that both c-MYC and HDAC 8 are critical targets and targeting these two targets with siRNA inhibited cell growth by 86% in vitro. The combination of siRNAs inhibited tumor growth in vivo by 80%, therefore, inhibiting more than one target is critical for the successful treatment of tumors in vivo.

5. Conclusion

Neuroblastoma is the most frequently diagnosed extracranial solid tumor in children. These tumors account for 15% of childhood deaths from cancer. Survival in one- year-old children is <30% despite aggressive therapies.

We used mouse neuroblastoma tumor model and identified MYC and HDAC8 are the critical targets in neuroblastoma tumorigenesis. Treatment of the tumors in mice with the combination of siRNA-MYC + siRNA-HDAC8 inhibited both the targets MYC and HDAC8 simultaneously and inhibited the growth of tumor by 80%. Therefore, inhibiting more than one target is critical for the successful treatment of tumors in vivo.

Acknowledgements

Conflicts of interest

The author declares that they have no conflicts of interest.

Declarations

Ethics approval: Mice experiments were performed with the approval of the institutional Animal Care and Use Committee, IACUC at Nanospectra Biosciences Inc. Houston, Texas.

Grant support

Author details

Nagindra Prashad
Genetics in Medicine, Houston, TX, USA

*Address all correspondence to: nagindra.prashad@gmail.com

IntechOpen

References

[1] World Health Organization. 2014. Chapter 5. 16.

[2] Maris JM, Hogarty MD, Bagatell R, Cohn SL.. Neuroblastoma. *Lancet*. 2007;369 (9579):2106-2120.

[3] Chang TC, Yu D, Lee YS, Wentzel EA, Arking DE, West KM, Dang CV, Thomas-Tikhonenko A, Mendell JT. Widespread microRNA repression by Myc contributes to tumorigenesis. *Nat Genet*. 2008;40(1):43-50.

[4] O'Donnell KA, Wentzel EA, Zeller KI, Dang CV, Mendell JT. C-myc regulated micrornas modulate e2f1 expression. *Nature*. 2005;435(7043):839-843.

[5] Dang CV. C-myc target genes involved in cell growth, apoptosis, and metabolism. *Mol Cell Biol*. 1999;19(1):1-11.

[6] Richon VM, Sandhoff TW, Rifkind RA, Marks PA. Histone deacetylase inhibitor selectively induces p21WAF1 expression and gene-associated histone acetylation. *Proc Natl Acad Sci USA*. 2000;97(18):10014-10019.

[7] Oehme I, Deubzer HE, Wegener D, Pickert D, Linke JP, Hero B, Kopp-Schneider A, Westermann F, Ulrich SM, von Deimling A, Fischer M, Witt O. Histone deacetylase 8 in neuroblastoma tumorigenesis. *Clin Cancer Res*. 2009;15(1):91-99.

[8] Glick RD, Swendeman SL, Coffey DC, Rifkind RA, Marks PA, Richon VM, La Quaglia MP. Hybrid polar histone deacetylase inhibitor induces apoptosis and cd95/cd95 ligand expression in human neuroblastoma. *Cancer Res*. 1999;59(17): 4392-4399.

[9] Coffey DC, Kutko MC, Glick RD, Butler LM, Heller G, Rifkind RA, Marks PA, Richon VM, La Quaglia MP. The histone deacetylase inhibitor, CBHA, inhibits growth of human neuroblastoma xenografts in vivo, alone and synergistically with all-trans retinoic acid. *Cancer Res*. 2001;61(9):3591-3594.

[10] Prashad N. Mir-665 targets c-myc and hdac8 to inhibit murine neuroblastoma cell growth. *Oncotarget*. 2018; 9(69):33186-33201.

[11] Liang Y, Gao H, Lin SY, Sirna-based targeting of cyclin e overexpression inhibits breast cancer cell growth and suppresses tumor development in breast cancer mouse model. *PLOS ONE*. 2010;5(9):e12860.

[12] Uchida H, Tanaka T, Sasaki K, Kato K, Dehari H, Ito Y, Kobune M, Miyagishi M, Taira K, Tahara H, Hamada H. Adenovirus mediated transfer of sirna against survivin induced apoptosis and attenuated tumor cell growth in vitro and in vivo. *Molecular Therapy*. 2004;10(1):162-171.

[13] Oh BY, Lee RA, Kim KH. Sirna targeting livin decreases tumor in a xenograft model for colon cancer. *World Journal of Gastroenterology*. 2011;17(20):2563-2571.

[14] Zhang X, Ge YL, Tian RH. The knockdown of c-myc expression by RNAi inhibits cell proliferation in human colon cancer HT-29 cells in vitro and in vivo. *Cell Mol Biol Lett*. 2009;14(2):305-318.

[15] Prashad N. Targeting Myc and Hdac8 with a combination of SiRNAs inhibits Tumor Growth in murine Neuroblastoma Xenograft Model. Journal of Cancer Biology and Therapeutics. 2020; 6(1): 301-307

[16] Khandelia P, Yap K, Makeyev EV. Streamlined platform for short hairpin RNA interference and transgenesis in cultured mammalian cells. *Proc Natl Acad Sci USA*. 2011;108(31):12799-12804.

[17] Welch C, Chen Y and Stallings RL MicroRNA-34a functions as a potential tumor suppressor by inducing apoptosis in neuroblastoma cells. Oncogene. (2007); 26: 5017-5022

[18] Wei JS, Song YK, Durinck S, Chen QR, Cheuk AT, Tsang P,Zhang Q, Thiele CJ, Slack A, Shohet J, Khan J. The MYCN oncogene is a direct target of miR-34a. Oncogene. 2008; 27:5204-13.

[19] Li T, Xue Y, Wang G, Gu T, Li Y, Zhu yy, Chen L Multi-target sirna: therapeutic strategy for hepatocellular carcinoma. *J Cancer. 2016; 7: 1317-1327*

Edited by Pasquale Cianci,
Enrico Restini and Amit Agrawal

Pheochromocytoma, paraganglioma and neuroblastoma are the most common neural crest-derived tumors in adults and children, respectively. These neoplasms are associated with significant morbidity and mortality. Some international studies currently underway are researching and evaluating the presence of any similarities and differences between these tumors. Hopefully, future results will reveal several potential novel genes and pathways that might have major roles in the pathogenesis and progression of these neoplasms. This book discusses epidemiology, genetics, and treatment of these malignancies.

IntechOpen